INDEX

Summary

Single point mutations in Connexins 26 or 30 (Cx26, Cx30), codified respectively by GJB2 and GJB6 gene of the DFNB1 locus, provoke genetic non syndromic hearing deafness in pre lingual stage. In the inner ear, Cx26 colocalizes with Cx30 between supporting and epithelial cells of the organ of Corti (OoC) cells, in the spiral limbus, the spiral ligament and the stria vascularis, where they may form heteromeric connexons [1], [2]. The rescue of the expression of wild type connexin is one of the possible therapies for patients, and this can restore cellular network communication of defective connexin gap junctions and hemichannels [3].

In this work we characterized by immunofluorescence the expression of connexin 26 and 30 in the double mutant $Cx26^{Sox10Cre}$ mice during inner ear development, from P5 to adult age, specially in the OoC. We addressed kind of cellular degeneration, more evident in the basal turn of the cochlea, by the absence of the connexin channels. In adult mice, partial obliteration of Cxs leaded to a profound hearing loss, probed by ABR registrations, and a reduction of endocochlear potential. Cochlear organotypic cultures from mutant mice probed by gap-FRAP experiments presented an unpaired cell-cell communication.

We have also described an *in vivo* gene therapy approach that can be used to restore the expression of Cxs in mice using a Bovine Adeno Associated virus, BAAV. The BAAV is a very safe tool because it is not toxic, not pathogenic, and replicative defective in host cells. The transduction of genes occurs mainly on supporting cells, where the connexins are expressed [3].

Our studies identified which age is resonable to start a gene therapy in order to get the best results on hearing. For this therapeutic study, technique such as canalostomy, which previously were described in adult mice, were standardized in P4 mice. We reported for the first time that this kind of surgery in such young mice is not affecting hearing function, and that, so far, we can manipulate gene expression *in vivo*, by deleting Cx26 gene in few cells in $Cx26^{loxP/loxP}$ mice by a Cre recombinase, codified by the BAAV genome.

Riassunto dell'attività svolta

Mutazioni puntiformi nelle Connessine 26 o 30 (Cx26, Cx30), codificate rispettivamente dai geni GJB2 e GJB6 nel locus DFNB1, provocano sordità ereditaria non sindromica in età perlinguale. Nell'orecchio interno, la Cx26 colocalizza con la Cx30 tra le cellule epiteliali e di supporto dell'Organo di Corti (OdC), nel limbo spirale, nel ligamento spirale e nella stria vascularis, dove possono formare connessioni eteromerici [1], [2]. Il ripristino dell'espressione delle connessine sane è una possibile terapia per pazienti non udenti, che permetterebbe il recupero delle comunicazioni della rete cellulare attraverso giunzioni gap ed emicanali di connessine funzionali [3].

In questo lavoro, abbiamo caratterizzato, attraverso tecniche di immunofluorescenza, l'espressione delle Cx26 e Cx30 in topi transgenici $Cx26^{Sox10Cre}$, durante lo sviluppo dell'orecchio interno, da P5 all'età adulta, in particolare nell'OdC.

Abbiamo notato una degenerazione cellulare maggiormente evidente nel giro basale della coclea, dovuto all'assenza di canali di connessine. Nei topi adulti, si è notata una marcata perdita uditiva dovuta alla parziale mancanza di connessine, a seguito di registrazioni di ABR, e una riduzione del potenziale endococleare.

Esperimenti di gap-FRAP condotti in colture organo tipiche di coclea dai topi mutanti hanno rivelato una notevole riduzione delle comunicazioni cellulari.

Abbiamo inoltre descritto un approccio *in vivo* per una terapia genica, che potrebbe essere usato per ripristinare l'espressione delle connessine, utilizzando un virus adeno-associato bovino (BAAV). Tale virus rappresenta uno strumento molto sicuro, poiché non è tossico, non è patogeno e non si replica nelle cellule ospiti. La trasduzione attraverso questo vettore interessa soprattutto le cellule di supporto, dove sono maggiormente espresse le connessine [3].

I nostri studi hanno identificato la migliore età da cui iniziare una terapia genica, al fine di ottenere i risultati migliori. Per questi studi terapeutici, abbiamo perfezionato una tecnica ampiamente utilizzata in topi adulti, applicandola in topi di 4 giorni. Abbiamo verificato, per la prima volta, che questa metodica anche applicata a topi

così giovani non interferisce con la funzionalità uditiva. Inoltre, ad ora, abbiamo potuto manipolare l'espressione genica in vivo, eliminando il gene della Cx26 in alcune cellule di topi $Cx26^{loxP/loxP}$ attraverso l'espressione di una Cre ricombinasi codificata dal genoma del BAAV.

Original publications

Part of the data reported in the present thesis has been published in the following papers:

I. Anselmi F, Hernandez VH, Crispino G, Seydel A, Ortolano S, Roper SD, Kessaris N, Richardson W, Rickheit G, Filippov MA, Monyer H, Mammano F.(2008) ATP release through connexin hemichannels and gap junction transfer of second messengers propagate Ca^{2+} signals across the inner ear. Proc Natl Acad Sci U S A. 105, 18770-5.

II. Ortolano S, Di Pasquale G, Crispino G, Anselmi F, Mammano F, Chiorini JA. (2008) Coordinated control of connexin 26 and connexin 30 at the regulatory and functional level in the inner ear. Proc Natl Acad Sci U S A. 105, 18776-81.

III. Majumder P, Crispino G, Rodriguez L, Ciubotaru CD, Anselmi F, Piazza V, Bortolozzi M, Mammano F. (2010) ATP-mediated cell-cell signaling in the organ of Corti: the role of connexin channels. Purinergic Signal. 6, 167-87.

IV. Bortolozzi M, Brini M, Parkinson N, Crispino G, Scimemi P, De Siati RD, Di Leva F, Parker A, Ortolano S, Arslan E, Brown SD, Carafoli E, Mammano F. (2010) The novel PMCA2 pump mutation Tommy impairs cytosolic calcium clearance in hair cells and links to deafness in mice. J Biol Chem. 285, 37693-703.

V. Schütz M, Scimemi P, Majumder P, De Siati RD, Crispino G, Rodriguez L, Bortolozzi M, Santarelli R, Seydel A, Sonntag S, Ingham N, Steel KP, Willecke K, Mammano F. (2010) The human deafness-associated connexin 30 T5M mutation causes mild hearing loss and reduces biochemical coupling among cochlear non-sensory cells in knock-in mice. Hum Mol Genet. 19, 4759-73. (Results of this article were chosen to be used as a cover page of the Magazine)

INTRODUCTION

Anatomy and Physiology of the ear and hearing

The ear is the organ that permits us to feel sounds. Hearing is one of the most important sense for animal species, and is fundamental to escape from predators or to hunt food. For humans, it represents mostly a tool to communicate and live in society. Hearing function translate acoustic stimuli in electrical signals, to be transmitted to the temporal cortex, by a precise pathway and a subtle anatomy.
The external ear collects sound and channels via the ear canal to the tympanic membrane, or eardrum. As oscillations in air pressure hit on the eardrum, its vibrations are transmitted to the middle ear's ossicles, named malleus, incus, and stapes. These tiny bones are directly coupled to the oval window, and so their vibrations are conveyed to the inner ear (**Figure 1**).

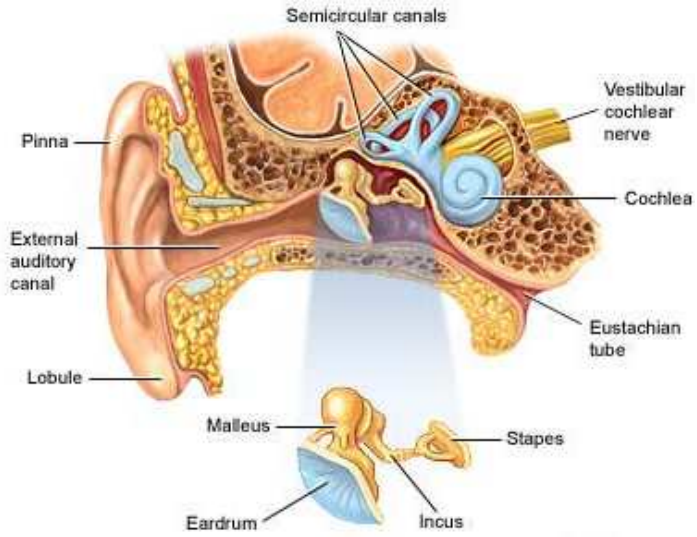

Figure 1 Scheme showing the human external, middle and inner ear, and a magnification of the middle ear's ossicles.

The *inner ear* is situated within the petrous portion of the temporal bone and is composed of the *vestibular system* (semicircular canals, utricle, and saccule), which senses linear and angular acceleration and inclination of the head with

respect to gravity, and the *cochlea*, which mediates sound perception. In the inner ear, *membranous labyrinth* is contained within the *bony labyrinth*. The bony labyrinth consists of the vestibular system (composed by the vestibule and the *semicircular canals*) and the spirally coiled cochlea. Within each structure is the corresponding portion of the membranous labyrinth: the vestibule contains the utricle and the saccule, each semicircular canal contains a semicircular duct, the cochlea the cochlear duct (**Figure 2**).

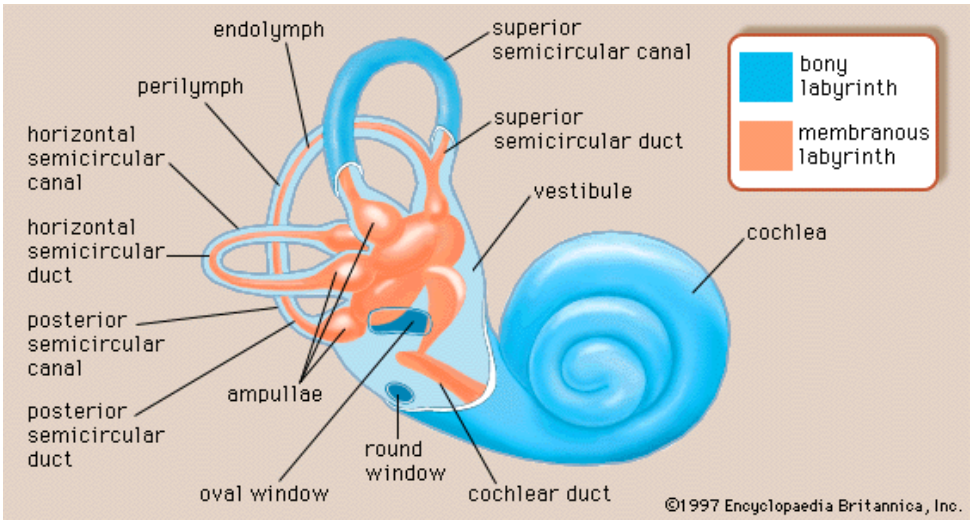

Figure 2. The inner ear is composed of the vestibular system (*semicircular canals*, utricle, and saccule) and the *cochlea*. The *oval window*, where the footplate of the *stapes* inserts, and the *round window* are located at the basal end of the cochlea. The stapes footplate, within the oval window, applies pressure to the fluid filling the cochlea.

The cochlea is a spiral tube that is coiled around a central pillar, the *modiolus*. A thin bony shelf, the osseous spiral lamina, winds around the modiolus like the thread of a screw. It projects about halfway across the cochlear canal, which is divided into three compartments: an upper chamber called the *scala vestibuli* (vestibular ramp), a lower chamber called the *scala tympani* (tympanic ramp) and a middle chamber called *scala media* (**Figure 3**). The scala vestibuli and scala tympani, which are filled with a fluid called *perilymph*, communicate with each other at the apex of the cochlea through a foramen called *helicotrema*. Instead, the scala media ends blindly at both ends and is filled with *endolymph*. It is delimited by the

upper surface of the *organ of Corti* (OoC), by the *stria vascularis* and by *Reissner's membrane*, which consists of only two layers of flattened cells. A low ridge, the *spiral limbus*, rests on the margin of the *lamina spiralis ossea* and provides the attachment for the *tectorial membrane* that surmounts the OoC (**Figure 3**). Named after marquis Alfonso Corti, the Italian anatomist who first described it in 1851, the OoC is an avascular sensory epithelium, seated on the *basilar membrane* (BM), which comprises parallel rows of *sensory hair cells* and several types of *supporting cells*. The basilar membrane together with the overlying OoC and the scala media form the *cochlear duct*. The OoC is covered by the *tectorial membrane*, an acellular gelatinous structure floating in endolymph and originating from the spiral limbus as a thin fibrillar layer that becomes thicker as it extends over the OoC. The most striking feature of the OoC, when viewed in cross section, is *the tunnel of Corti* formed by two rows of *pillar cells*. Resting directly on the BM, these cells have adjoining, widely spaced bases that taper upward into slender processes. These, in turn, expand and interlock in the upper surface of the organ of Corti, the *reticular lamina*. The arch separates a single row of pear-shaped, *inner hair cells* (IHCs) from three rows of cylindrical *outer hair cells* (OHCs).

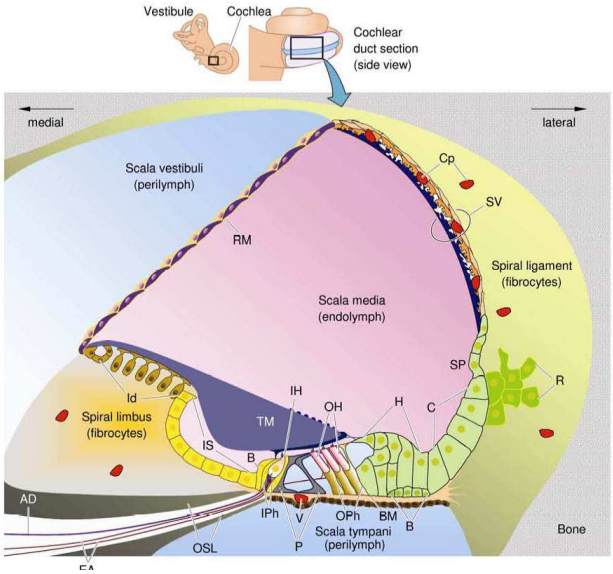

Figure 3. Schematic diagram of a cross section of the cochlear canals. Scala media (or cochlear duct, filled with endolymph) lies between the larger vestibular and tympanic scalae (filled with perilymph). The base of scala media is formed by the osseous spiral lamina (OSL) and the

basilar membrane (BM). Resting on the basilar membrane is the organ of Corti, which contains sensory inner hair cells (IH) and outer hair cells (OH), separated by pillar cells (P) forming the tunnel of Corti. The IHC is synaptically connected to afferent dendrites (AD) of type I spiral ganglion neurons. Efferent axons (EA) arising from small neurons in the ipsilateral lateral superior olivary complex and large neurons of the medial efferent system from both sides of the medial superior olivary complex effect a feedback control to the inner hair cell/type I afferent synapse and form axo–somatic contacts with outer hair cells, respectively. Each OHC is supported by an outer phalangeal cell (OPh), or supporting cell of Deiters, which holds the base of the hair cell in a cup–shaped depression. From each Deiters' cell, a phalangeal projection extends upward to the stiff membrane, the reticular lamina that forms the upper layer of the OoC. The apices of the OhC are firmly held by the reticular lamina, but the cell bodies are suspended in a fluid, the cortilymph, that fills the space of Nuel and the tunnel of Corti. The IHC are supported and enclosed by the inner phalangeal cells (IPh), which rest on the thin outer portion, called the tympanic lip, of the spiral limbus. The latter rests on the margin of the osseous spiral lamina and hosts interdental cells (Id) and fibrocytes (not shown). The inner border cell (B) and cuboidal epithelial cells line the spiral limbus on the inner sulcus (IS) side. On the top of the IHC, stereocilia are arranged in parallel rows whereas, on the OHC stereocilia form a W pattern. The longest stereocilia of the OHC make contact with the acellular structure forming the tectorial membrane (TM), which covers the reticular lamina reaching the cells of Hensen (H). Two other types of epithelial cells, the cells of Claudius (C) and Böttcher (B), cover the outer sulcus. At the upper margin of the outer sulcus is the spiral prominence (SP) followed by the stria vascularis (SV). Some cells of the outer sulcus send projections, called root cells (R), into the substance of the fibrous spiral ligament, which lies between the stria vascularis and the bony wall of the cochlea and also host numerous fibrocytes (not shown). Like the adjacent SV, it is well supplied with blood capillaries (Cp). The vas spiralis (V) is a blood vessel running in the tympanic layer of the basilar membrane just beneath the tunnel of Corti. The transparent vestibular membrane of Reissner (RM), which consists of only two layers of flattened cells, stretches from the SV to medial margin of the spiral limbus. (Figure extracted from Schultz et al., 2010)[4]

Cochlear hair cells are polarized neuroepithelial cells with primary sensory synapses at their basal end. The characteristic feature of the sensory hair cells is the apical hair bundle, formed by a highly organized array of stereocilia, which contains the molecular apparatus devoted to *mechanosensory transduction*. Stereocilia are graded in height, becoming longer on the side away from the *modiolus*. The tallest stereocilia of the OHCs are firmly embedded in the tectorial membrane, whereas the stereocilia of the IHCs are free standing. Stereocilia in a

bundle are interlinked by *tip links*, fine extracellular filaments that connect adjacent stereocilia along the *sensitivity axis [5]*. From each Deiters' cell a projection extends upward to the reticular lamina, which is formed by the apposition of the apical poles of pillar cells, OHCs and Deiters' cells. Beyond the OHCs and the Deiters' cells are three other types of epithelial cells, usually called Hensen's, Claudius', and Boettcher's cells. Supporting Hensen's cells are characterized by the presence of abundant lipid inclusions and mitochondria located near their lateral and apical membranes [6]. Their processes are facing the endolymphatic compartment [7], which is a common feature of transporting epithelia [8]. They are adjacent to the outermost row of the OHCs and contact the BM. All cell apices forming the reticular lamina are firmly interlocked by *tight junctions*. The tight junction network extends all over the scala media surface of the OoC and into the Reissner's membrane, thus preventing the mixing of endolymph and perilymph. The borders of the endolymphatic space are thus the scala media side of the "upper" surface of the OoC, the stria vascularis and the Reissner's membrane (**Figure 3**). Perilymph is similar, but not identical, in composition to other extracellular fluids of the body, such as cerebrospinal fluid: the concentration of Na^+ is high, while concentration of K^+ is low. Perilymph is apparently formed locally from the blood plasma by transport mechanisms that selectively allow substances to cross the walls of the capillaries. However it is unlikely that the cerebrospinal fluid is involved in the normal production of perilymph [9]. A fluid similar to perilymph (sometimes referred to as *cortilymph*) fills the spaces within the organ Corti (tunnel of Corti and space of Nuel). Endolymph is unique among extracellular fluids of the body as its K^+ concentration is much higher than its Na^+ concentration (**Table 1**). A second striking feature of endolymph is its electrical potential, which is approximately 80 mV more positive than the potential of perilymph (usually taken as reference). This voltage difference is known as the *endocochlear potential* (EP) [10].

	Perilymph (scala vestibuli)	Perilymph (scala tympani)	Endolymph (scala media)
Na^+	141	148	1.3
K^+	6.0	4.2	157
Ca^{2+}	0.6	1.4	0.023
Cl^-	121	119	132
$HC03^-$	18	21	31

Table 1. Ionic concentrations of perilymph and endolymph (in mM) (from Marcus in Cell Physiology *source book [11]*)

When vibrations are transmitted to the cochlear fluids, a pressure wave travels down the scala vestibuli from base to apex, through to the scala tympani and ending at the round window. The two external scalae and the central scala media are acoustically coupled, and the pressure wave passing through Reissner's membrane is applied to the basilar membrane. The basilar membrane's mechanical properties vary with position along the cochlea: the collagen fibers in the base are shorter and stiffer than those in the apex, which are longer and more flexible [12]. These characteristics have a profound effect on the basilar membrane's response to vibrations; the amplitude of a pressure wave changes as it travels down the basilar membrane, with the peak amplitude's position dictated by the stimulus frequency [13]. Accordingly, mechanical responses to auditory stimuli of high frequency peak at the base, while lower frequencies induce peak responses near the apex (**Figure 4**).

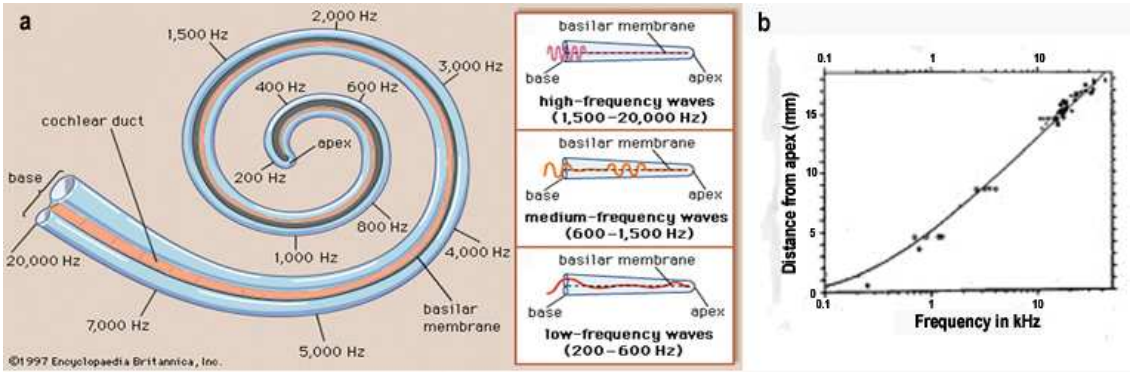

Figure 4 (**a**) Traveling wave peak at frequency-dependent locations, higher frequencies peaking closer to more basal location. Peak position is an exponential function of input frequency because of the exponentially graded stiffness of the basilar membrane. Part of the stiffness change is due to the increasing width of the membrane and part to its decreasing thickness. (**b**) Relationship between peak frequency (Hz) and distance from apex (nm). From [14].

Upon the basilar membrane sits the organ of Corti, containing 15,000–20,000 hair cells in the human auditory system, organized into one row of inner hair cells and three rows of outer hair cells. The less abundant inner hair cells are the primary sensory cells of the auditory system, with 90%–95% of the cochlear afferent innervations; they provide the major input to the auditory centers of the central nervous system. The outer hair cells are endowed with many efferent synapses and play a central role in signal amplification. When the hair bundle is deflected by a mechanical stimulus, it responds as a unit; stereocilia move as rigid rods, without any flexion [15], [16]. Mechanoelectrical transduction begins with hair-bundle deflection. This deflection triggers opening of a nonselective cation channel, the transduction channel [17], that opens within 50 µs [18], [19], and has a fairly large conductance of ~100 pS in high Ca2+, as measured by single-channel recording [20], [21]. Deflection movement toward the tallest stereocilia opens channels; an opposite movement toward the shortest stereocilia closes channels [22]. Although an indispensable fraction of the receptor current is carried by Ca^{2+} ions [23], [24], more than 70% is due to K^+ influx [17], [25]. This inward K^+ current is a manifestation of the unusually high K+ concentration (~150 mM) in the endolymph. Moreover, the receptor current is enhanced by the endolymph's extracellular potential of +80 mV, which gives rise to a +150 mV electrical driving force for K^+

and Ca^{2+} entry. As hair cells depolarize voltage-dependent Ca^{2+} channels near basolateral synapses open; elevated Ca^{2+} levels stimulate the neurotransmitter release at the glutamatergic synapses, initiating signal propagation to afferent neurons [26].

K^+ homeostasis in the inner ear

In the mouse, a mature ionic composition of endolymph is known to be reached at the end of the first postnatal week. The EP develops 5 to 6 days after birth (P5-P6) and reaches adult values at P17-18 [27]. The endolymphatic K^+ concentration remains unchanged during the rapid increase of the EP [28]. Thus the EP and the high K^+ concentration arise independently during the development of the cochlea. A certain degree of independence had been inferred from the results of anoxia experiments. Anoxia caused a decay to zero of the EP with 1-2 min [29]. Few more minutes later, the positive EP was replaced by a negative potential, called –EP, thought to be a diffusion potential arising from the high K^+ concentration in the endolymph, which could take several hours to disappear as the ions equilibrated [30].

The current understanding of the molecular processes underlying these phenomena is based on the structure of the stria vascularis, which consists of two barriers formed by the *marginal cells* and the *basal cells* (**Figure 5**). Each barrier consists of a continuous sheet of cells joined by tight junctions. Between the two layers is the *intrastrial space*, where the potential is +90 to +100 mV relative to perilymph, and a discontinuous layer of *intermediate cells*. As described in Table 1, ionic composition of the endolymph is quite unusual: K^+ concentration is high, while conversely Na^+ levels are low; the contiguous perilymph, instead, resembles a general extracellular fluid. From the endolymph, K^+ ions enter the sensory cells through mechanoelectrical transduction channels located at their apical pole [31] and are secreted from their basolateral side mostly through KCNQ4, but also KCNN2 (SK2) and KCNMA1 (BK) K^+ channels [32], [33].

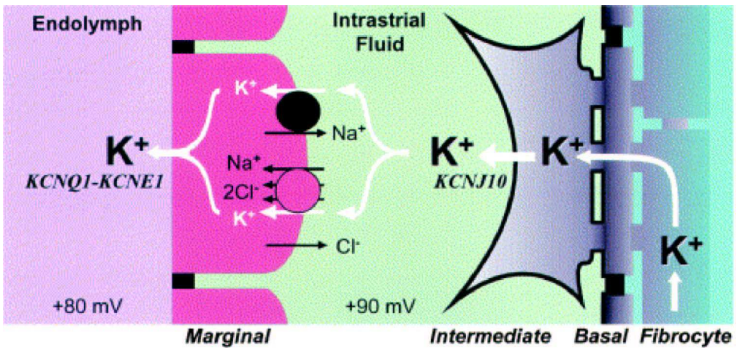

Figure 5. Schematic cross-section through stria vascularis. Stria vascularis consists of two barriers comprised of cells that are joined by tight junctions. One barrier is composed of marginal cells and the other of basal cells. Strial marginal cells secrete K^+ into endolymph. The endocochlear potential is generated across the basal cell barrier. Basal cells are joined by gap junctions to intermediate cells on the intrastrial side and to fibrocytes on the spiral ligament side. The molecular mechanism that generates the endocochlear potential is understood to be the KCNJ10 K^+ channel in the intermediate cells. From Marcus, 2000

The K^+ released from the sensory cell is maintained in the extremely specialized and tight insertion of the OHC base into the cup region of its supporting Deiters' cell, from where it is likely taken up by the K-Cl co-transporters Kcc4 [34] and Kcc3 [35]. The genetic disruption of these K-Cl co-transporters causes deafness in mice [34], [35]. These proteins direct potassium into the epithelial cell gap junction system of the supporting cells [36], Deiter's cells and other supporting cells of the OoC are essential to cochlear ion homeostasis. These cells belong in distinct gap junction networks formed by nonsensory epithelial cells [37], [38], including interdental cells of the spiral limbus, inner sulcus cells, organ of Corti supporting cells, outer sulcus cells, and cells within the root processes of the spiral ligament [39]. Therefore, immediately after being released from the hair cells, a substantial proportion of the K^+ ions is likely to be taken up into these syncytia that may be an integral part of the recycle scheme [36].

K^+ very probably enters stria vascularis via a connective tissue cell gap junction system, between spiral ligament fibrocytes and stria vascularis basal cells. From basal cells it could pass through gap junction channels into intermediate cells. KCNJ10 passively secretes potassium from the high concentration in the cytosol of intermediate cells to the 1-2 mM intrastrial fluid [40], generating this way the

endocochlear potential [41], [42]. From this peculiar extracellular milieu, potassium is taken up by marginal cells; they are not interconnected by gap junctions. K^+ enters via a $Na^+/2Cl^-/K^+$ cotransporter; a Na^+/K^+-ATPase extrudes sodium, thus establishing a sodium gradient that energizes the $Na^+/2Cl^-/K^+$ co-transporter for an efficient K^+ uptake. Potassium is then passively secreted back into endolymph through the KCNQ1/KCNE1 K^+ channel [43], [42]; the driving force for this release comes from the small positive membrane potential across the apical membrane of strial marginal cells [44], [45].

Although the pathway of K^+ through stria vascularis and through the hair cells is well established, the path from the hair cells toward stria vascularis lacks definitive experimental evidence, and a previous alternative hypothesis consisted in K^+ flux through perilymph towards spiral ligament [46], [47]. The basilar membrane could be easily crossed by K^+ ions [48], while sudden changes in K^+ concentration around the hair cells could be buffered by supporting cells. Therefore, it has been proposed that intercellular transport across the gap junction network of this connective tissue participates in K^+ recirculation. After reaching the stria vascularis, K^+ ions are released by intermediate cells into the strial luminal site and are finally taken up by strial marginal cells to be secreted back into endolymph [49], [50]. However, the hypothesis of K^+ flowing mainly through the supporting cells syncytium and never entering the perilymph is backed by the phenotypes of Cx26- [51], Cx30- [34] and KCC4-knockout mice [52]. K^+ cycling within the cochlea is not limited to the current loop through the sensory cells. Part of the current that is generated by stria vascularis is carried through outer sulcus and Reissner's membrane cells [53]. Moreover, studies in animals in which the hair cells have been destroyed indicate that alternative pathways exist also for the route through the sensory hair cells, owing to the unaltered endocochlear potential, K+ concentration and endolymphatic volume [54]. To some extent, the passage through KCNJ10 could be dodged as well, even if that abolishes the endocochlear potential [40], [55]. The critical role K^+ plays for endolymph homeostasis and sensory transduction renders it likely that the rate of K^+ secretion is controlled by the presence of K^+ near the basolateral membrane of strial marginal cells [9] as

well as by factors that link the rate of K^+ secretion to the systemic status. Strong evidence has been obtained for the presence of purinergic [56], muscarinic [57] and adrenergic receptors [58] that act as control mechanisms. P2Y2 subtype of purinergic receptors are expressed on the apical membrane of strial marginal cells, whereas P2Y1 and P2Y2 coexist on the basolateral membrane. The apical P2Y2 receptors down regulate K^+ secretion via the DAG-protein kinase (PKC), while basolateral P2Y1 and P2Y2 receptors increase K^+ secretion followed by a decline, due to the production of IP3 and elevation of cytosolic Ca^{2+} [59]. The basolateral membrane of strial marginal cells, moreover, contains β1-adrenergic receptors [60] that control the rate of metabolism [61], the activity of Na^+/K^+-ATPase [62], [63] and the rate of transepithelial K^+ secretion [60]. β-adrenergic receptors cause an elevation of the cytosolic cAMP concentration that stimulates KCNQ1/KCNE1 K^+ channel in the apical membrane of strial marginal cells to secrete K^+ [60]. The choice of K^+ as charge carrier over Na^+ has major advantages. First, that a K^+ influx in the cytosol causes a subtle change in concentration, being K^+ the most abundant ion in this compartment. The most important aspect, however, is in that influx and extrusion of K^+ are energetically inexpensive for the sensory cell since both occur down an electrochemical gradient (–80 mV resulting from the difference in concentration of the two fluids). Contributing to this gradient is the resting membrane potential of the sensory cells (–60 mV relative to perilymph) that is mainly determined by their K^+ selective channels in the basolateral membrane. This steep ~-150 mV gradient generates a substantial driving force for K^+ ions, resulting in a continuous flux of K^+, known as the standing current, through the reticular lamina, flowing particularly through the sensory cells [64]. It is worth emphasizing that currently there is no direct evidence for the cycling of K^+ ions through cochlear gap junction (GJ) channels [65].

Gap Juntions- Connexins

Intercellular signaling is fundamental to the complex biological functions, include synaptic transmission, hormone-receptor signaling, and cell adhesion. These

processes are all mediated by membrane proteins such as ion channels, G-protein coupled receptors (GPCRs), or receptor tyrosine kinases. Gap junctions are unique because mediate intercellular signals by connecting the cytoplasms of two neighboring cells.

They are expressed in a wide variety of cells, organs, and tissues, and play essential roles in a variety of biological processes. Gap junction channels are selective for small molecules, voltage-dependent gating, and response to Ca^{2+}, pH and phosphorylation [66], [67].

Gap junctions were identified in the '60s, with histological studies [68]; the term "gap junction" refers to the plaques or maculae containing hundreds of intercellular channels spanning the two plasma membranes that appear in electron microscopy studies in almost all tissues. They are involved in development, cell differentiation, growth and proliferation, electrical activation of the heart and of smooth muscles, neuronal signaling, hormone secretion, sensory transduction, wound healing, lens transparency and immune functions [69]. In the developing brain, for example, gap junctions are expressed in periventricular precursor cells and mediate synchronous Ca^{2+} oscillations, which coordinate and regulate the proliferation of neural cells [70], [71]. The neural cells migrate along with the radial glial cell [72], and the expression pattern of connexins appears to be associated with neural differentiation [73].

A gap junction contains clusters of tens to thousands of intercellular channels called ''gap junction channels,'' each of which is formed by the end-to-end docking of two hemichannels, also referred to as ''connexons.'' Each connexon is composed of six connexin subunits surrounding the central pore. Some of them are expressed in a single cell type and form heteromeric (more than two different connexins in a connexon) or heterotypic (a gap junction channel with different connexons) channels, conferring further diversity in their composition and function [74], [75] (**Figure 6**).

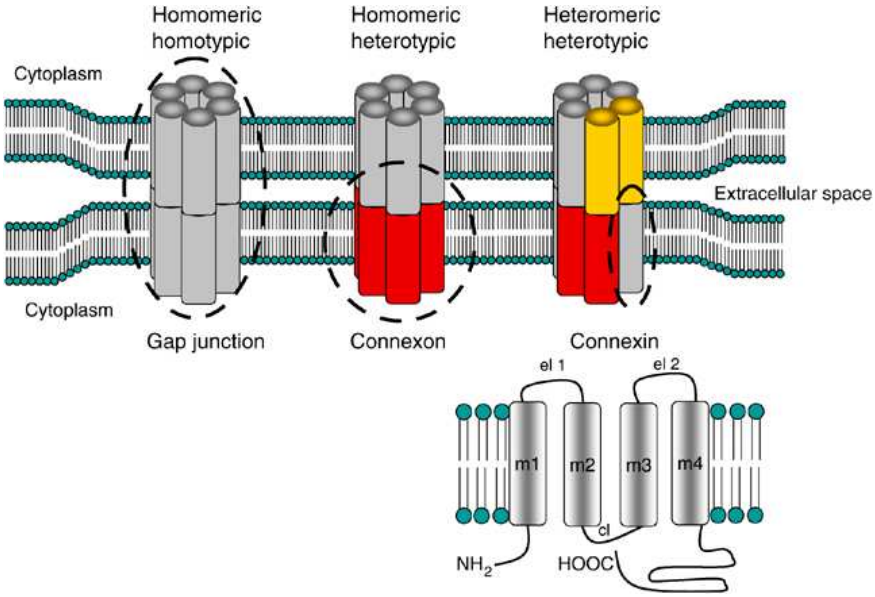

Figure 6. Representative scheme of connexin and gap junction channels. [76]

Outside the plasma membrane, these proteins could be seen in the ER and Golgi in some disease-associated mutants. Although not glycosylated, most connexins do pass through the Golgi, and oligomerize late in their biosynthesis [77]. There is also some evidence for non-Golgi transport of Cx26 [77], [78]. Hemichannels are inserted into the membrane, where they remain in a predominantly closed state until recruited to the outside of existing plaques within the membrane [79]. Removal of old connexins can occur through 'budding off' of whole pieces of the plaque, to form annular gap junction vesicles within one cell [80]. Both lysosomal and proteasomal degradation pathways for connexins have been reported [81]. Gap junctions are dynamic with an *in vivo* half-life of ~5 h in liver hepatocytes [82] and 1.3 h in the heart [83]. In some cell types or for some connexins, more stable subgroups of proteins may exist: for instance, Cx56 in lens cultures was found to have a subpopulation that had a long half-life of over 36 h [84].

To date, more than 20 different connexins have been identified in the human genome, and have been classified and named according to their molecular weight [85], [86], [69], or to their molecular homology; they are grouped into α, β, δ subtypes [87]. Generally, heterotypic channels behave consistent with an in-series combination of homomeric channels, although rectifying channels can be produced

[88]. Interactions between connexins seem to be somehow selective. Heterotypic coupling tends to occur, with some notable exceptions, within a homology group i.e. α or β [74], dictated by sequences, possibly as few as a couple of residues, in the second extracellular loop. Within a single plaque, some connexins will segregate, while others mix [89], [90], which suggests that formation of heteromeric channels is also selective. Signals that regulate hetero-typic docking of different connexons have been identified mainly in the extracellular loops [91], [92]. Other than the preferential interactions just described, no common properties link the members of connexin groupings, which have been derived from sequence alignments of the connexins.

The primary function ascribed to gap junctions has been the transfer of ions and metabolites under about 1200 Da, with a maximal diameter of approximately 1.5 nm, between cells in contact, and this transfer through Gj is mediated by passive diffusion. Although this may seem to be a ‘housekeeping' function, several studies have revealed a surprising diversity in the permeability properties of gap junctions composed of different connexins to natural permeants such as ATP, AMP, adenosine and glutathione, InsP3 and even different cyclic nucleotides [93], [94], [95]. Thus, differences in the selectivity for second messengers may play an important role in organ function. The electrical unitary conductance (i.e. the conductance of a single gap junction channel) varies widely (25 pS for Cx45, 350 pS for Cx37), yet, the sequence of monovalent cation selectivity is the same (K^+>Na^+>Li^+>TEA) for different connexins [96]. One of the properties that modulate transfer selectivity is the charge of the passing molecule or ion [97]. Studies in vitro have shown that selectivity and permeability of the Gj depend on the type of Cx forming the channel [93], [95], [98], [99], [100]. Tracers of different molecular weights and charges delivered intracellularly to a single cell, such as Lucifer Yellow (LY, 443 Da, -2), propidium iodide (414 Da, +2), and ethidium bromide (314 Da, +1), have been used to evaluate the selectivity and permeability of the gap junction composed of different Cxs in vivo [98]. Homomeric connexons made of Cx32, expressed in liver parenchymal cells, permitted the transmission of InsP3 between cells and the spread of InsP3-triggered Ca^{2+} wave [101]. It has also been shown

that Cx32 is permeable to both cAMP and cGMP, whereas heteromeric connexons composed of Cx32 and Cx26 lose permeability to cAMP, but not to cGMP [95]. These intercellular channels directly connect the cytoplasm of one cell with the cytoplasm of a neighboring cell [102], but rather than constituting mere passive pores they can open or close in response to environmental and intracellular conditions, like variations in pH, calcium concentration, phosphorilation and voltage. Gap junction channels typically remain open at rest: as they close, cells uncouple from each other electrically and metabolically. Uncoupling is mainly a protective device for isolating healthy cells from damaged neighbors, but in some cells there is evidence for channel gating sensitivity to nearly physiological $[Ca^{2+}]_i$ and $[H^+]_i$, suggesting that modulation of channel permeability by these ions may be relevant to normal cell functions as well [103]. While it is clear that Ca^{2+} affects channel gating, the $[Ca^{2+}]_i$ that activates the gating mechanism is still uncertain, and may vary among connexins and cell types [104, 105]: evidence for gap junction channel sensitivity to nanomolar [Ca2+]i has been confirmed in astrocytes co-injected with lucifer yellow and Ca^{2+}. In these cells, the blockage of cell–cell dye diffusion was linearly related to $[Ca^{2+}]_i$ ranging from 150 to 600 nM [106]. In contrast, higher $[Ca^{2+}]_i$ appear to be needed to uncouple cardiac myocytes [107]. Also the sensitivity to pH varies among cell types and is at least in part related to the type of connexin expressed. A soluble cytosolic intermediate has been proposed to mediate the Ca^{2+}/H^+-induced cell–cell uncoupling, that could be calmodulin (CaM; [108]) or protonable amminosulphonates [109].

Electrophysiological studies have demonstrated that gap junctions have several gating mechanisms. At least two regulation mechanisms respond to the transjunctional voltage (Vj), Vj gating (fast) and loop gating (slow) [110].Gap junctions can also be gated by the membrane voltage (Vm), termed Vm gating, and by chemical factors such as phosphorylation, pH and Ca^{2+}, known as chemical gating [111]. Molecular mechanisms which mediate voltage-induced closure of gap junction channels must be different [69]. Chemical uncouplers like calcium and protons activate a chemical gate that behaves in terms of kinetics and efficiency identically to the slow *Vj* gate [112], [110], probably reflecting complex

conformational changes that require the participation of all connexins in a gap junction channel. Changes in membrane potential (*V*m) activate an additional gate (*V*m gate), which is only present in few connexin channels. Although chemical gate and slow *V*j gate are usually referred to as separate gates, evidence is accumulating in favor of the idea that they may in fact be the same [113].

Each monomer of connexin has four transmembrane alpha helices (TM1-TM4) and two extracellular loops (E1, E2), an N-terminal region (NT), a cytoplasmic loop (CL), and a C-terminal tail (CT). Three highly conserved cysteine residues make disulfide bonds between the loops [114], which are essential for the formation of functional gap junction channel [115].

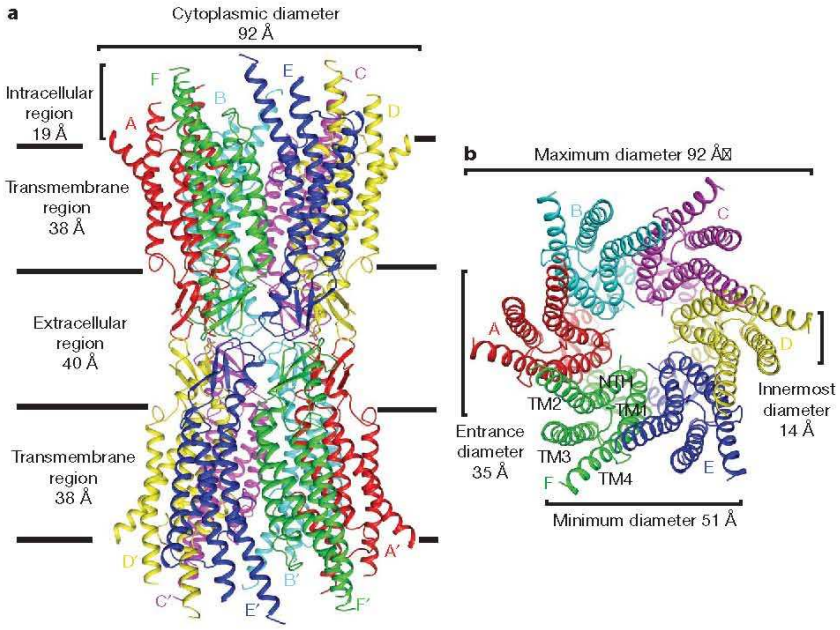

Figure 7. Overall structure of the human Cx26 gap junction channel in ribbon representation.(a) Side view of the Cx26 gap junction channel with the locations of plasma membranes and scale of each region. Each subunit is colored differently, and those associated with the crystallographic two-fold axis are in the same color. (b) Top view of the Cx26 gap junction channel representing the arrangement of the transmembrane helices and the N-terminal helix. The channel has a hexagonal appearance with the largest outer diameter of ~ 90 Å and a pore entrance of ~ 40 Å (Extracted from Maeda and Tsukihara, 2010 [116], Maeda et al., 2009 [117])

The crystal structure of the human connexin 26 (Cx26, also known as GJB2) at 3.5Å resolution, shows two membrane-spanning hemichannels and the arrangement of the four transmembrane helices of the six protomers forming each hemichannel. The hemichannels feature a positively charged cytoplasmic entrance, a funnel, a negatively charged transmembrane pathway, and an extracellular cavity. The pore is narrowed at the funnel, which is formed by the six amino-terminal helices lining the wall of the channel, which thus determines the molecular size restriction at the channel entrance. The structure of the Cx26 gap junction channel also has implications for the gating of the channel by the transjunctional voltage (**Figure 7**) [117].

Two major connexins, Cx26 and Cx30, are coexpressed and form homo- and hetero-gap junctions in the inner ear [118], [36], [119], and mutations in these proteins are known to be associated with hearing loss [120], [120], [121], underscoring the importance of gap junctional communication in auditory function.

Connexins: Cochlear distribution and hearing loss

Hearing loss (HL) is the most common birth defect and the most prevalent sensorineural disorder in developed countries [122]. One in 500 newborns presents with HL in excess of 40 decibels (dB); by adolescence, prevalence increases to 3.5 per 1000 [123]. Hereditary HL is nearly always *monogenic*; deafness *loci* are given the prefix DFN, followed by a number indicating the order in which they were discovered. Updated lists of loci and cloned genes are provided by a number of Web sites, but most notably by the Hereditary Hearing Loss Homepage at http://hereditaryhearingloss.org.

The pattern of inheritance can be dominant (DFNA), recessive (DFNB), X-linked and mitochondrial. Inherited hearing loss can be separated into non-syndromic deafness, in which there are no additional abnormalities affecting other organs, and syndromic deafness, which is accompanied by other specific abnormalities. Many genes are involved in the different types of deafness (syndromic and non-syndromic). Non-syndromic hereditary deafness is mainly (80%) due to recessive

genes (or mutations). It is believed that more than one hundred genes could be involved in hearing impairment. Several of these genes have been identified recently by positional cloning or positional candidate gene approaches [124]. The complex deafness DFNB1 locus (13q11-q12), has been shown to contain the genes encoding for Cx26 (GJB2) and Cx30 (GJB6) within 50 kb of each other [125]. Deafness-causing mutations have been reported in other connexin genes, such as: *GJB1* (Cx32), which is also responsible for X-linked Charcot-Marie-Tooth disease type I [126]; *GJB3* (Cx31), involved in deafness [127] or a skin disease (erythrokeratodermia variabilis) [128] depending on the location of the mutation; and *GJA1* (Cx43), involved in recessive deafness [129]. However DFNB1 mutations are responsible for about half of all cases prelingual hearing loss in most populations [122, 130, 131]. The carrier rate in the general population for a recessive deafness-causing GJB2 mutation is approximately 1 in 33 (http://www.ncbi.nlm.nih.gov/books/NBK1434/). More than 50 distinct recessive mutations of *GJB2* have been described, including nonsense, missense, splicing, frame-shift mutations and inframe deletions [132]. A large French dominant family affected by pre-lingual deafness showed linkage to chromosome 13q12 (DFNA3), the same region to which DFNB1 had been mapped [133]. An interaction between *GJB2* mutations and a mitochondrial mutation appears to be the cause of hearing impairment in some heterozygote patients [134].

Several connexins have been detected in the adult mammalian cochlea [39], [119]. Gap junctions are found in two networks of cells: the *epithelial network* of supporting cells and the *connective tissue network* of fibrocytes and cells of the stria vascularis [39], [135] (**Figure 8**).

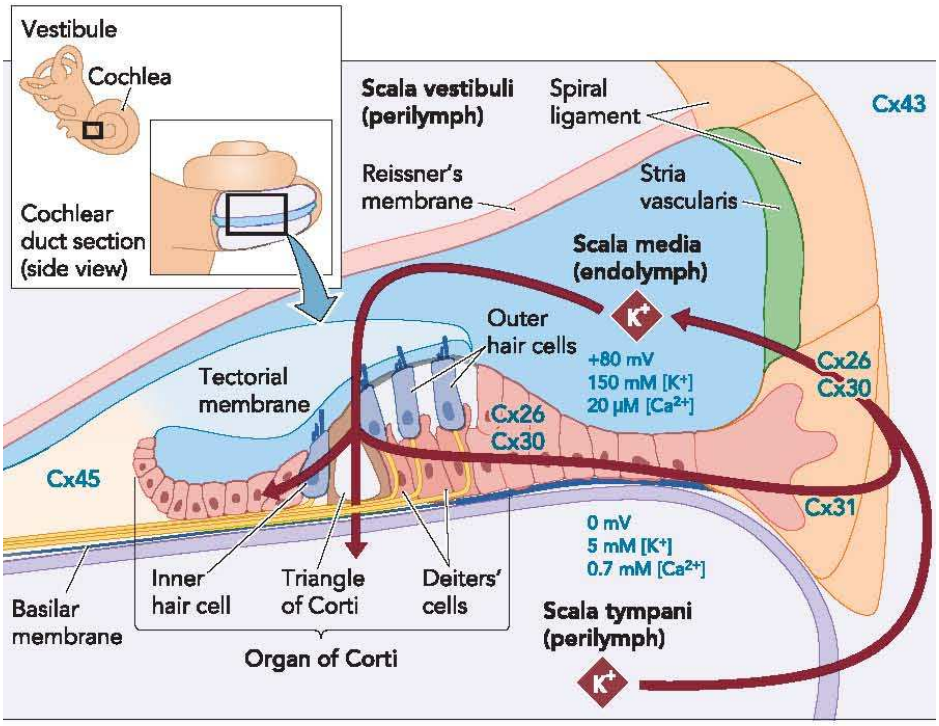

Figure 8. Schematic view of selected K^+ recycling process, connexin and ionic distribution in the inner ear. Figure extracted from Mammano et al., 2007. [136]

Cx26 is the most prominent connexin expressed in the inner ear, proximal tubules of the kidney, the liver and the rat placenta [137]. The most common mutation associated with recessive deafness is a single-base deletion (35delG) within the *GJB2* gene that results in a frameshift at position 12 in the coding sequence of Cx26 and premature termination of the protein [138], [120], [139], [140]. The precise guanine residue deleted cannot be determined as there are normally six consecutive guanine residues from aminoacids (a.a.) positions 30 to 35, and an equivalent mutation has also been described as 30delG in some studies [138], [141]. Because this mutation is common in several ethnic backgrounds, the six repeating guanine residues may represent a "mutational hotspot" within the Cx26 locus, which may explain the prevalence of this mutation in patients with recessive deafness [142]. Besides 35delG, several other Cx26 recessive mutations have been reported. Mutations might affect the correct trafficking and targeting of connexins to the membrane, as demonstrated for the W77R, V37I, S113R, M163V

and R184P mutations. Affected proteins, in fact, do not reach the plasma membrane and are retained into intracellular compartments [143]. In other cases, e.g. V84L and V95M, mutations occur in domains crucial for the control of channel activity and produce a channel with altered functionality, although the proteins appear correctly targeted to the plasma membrane [144], [145, 146]. One well-characterized example of dominant non-syndromic deafness was attributed to a G-to-C transition that resulted in a tryptophan-to-cysteine substitution at a.a. position 44 (W44C) [147]. Functional analysis of this mutant revealed the inability of W44C mutant channels to allow passage of the fluorescent dye Lucifer Yellow when expressed in HeLa cells [143]. W44C also altered channel activity, when coexpressed with wild-type Cx26 [143]. Additional examples of dominant non-syndromic deafness caused by Cx26 mutations are R143Q and C202F. The R143Q mutant affects a highly conserved residue within the third transmembrane domain of Cx26 [148], whereas the C202F mutation occurs in the fourth transmembrane domain of Cx26 and patients with this mutation exhibited a later onset of hearing loss, with effects becoming evident between 10 and 20 years of age [149]. Cx26 colocalizes with Cx30 between supporting cells, in the spiral limbus, the spiral ligament and the stria vascularis, where they may form heteromeric connexons [1], [2].

Cx30 is also found in adult mouse brain and skin [150], is encoded by *GJB6* (which maps to 13q12) and its a.a. sequence shares 77% identity with that of Cx26 [151]. In addition to Cx26 and Cx30, several other connexins are known to be expressed in the inner ear. To date, only a single dominant mutation in *GJB6* has been associated with a rare variant of non-syndromic hearing loss. Replacement of threonine by methionine (T5M) occurs at the amino-terminal end of Cx30 and *in vitro* studies demonstrated the functional impairment of homomeric-homotypic channels formed by the mutant protein, despite normal assembly into gap junctional plaques [121, 152]. Rare deletions in *GJB6* have been identified and supposed to cause autosomal recessive DFNA1 [153], [154].

The physiological role of connexin in the inner ear was studied by Anselmi et al., 2008. The intracellular calcium signals (ICS) propagation was triggered by the

release of ATP. In the inner, ATP ear acts as an IP_3-generating agonist and evokes Ca^{2+} responses that have been linked to noise-induced hearing loss and development of hair cell-afferent synapses. Studies using knock mice for P2X7 receptor or pannexin-1 have conclusively demonstrated that connexin 26 and 30 play a dual role in the ICS of inner ear: as hemichannels, they promote ATP release, sustaining long-range ICS propagation; as GJ channels, they allow diffusion of Ca^{2+}-mobilizing second messengers across coupled cells (**Figure 9**).

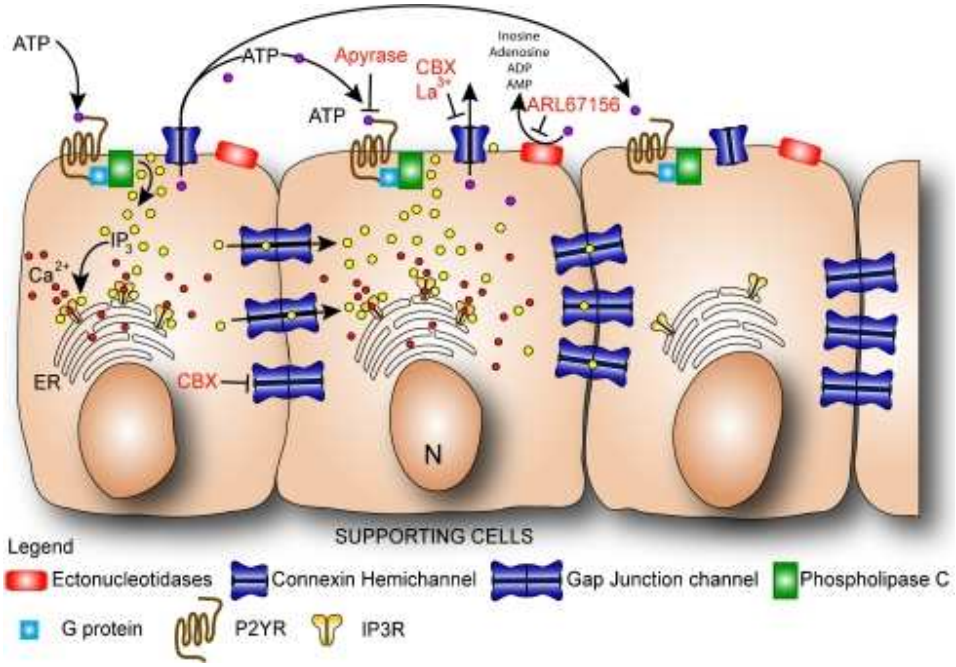

Figure 9. Schematic representation of ICS propagation across the network of GJ coupled cochlear supporting and epithelial cells. CBX, carbenoxolone, is a non-specific inhibitor of connexin hemichannels and GJ channels [155]; ARL67156, 6-N,N-diethyl-D-β-ydibromomethylene adenosine tri-phosphate, originally named FPL 67156, is a commercially available inhibitor of ecto-ATPases [156]. Apyrase is an enzyme that catalyzes the hydrolysis of ATP to yield AMP and inorganic phosphate [157], [158]. La^{3+} is a blocker of connexin hemichannels [159] that does not affect GJ channels when applied extracellularly to cochlear cultures [160]. P2YR, G-protein coupled P2Y receptor; IP_3R, receptor for inositol 1,4,5-trisphosphate (also commonly known as triphosphoinositol, abbreviated $InsP_3$ or IP_3). Scheme modified from Majumder et al., 2010 [65].

Data supporting these notions were identified using organotypic cultures obtained from P5-P6 mice. Photostimulating the lesser ephitelial ridge (LER) with caged

inositol (3,4,5) tri-phosphate (IP_3) resulted in transfer of ICS in the lateral direction, from LER cells to greater epithelial ridge (GER) cells across the hair cell region (HCR) of medial and basal cochlear turns (CTs). The photostimulation of the greater epithelial ridge (LER) with caged IP3 resulted in ICS transfer mostly in the basal turn. In vitro, the LER cells displayed impressive rhythmic activity with oscillations of cytosolic free Ca^{2+} concentration ($[Ca^{2+}]_i$) coordinated by the propagation of Ca^{2+} wavefronts sweeping repeatedly through the same tissue area along the coiling axis of the cochlea. Oscillations evoked by uncaging IP_3 or by applying ATP differed greatly, by as much as one order of magnitude, in frequency and waveform rise time. ICS evoked by direct application of ATP propagated along convoluted cellular paths in the LER, which often branched and changed dynamically over time. These data shows that functional maturation of the cochlea requires differentiation and proper organization of non-sensory cells in the organ of Corti and cochlear lateral wall and the acquisition and maturation of mechanoelectrical transduction in hair cells occur in a gradient from the base to the apex of the cochlea, with IHCs differentiating prior to OHCs [161]. The release of ATP is more prominent in the GER region, especially from the basal to apical portion [65].

The connexin 26 and 30 expression follows up the Organ of Corti maturation, been expressed strongly from basal to apex, with homogeneous expression in the GER region. In early postnatal stage, the GER region hosts a uniform population of tall columnar cells. These transient cells are replaced by cuboidal cells as GER is retracted and the proper inner sulcus becomes clearly defined in the mature OoC.

Knockout and knockin animals are key tools to understand the physiopathology of GJB genes. The Cx30 T5M (Threonine methionine residue in the N-terminus 5) knock in mouse expressed the human mutation associated with prelingual non-syndromic deafness. Unfortunately the mouse model expresses a mild phenotype compared to human, with middle/high-frequency hearing loss, which means a significant increase in the hearing thresholds of about 15 dB at all frequencies. The western blot analysis showed significantly down-regulated the expression levels of Cx26 and Cx30 in adult mice. The transfer of the fluorescent tracer calcein

between cochlear non-sensory cells was reduced, as was intercellular Ca^{2+} signalling due to spontaneous ATP release from connexin hemichannels [4]. Another mouse model, Cx26S17F conditional knockin mouse, in heterozygosis shows similar phenotype of the human disease. The heterozygous mice show hyperplasia of tail and foot epidermis, wounded tails and annular tail restrictions, and are smaller than their wild-type littermates. Analyses of auditory brainstem responses (ABRs)

indicate an ~35 dB increased hearing threshold in these mice, which is likely due

to the reduction of the endocochlear potential by 20-40%. The Cx26S17F protein does not form functional gap junction channels or hemichannels, alters epidermal proliferation and differentiation. In the inner ear, reduced intercellular coupling by heteromeric channels composed of Cx26S17F and Cx30 could contribute to hearing impairment in heterozygous mice, while remaining wild-type Cx26 may be sufficient to stabilize Cx30 and partially maintain cochlear homeostasis [162].

Ortolano et al., 2008 provided strong evidence for the importance of coordination between Cx26 and Cx30 expresion. The expression of Cx26 was strongly downregulated in Cx30 knockout animals at transcriptional and protein level in LER cells. Overexpression of Cx30 on Cx30ko mice by bovine adeno associated gene transduction restores the Cx26 expression. Recombinant gap junction channels were functional, leading to a rescue of cell-cell coupling and ICS propagation. The ablation of Cx26 by transduction of $Cx26^{loxP/loxP}$ cultures with a Cre recombinase vector caused the Cx30 downregulation and ICS failure. This coordinated regulation of Cx26 and Cx30 expression appears to occur as a result of signaling through PLC and the NF-kB pathway. Application of ATP in Cx30ko cochlear cultures resulted in increased Cx26 transcript.

Targeting ablation of inner ear connexins

Gene targeting of connexins in mice has provided new insights into connexin function and the significance of connexin diversity [163]. Complete removal of the Cx26 gene results in neonatal lethality, thereby preventing analysis of its function in hearing [164]. This limitation was overcome through the generation of a cochlear specific knockout of Cx26 using the Cre–*loxP* system [51], successfully deleting Cx26 in the epithelial gap junction network without affecting Cx26 expression in other organs. Animals with this deletion are a model of recessive deafness and displayed normal patterns of cochlear development, but showed an increase in postnatal cell death within the cochlea along with significant hearing loss. The initiation of cell death was found to occur in supporting cells surrounding IHCs (i.e. inner phalangeal and border cells), and coincided with the onset of audition. It was hypothesized that loss of Cx26 prevented recycling of K+ after sound stimulation, and that elevated K+ in the extracellular perilymph inhibited uptake of the neurotransmitter glutamate, which accumulated and resulted in cell death [51]. While the evidence concerning Cx26 is compelling, this hypothesis becomes more complex when considering the activity of Cx30 in the inner ear. Lautermann *et al*. [165] have shown that Cx26 and Cx30 normally colocalize within the cochlea, and tissue-specific deletion of the Cx26 gene did not alter expression patterns of Cx30 [51]. This observation complicates the role of gap junctional disfunction in the onset of deafness due to the fact that Cx30 passes K+ in an efficient manner [166] but could not prevent hearing loss in the absence of Cx26. Thus, the presence of a single type of connexin with similar ionic selectivity was unable to rescue the phenotype observed in these mice. Similar to the tissue-specific loss of Cx26, deletion of Cx30 in mice resulted in hearing loss, but did not alter the development of the inner ear [52]. Although development was normal, Cx30 knockouts lacked the EP, but maintained the normal [K^+] of the endolymph. In addition, Cx30 knockouts also presented increased apoptosis within the cochlear sensory epithelium. Deletion of Cx30 did not alter the cochlear Cx26 expression in adult mice [52], but in cochlear organotypic cultures Cx26 levels were downregulated in the supporting cells of the OoC [3]. The loss of both Cxs before the onset of

hearing altered biochemical coupling in the OoC, as ICS and ATP signaling were inhibited [160], thus affecting correct tissue development.

Gene delivery in the mouse inner ear

Molecular therapy could be a good alternative to acoustic prosthesis in case of hereditary deafness. It could be actuated early in the postnatal period and permit the acquisition of normal speech ability. The idea is to introduce in the inner ear a normal protein, to compensate for a mutant one. Several are the proteins whose mutations cause deafness, expressed in the different compartment of the ear. Murine deafness models help to understand the mechanisms at the basis of hearing impairment, but are also fundamental to approach to gene therapy to be applied, in a future, to humans.

Delivery techniques are the same commonly used in otolaryngology in humans, for the great similarity between murine and human inner ear anatomy (**Figure 10**).

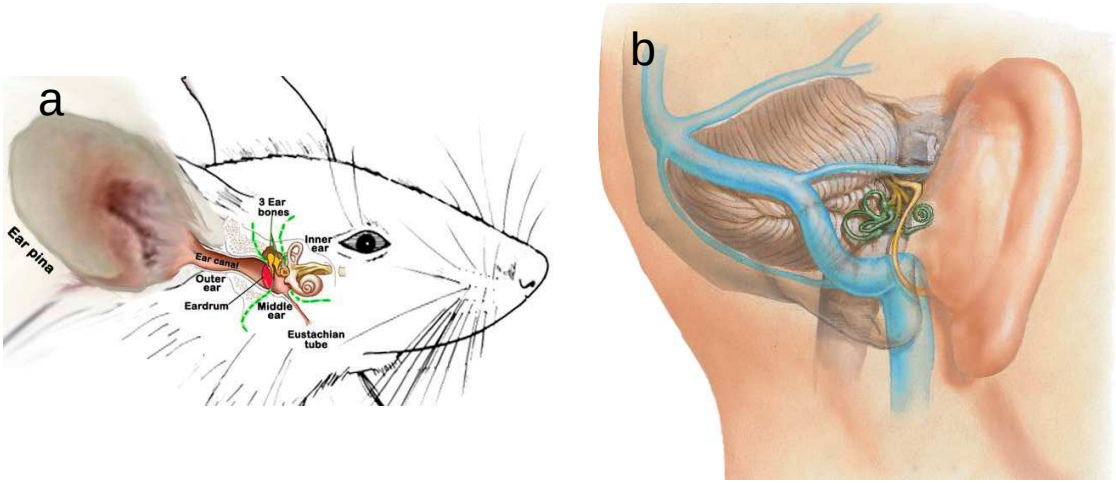

Figure 10. Murine (a) and human (b) inner ear localization.

These approaches include delivery directly in the cochlea or in the vestibular system. In the first case, instillation is performed through an intact round window membrane with a gelatin sponge or a direct injection through the round window membrane; or by infusion with pump through cochleostomy [167]. [168]. Unfortunately, these techniques damage the inner ear, altering auditory function

[169]. Moreover, the presence of a different structure, called *bulla*, that surrounds the murine cochlea and that is not present in humans, makes these surgeries a little more industrious and invasive. More recent findings, vestibular approaches were identified as more appropriate to maintain unaltered physiology of the inner ear [170]. Introduction of drugs, in that way, could be done through the uticulus or through one of the semicircular canals [170], in both cases without affecting hearing. Also, at least for mice, electroporation *in utero* can be actuated in embryo, immediately after the otic capsule appearance [171]. But this technique is very difficult and the risk of mortality for the dam or embryos is very high.

Several particles have been used in the attempt to optimize gene expression. Vectors successfully studied *in vivo* include cationic liposomes, adeno-associated virus, adenovirus, lentivirus, herpes simplex virus and vaccinia virus. Most of these are viral vectors, highly pathogenic for humans, and considered immunologically active, although modified to make them safer. Moreover, virus such as lentivirus transduce efficiently nervous cells. For a gene therapy focused on connexins, it is necessary a vector whose tropism is specific for supporting cells of the inner ear.

In 2004 a new vector was cloned and characterized, a bovine adeno-associated virus (BAAV) [172], that has been used in cochlear cultures from Cx30ko mice to restore connexins channels activity [3]. The transduction of this virus occurred mainly in connexins expressing cells. *In vivo*, in the cochlea, the vector was used to transduce supporting cells of guinea pig cochlea [173] and, in rat culture, neuroepithelial cells [174].

MATHERIALS AND METHODS

Transgenic Mice and Genotyping

The background strains of the transgenic mice used in this study are as follows: Cx30 KO [52], mixed C57BL/6 and 129/Ola; Cx26$^{loxP/loxP}$ [51] mixed C57BL/6 and 129/SvPasCrl; Sox10-CRE [175], mixed BL6CBAF1 and 129/ Sv. Genotyping for Cx30 KO [52] was performed by standard PCR on extracted mouse tail tips. Primer pairs were specific for the WT alleles. Thus, the primers for Cx30 were as follows: Cx30F, 5´-GGTACCTTCTACTAATTAGCTTGG-3´; and Cx30R, 5´-AGGTGGTACCCATTGTAGAGGAAG- 3´. To visualize the deletion, primers specific for the *lacZ* region (which flanks the deleted allele) were used in combination with the corresponding WT forward primer: Cx30lac, 5´-AGCGAGTAACAACCCGTCGGATTC-3´. Targeted ablation of Cx26 in the otic capsule was achieved by crossing Cx26$^{loxP/loxP}$ mice [51] with Sox10-Cre mice [175, 176]. Double transgenic mice were detected by screening for the presence of the two insertions, *loxP* and *Cre*, by PCR on extracted mouse tail tips by using the following primers (see supplementary materials in ref. [51]): Cx26F, 5´-CTTTCCAATGCTGGTGGAGTG-3´; Cx26R, 5´-ACAGAAATGTGTTGGTGATGG-3´; CreF, 5´-CTAAACATGCTTCATCGTCGGTCCG-3´; and CreR, 5´-CGTAACAGGGTGTTATAAGCAATC-3´. Animal handling was approved by the Committee for Animal Care and Use of the University of Padua, Italy.

Molecular cloning

The coding region of wild-type CMVmCx26, CMVmCx30, GFAPmCX26 and GFAPmCx30 were amplified from constructs available in the laboratory using oligonucleotide primers to introduce the desired restriction enzyme sites at the 5′ and 3′ termini of the desired sequence. The following primers were used:

CMVmCx26for: 5’-CGTGAGCTCTAGTAATCAATTACGGGG -3’

CMVmCx30rev:5’- GGCAAGCTTTTAACTTGGGAAACTTGTG-3’

GFAPmCX26for:5’- CGTGAGCTCTAGTAATCAATTACGGGG -3’

GFAPmCx30rev: 5’- GGCAAGCTTTTAGACTGGTCTTTTGGAC -3’

which introduced SacI–HindIII sites.

The resulting PCR products were digested with the two enzymes and ligated into the respective sites of PDT1.1 followed by transformation into *Escherichia coli* (TOP10). Mini plasmid preparation and restriction enzyme analysis were performed to identify positive clones. All constructs were sequenced using the Dye Terminator (Perkin–Elmer, Wellesley, MA), as recommended by the manufacturer, to verify that PCR amplification did not introduce mutations.

BAAV Production and Quantification

Semiconfluent 293T cells were transfected by calcium phosphate with four required plasmids (transgene vector, pAd12, and bovine adeno-associated virus (BAAV) AAV2-Rep plus BAAV-Cap). In the case of BAAVCx26, AAV-2 inverted terminal repeats (ITRs) were used in the vector plasmid. Forty-eight hours after transduction, cells were harvested by scraping in harvesting buffer (140 mM NaCl, 5 mM KCl, 0.7 mM K2HPO4, 25 mM Tris-HCl, pH 7.4) and the cell pellet was concentrated by low-speed centrifugation. Cells were lysed in harvesting buffer containing 0.5% deoxycholate and 100 U/ml DNase (Benzonase; Sigma) and incubated for 30 min at 37℃. Following 10 min of l ow-speed centrifugation, the vector was purified using CsCl gradients. Particle titers were determined by qPCR, and biological activity was tested on packaging cells, as previously described [177]. For viral titration, a dilution of the viral preparation was added to a PCR mixture containing 1X SYBR Green Master Mix (Applied Biosystems/Applera) and 0.25 pmol/µl forward and reverse primers. Amplification was measured using a sequence detector (ABI 7700; Applied Biosystems). Specific primers for CMV were designed with the Primer Express program (Applied Biosystems): CMV forward 5´-

CATCTACGTATTAGTCATCGCTATTACCAT-3´ CMV reverse 5´-TGGAAATCCCCGTGAGTCA-3´. Following denaturation at 96℃ for 10 min, cycling conditions were 96℃ for 15 sec and 60℃ fo r 1 min for 40 cycles. The viral DNA in each sample was quantified by comparing the fluorescence profiles with a set of DNA standards. The AAV particle titers were in the range of 10^{12}-10^{13} particles/ml.

Quantitative PCR (qPCR) of mRNA

mRNA was extracted from freshly isolated P5 whole cochleae or microdissected LER cells using RNAeasy kit (Qiagen). The same procedure was applied to organotypic cultures 48 h after *in vitro* transduction with BAAV constructs. cDNA was obtained by reverse transcription of mRNA with Oligo$(dT)_{12}$-18 (Invitrogen) and Omniscript Reverse Transcriptase (Qiagen) for 1 h at 37 ℃. qPCR was performed on cDNA (obtained as described previously) to amplify Cx26 and Cx30 and was normalized to GADPH expression. Connexin expression relative to GADPH was estimated according to the method described by Pfaffl [178]. Amplification was carried out using SYBER Green (Applied Biosystems) on the ABI 7700 sequence detection system equipped with ABI Prism 7700 SDS software (Applied Biosystems) through the following amplification cycles: 50℃: 2', 95℃: 10', 95℃: 15', 60℃: 1' (40 cycles). Primers used are as follows:

Cx26f: 5'- TCACAGAGCTGTGCTATTTG- 3'

Cx26r: 5'- ACTGGTCTTTTGGACTTTCC- 3'

Cx30f: 5'- GGCCGAGTTGTGTTACCTGCT- 3'

Cx30r:5'- TCTCTTTCAGGGCATGGTTGG- 3'

GADPHf: 5'- TTGGGTACACTACACTGAGGACC- 3'

GADPHr: 5'- TTGAGAGCAATGCCAGCCC- 3'

Anaesthesia in adult and in P4 mice

To record auditory brainstem responses and perform canalostomy, adult mice were anaesthetized with an intraperitoneal injection of zolazepram (25 mg/g) and xylazine (10 mg/g). For Canalostomy in P4 pups, doses are Xilor 0,45 µg/g and Zoletil100 0,15 µg/g, diluted in physiological solution. Supplemental doses were administered as needed. To measure endocochlear potential, mice were anaesthetized with 0.01 ml/g body weight of 20% urethane. During all surgical procedures, the body temperature was kept at 38℃ by a feedback-controlled heating pad.

In vivo recordings of endocochlear potential (EP) and auditory brainstem responses (ABR)

These recordings were performed in mice $Cx26^{loxP/loxP}$ and $Cx26^{Sox10Cre}$ **,** aged between P18 and P90, or 4 weeks after surgery. For EP, after induction of anesthesia, a tracheal cannula was inserted and the bulla opened to reveal the cochlea. A small hole was made in the bony wall of the cochlea over the basal turn scala media, and a micropipette electrode filled with 150 mM KCl was advanced through the hole and through the spiral ligament of the lateral wall into the scala media. The potential difference between the scala media and a reference silver/silver chloride pellet under the dorsal skin was recorded [179]. To record ABR, mice were anaesthetized and submitted to acoustic stimuli. Each recording procedure lasted up to 70 min. Acoustic stimuli were produced in the free field within a foam-padded, shielded acoustic chamber by a System 3 Real-time Signal Processing System combined with an ES1 electrostatic speaker (Tucker-Davis Technologies, Alachua, FL, USA) positioned 4 cm lateral to the left ear of the mouse [180]. Stimuli were calibrated by means of an ECM8000 measurement microphone (Behringer International GmbH, Willich, Germany), mounted on the

800B Larson-Davis sound level meter and placed in the position to be occupied by the mouse ear. Stimuli consisted of tone bursts (1 ms rise/decay; 3 ms plateau) at 8, 14, 20, 26 and 32 kHz, and clicks (0.1 ms) delivered at a repetition rate of 13 Hz. A maximum peak equivalent sound pressure level (SPL) of 100 dB (re: 20 mPa) was employed for clicks as well as tone bursts. Decreasing SPLs of 10 dB were employed, starting from a maximum of 100 dB SPL. To minimize contralateral acoustic stimulation, the outer ear canal of the right ear was filled with condensation vulcanizing silicone mixed with hardener paste (Otoform A flex, in double cartridges; Dreve Otoplastik, Unna, Germany) delivered through a mixing canulas (diameter 5.4 mm) and dispensed by an injector (DS50; Dreve Otoplastik). Acquisition and analysis time was 12 ms for each single stimulus. Responses were recorded between subcutaneous needle electrodes inserted at the vertex (active), ventrolateral to the left ear (reference) and above the tail (ground). Potential differences were amplified (50 000×) with an isolated instrumentation amplifier, band-pass-filtered below 100 Hz and above 8000 Hz and digitized at a rate of 40 000 samples per second. Response waveforms were typically obtained from averages of 400 stimuli presented at the rate of 13 per second for each stimulus condition, saved in the non-volatile memory of a computer and finally displayed on a computer screen.

Analysis of auditory brainstem responses

Lab WIEW software (version 8.0.1; National Instruments, Austin, TX, USA) was used for measurements and analysis of amplitude and latency of auditory brainstem responses. To reduce noise and abrupt transitions in the temporal domain, traces were smoothed digitally by low-pass finite-impulse response filtering with equi-ripple characteristics using the Parks–McClellan algorithm. Low-pass frequency was fixed two octaves below the original sampling frequency. For quality control, the smoothed trace was checked against the original trace on the computer display. Wave amplitudes were calculated by a peak detection algorithm as the difference between the two values represented by response maxima (peak)

and minima (valley). The algorithm fitted a quadratic polynomial curve to sequential groups of data points (the number of data points used in the fit was 3). Peak latencies were determined relative to the onset of the acoustic stimulus. Wave IV was the most stable and robust evoked response at all intensity levels and for all types of stimulus. The corresponding peak was therefore utilized to estimate auditory brainstem response threshold, defined as the lowest SPL at which any peak could be detected above the residual noise by an experimentally experienced observer blind with respect to genotype. If no wave was detected at maximum intensity stimulation, a nominal threshold of 110 dB SPL was assigned. If any wave was detected at the minimum intensity stimulation of 1 or 10 dB SPL, a nominal threshold of the same level was assigned. Stimuli of lower intensities were not applied due to intrinsic limitations of the sound delivery system.

Canalostomy in posterior semicircular canal of adult mice

After induction of anaesthesia, mice were moved to the injection setup, under a dissection microscope (**Figure 11)**. Mouse head was maintained still by a muzzle-holder. A dorsal post-auricular approach allowed exposure of the posterior semicircular canal (PSC). A hole was made with the tip of a 33G needle, softly removing a part of the bony shell of the canal. A microsyringe with a 35G needle was slowly approached to break the membraneous PSC and access the endolymphatic space. The microsyringe movements are leaded by a micromanipulator. A drop of dentary cement was used to seal and avoid leakage of liquid. Then, 2µl WGA or bromophenol blue diluted in artificial endolymph (Marcus et al.) were injected at 3 nl/sec. Injection parameters were controlled by a micropump. Ten minutes after injection, the needle was slowly removed and the hole was closed with dentary cement.

Canalostomy in lateral semicircular canal of P4 mice

Mice were prepared as above, and mantained still by a piece of adhesive tape. A dorsal post-auricular approach allowed exposure of the lateral semicircular canal (LSC). A microsyringe with a 36G needle was slowly approached to make a hole in the PSC and access the endolymphatic space. The microsyringe movements are leaded by a micromanipulator. One microliter of dye solution diluted in artificial endolymph were injected at 3 nl/sec. Injection parameters were controlled by a micropump. After surgery, a solution of NaCl/Glucose was subcutaneously administered and pups grew with a step mother.

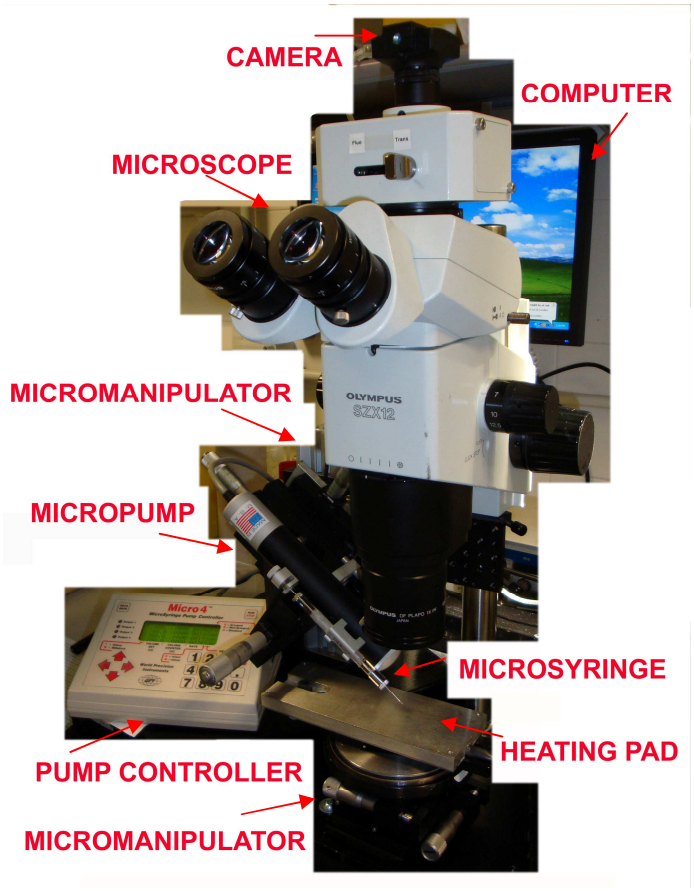

Figure 11. Setup for canalostomy.

Preparation of cochlear organotypic cultures

Cochleae were dissected from P5 mouse pups in ice-cold HEPES-buffered (10 mM, pH 7.2) Hanks' balanced salt solutions (Sigma, Milan) and placed onto glass cover slips coated with 136 mg/ml of Cell Tak (Becton Dickinson, Milan, Italy). Cultures were incubated in Dulbecco's modified Eagle's medium/F12 (Invitrogen, Leek, The Netherlands), supplemented with FBS 5% and maintained at 37℃ for 1 day.

Transduction of cochlear cultures with BAAV

Transduction of cochlear cultures with viral constructs was performed by adding purified vector at a final titer of 10^{11} particles/ml in culture medium devoid of FBS; cultures were kept in this medium at 37 ℃ for the first 24 h to favor viral transduction. Thereafter, cultures were maintained in DMEM/F12 supplemented with FBS up to 48 h before experiments.

Preparation of cochlear transversal sections for immunofluorescence

Cochleae were dissected from mice at different time points (P5- P9- P14- P30), fixed in 4% paraformaldehyde and decalcified overnight in ethylenediaminetetraacetic acid (0.3 M). After three washes in phosphate buffered saline (PBS), preparations were included in 3% agarose dissolved in PBS and cut perpendicularly to the modiolar axis in 100 µm thickness steps using a vibratome (VT 1000S; Leica Mikrosysteme Vertrieb GmbH, Wetzlar, Germany) set at speed 6 and frequency 6 (both on a scale of 10) and equipped with double-edge razor blades (Platinum, Gillette).

Immunohistochemistry and confocal imaging

Tissues were fixed in 4% paraformaldehyde for 20 min at room temperature and rinsed in PBS containing 2% bovine serum albumin (rinse solution). Cultures were permeabilized for 1 h at room temperature with 0.1% Triton X-100, dissolved in the rinse solution, whereas transverse slices were permeabilized for 3 h. In both preparations, Cx26 or Cx30 were immunolabelled by overnight incubation at 4℃ with specific polyclonal rabbit antibodies anti-Cx26 (Invitrogen, Leek, Cat. No. 51-2800) and anti Cx30 (Invitrogen, Cat. No. 71-2200) diluted in the rinse solution (2.5 mg/ml). Primary antibodies were omitted in negative controls. Cultures were then washed three times in PBS (5 min each time), whereas transverse slices were washed for 1 h each time. For cultures, secondary antibodies (Alexa Fluorw 488 goat anti-rabbit IgG, Invitrogen, Cat. No. A-11008) were applied at 5 mg/ml for 1 h at room temperature, while F-Actin was stained by incubation with Texas red-X phalloidin (Invitrogen, Cat. No. T7471) and nuclei were stained with 4′,6-diamidino-2-phenylindole, dihydrochloride (DAPI; Invitrogen, Cat. No. D1306), both diluted in the rinse solution (1:200). For transverse slices, incubation periods were extended to overnight. After washing for further three times in PBS, samples were mounted onto glass slides with a mounting medium (FluorSaveTM Reagent; Merk, Cat. No. 345789) and analysed using a confocal microscope (TCS SP5; Leica) equipped with an oil-immersion objective (either 40× HCX PL APO 1.25 N.A. or 63× HCX PL APO 1.4 N.A.; Leica). Alexa Fluorw 488 was excited by the 488 nm line of an air-cooled argon-ion laser (225 mW, Series 800; National Laser Company, UT, USA) and its fluorescence emission was recorded in a spectral window between 495 and 540 nm. Texas red was excited by the 561 nm line of a diode-pumped solid-state laser (10 mW, Model YLK 6110T, LasNova 60 yellow series 60; LASOS Lasertechnik GmbH, Jena, Germany) and its emission was collected between 600 and 690 nm. DAPI was excited by the 405 nm line of a diode laser module (50 mW, Radius 405-50; Coherent Inc., CA, USA) and its emission was collected between 410 and 440 nm. Laser line intensities and detector gains were carefully adjusted to minimize spectral bleed-through artifacts.

Calcein measurements and fluorescence recovery after Photobleaching

Focal irradiation of live cochlear cultures was used to photobleach calcein, as described previously [3, 65, 160]. Calcein is a polyanionic fluorescein derivative that exhibits fluorescence essentially independent of pH between 6.5 and 12. It has about six negative and two positive charges at pH 7 (net charge 24, MW 622) and permeates through gap junction channels in the immature organ of Corti [160]. In these experiments, the output of a TTL-controlled semiconductor laser module (or 50 mW, 405 nm, part number LGT 405-60, LG-Laser Technologies GmbH, Kleinostheim, Germany) was injected into a UV-permissive fibre-optic cable (single mode 0.1 N.A., mode field diameter 3.2+0.5 mm, part number P1-405A-FC-2; Thorlabs GmbH, Dachau, Germany); fibre output was collected through a collimating aspheric lens (5 mm effective focal length, part number HPUCO-23AS-6.2AS; LG-Laser Technologies GmbH), and the recollimated beam was directed onto a dichromatic mirror (440 dclp; Chroma Technology Corp., Bellows Falls, VT, USA) placed at 458 just above the objective lens of the microscope. By carefully adjusting the position of the fibre in front of the aspheric lens with a two-axis micromanipulator (part number HPT1, Thorlabs), we projected a sharp image of the illuminated fibre core (spot) onto the specimen focal plane selected by the (infinity corrected) objective lens. Under these conditions, the fibre-optic diameter determined accurately the laser-irradiated area, which encompassed one to few cells, depending on cell size and location within the sensory epithelium [65]**.** For staining with calcein, live cultures were incubated for 10 min at 37℃ in EXM (containing 138 mM NaCl, 5 mM KCl, 2 mM CaCl2, 0.3 mM NaH2PO4, 0.4 mM KH2PO4, 10 mM HEPES-NaOH and 6 mM D-glucose, pH 7.2, 320 mOsm) supplemented with 5 mM calcein-AM, plus 250 mM sulphinpyrazone and 0.01 w/v pluronic F-127 to prevent dye sequestration and secretion [181]. For recording, cultures were transferred on the stage of an upright fluorescence microscope (BX51; Olympus Corporation, Tokyo, Japan) and perfused in an EXM for 20 min at 2 ml/min to allow for de-esterification, and thereafter maintained in still EXM at

room temperature. Calcein fluorescence was excited and detected using a U-MGFHQ filter cube (Olympus) incorporating a BP460-480 excitation filter, a DM485HQ dichromatic mirror and a BA495-540HQ barrier (emission) filter. Cultures were imaged with a 60× water immersion objective (0.90 NA, Lumplan FL; Olympus) and fluorescence emission was monitored with a cooled charge-coupled device (CCD) camera (Sensicam QE, PCO AG, Kelheim, Germany). In all experiments, the effects of photobleaching due to sample illumination in the 460–480 nm spectral window were kept under control by carefully selecting the most appropriate inter-frame interval (4 s) while controlling light exposure (50 ms) with a mechanical shutter triggered by the frame-valid (FVAL) signal of the CCD camera. Baseline fluorescence in the 495–540 nm emission window was recorded for 2 min, followed by focal laser irradiation at 405 nm to bleach intracellular calcein. Laser irradiation intervals were adjusted to cause 50% photobleaching of the mean baseline fluorescence, which required 0.5 s for tall columnar cells of the greater epithelial ridge and 1.2 s for non-sensory cell of the lesser epithelial ridge (Fig. 5A). Fluorescence recovery after photobleaching was monitored for up to 10 min. Image sequences were acquired using software developed in the laboratory, stored on disk and processed off-line using the Matlab 7.0 software package (The MathWorks, Inc., Natick, MA, USA). For the analysis of fluorescence recovery after photobleaching, we delineated a region of interest (ROI) inside the bleached (b) area, plus an ROI in a proximal unbleached (u) area, and we computed the ratios of fluorescence intensities (fb/fu) at each time point, as described in Ortolano et al.[3], Anselmi et al. [160] and Majumder et al. [65].

RESULTS

A new mouse model for deafness: Cx26^{Sox10Cre}

Loss of connexin 26 in mammary epithelium during early pregnancy results in unscheduled apoptosis and impaired development [182]. For this reason, connexin26 full knockout mice present a lethal phenotype. Thus, studies for Cx26 function require a set of conditional knock out mice, whose deletion for Cx26 can be controlled and be specific for different tissues. Here, we concentrated on characterizing a novel conditional Cx26 null mouse model, Cx26^{Sox10Cre} [160]. These double transgenic mice are the result of the mating between Cx26$^{loxP/loxP}$ mice, carrying the floxed Cx26 [51], and Sox10Cre mice, which express a Cre recombinase under the Sox10 promoter [175] (**Figure 12**). Cx26 gene will be ablated in cells that express the Sox10 gene, *i.e.* cells deriving from the neural crest, and otic vesicle [183]. Of note, Cre recombinase transmitted via maternal germline will be activated only in Sox10-expressing cells, obliterating Cx26 gene only in these specific cells, whereas transmission via paternal germline will allow an early Cre activation in the whole embryo, deleting Cx26 in all cells, thus leading to embryos death.

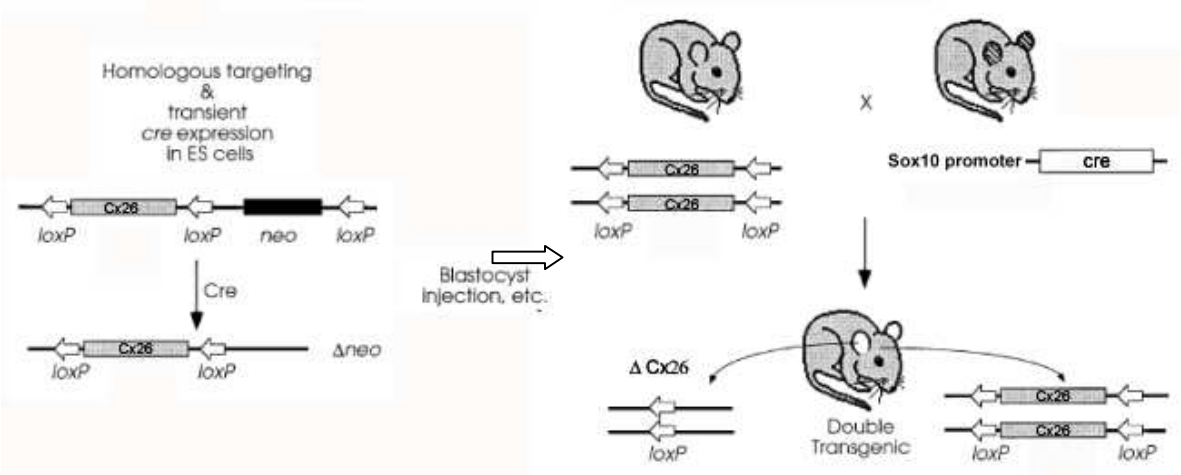

Figure 12. Conditional gene ablation by Cre recombinase (adapted from Sauer B., Methods, 1998 [184]).

Hearing impairment in Cx26^{Sox10Cre} mice

Hearing in Cx26$^{loxP/loxP}$ and Cx26^{Sox10Cre} mice was quantified by recording auditory brainstem responses, which are electrical signals evoked from the brainstem following the presentation of sound stimuli (**Figure 13a**). We measured the IV wave ABR thresholds for click and tone burst (8-14-20-26-32 kHz) stimuli in twelve Cx26$^{loxP/loxP}$ and in twelve Cx26^{Sox10Cre} mice, aged between P29 and P64 (**Figure 13b**). Compared to Cx26$^{loxP/loxP}$ mice, elevated hearing thresholds were found in Cx26^{Sox10Cre} mice for tone bursts at all frequencies, as well as for click stimuli, with a significant differences compared to wild type siblings ($p < 0.001$, ANOVA). Similar results were obtained from Connexin30 knockout mice (Cx30ko), whose hearing thresholds were dramatically reduced at all frequencies [4, 52] . EP recordings (**Figure 13c**) revealed a significant reduction ($P < 0.001$, ANOVA) of endocochlear potential (38 ± 2 mV for Cx26^{Sox10Cre} mice; 109 ± 3 mV for wild type siblings). For comparison, EP recordings from Cx30 ko mice yielded values around 4 mV [4], [52].

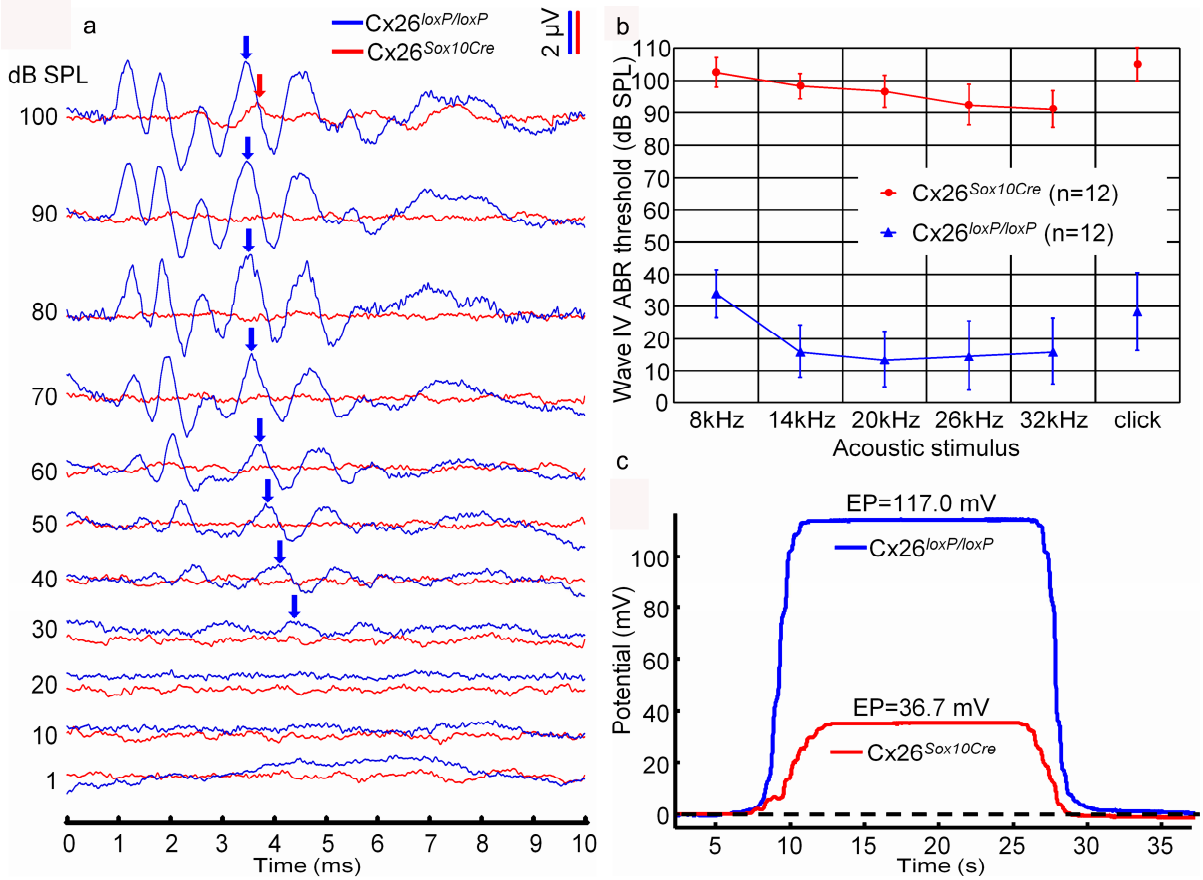

Figure 13. In vivo recordings from Cx26$^{loxP/loxP}$ and Cx26^{Sox10Cre} mice. (a) Representative ABR recordings in response to 14 kHz tone burst stimuli obtained from Cx26$^{loxP/loxP}$ (P32, blue line) and Cx26^{Sox10Cre} (P39, red line) mice. Note that in Cx26$^{loxP/loxP}$ mouse waves II, IV and V were detected down to 30 dB SPL, while in Cx26^{Sox10Cre} mouse no evoked responses were identified for intensities lower than 100 dB SPL. **(b)** ABR audiograms for tone bursts at 8-14-20-26-32 kHz and for click obtained from Cx26$^{loxP/loxP}$ (blue line, n=12) and in Cx26^{Sox10Cre} (red line, n=12) mice, aged between P29 and P64. Bars represent standard deviation. Note that click responses are plotted at an arbitrary point on the frequency axis (the position does not reflect the frequency content of click stimuli). **(c)** Representative recordings of Endocochlear Potential (EP) obtained from Cx26$^{loxP/loxP}$ (blue line) and Cx26^{Sox10Cre} (red line) mice, aged P38 and P41 respectively. Standards for reliable recording were: 1) stable EP during minimum 10 seconds and 2) a maximum difference of ±2mV between starting and final baseline potentials. EP was about 3 times lower in Cx26^{Sox10Cre} mice compared to Cx26$^{loxP/loxP}$ mice.

Connexin immunolabeling and Organ of Corti degeneration

To characterize connexin expression in Cx26^{Sox10Cre} transgenic mice, we performed immunolabeling with antibodies specific for Cx30 or Cx26 proteins at different time points: P5, P9, P14 and P30 (**Fig. 14, 15, 16**). Control cochleae presented with an increase of connexin expression after hearing onset, around P14, as previously reported [118] (**Fig. 14, 15, 16, panels i-p**). Inner hair cells (IHC) and outer hair cells (OHC) showed no sign of immunoreactivity to Cx26 or Cx30 antibodies, in accord with the notion that sensory cells are not coupled by gap junction to any other cell type in the organ of Corti (OoC). In cochleae from Cx26^{Sox10Cre} mice, Cx26 and Cx30 were still present in the spiral limbus, spiral ligament (**Figure 14, a-h**), as well as basal and intermediate cells of the *stria vascularis* (**Figure 15, a-h**). The latter finding is consistent with the residual EP levels measured in Cx26^{Sox10Cre} mice indicated above (**Figure 13b**). In contrast, Cx26 was not detected in the OoC of Cx26^{Sox10Cre} mice at all time points (**Figure 16, a-d**; corresponding control are shown in **Figure 16, i-l**). Connexin 30 was first downregulated at P5, while at P9 its expression started to raise and was virtually normal around P30 (**Figure 16, e-h**). The tunnel of Corti and the Nuel's space opened up at P9 in controls but not in the Cx26^{Sox10Cre} mice, similar to another conditional Cx26 knockout mouse model [185]. In **Figure 16, e-f**, joint Pillars cells were evident between IHC and OHC. Another striking difference was observed in the basal turn of P30 mutant mice, in which OoC degeneration was evident, affecting not only hair cells, as observed in Cx30 ko mice [186], but also non-sensory cells (**Fig. 15, 16**). The percentage of surviving hair cells was very low in the basal turn, and increased towards the apical turn **(Fig. 17b)**. In particular, cell loss was more pronounced for OHCs than for IHCs.

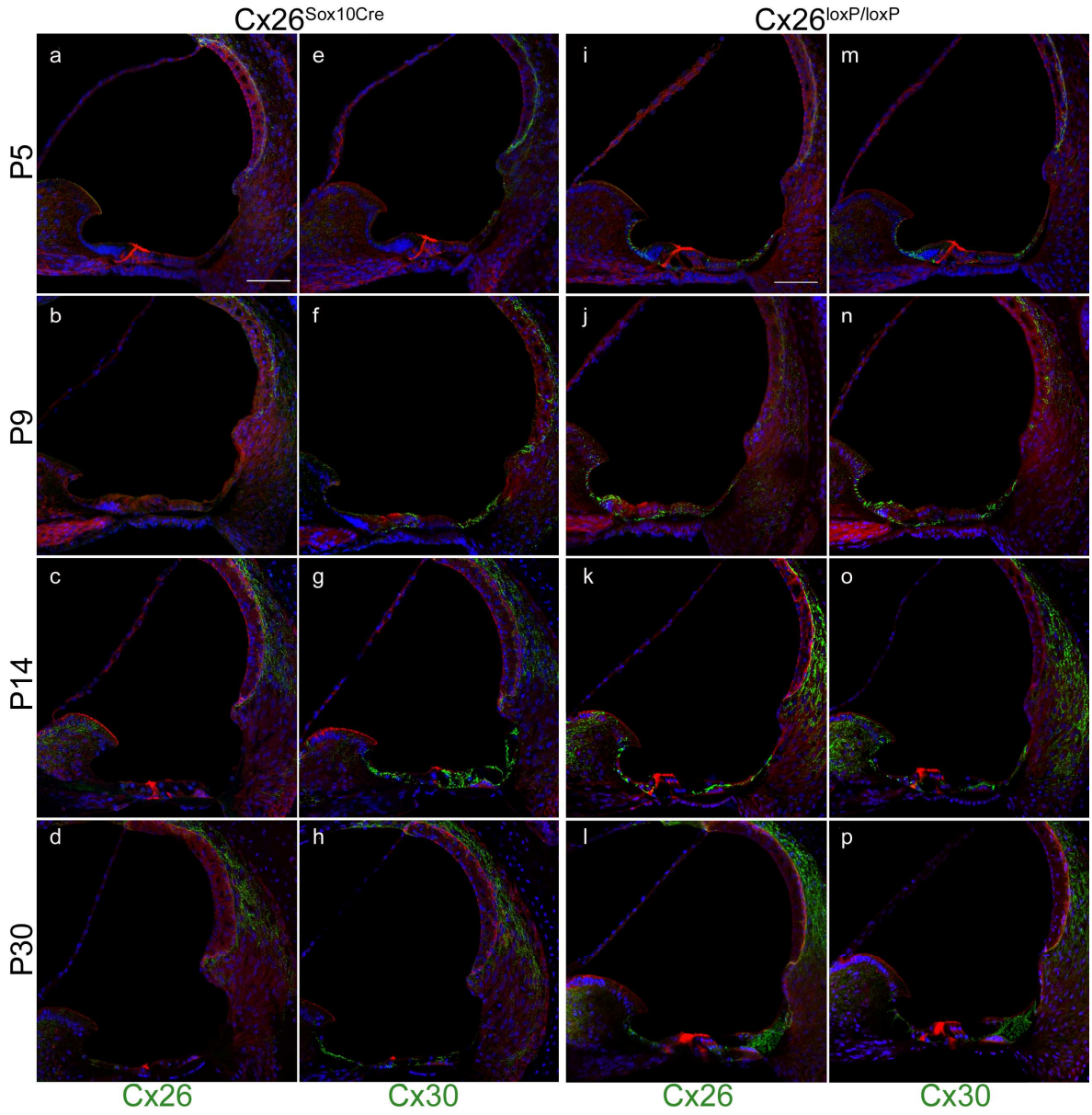

Figure 14. Connexin immunoreactivity in the scala media from Cx26^{Sox10Cre} and Cx26$^{loxP/loxP}$ mice. Maximal projection rendering of two consecutive midmodiolar confocal optical sections, taken at 1 mm intervals in the basal cochlear turn of Cx26^{Sox10Cre} (a- h) and Cx26$^{loxP/loxP}$ (i- p) on P5, P9, P14 and P30. Cx26 and Cx30 expression was analysed with specific antibodies (green), nuclei were stained with DAPI (blue) and actin filaments with Texas red conjugated phalloidin (red). Scale bar, 50 µm.

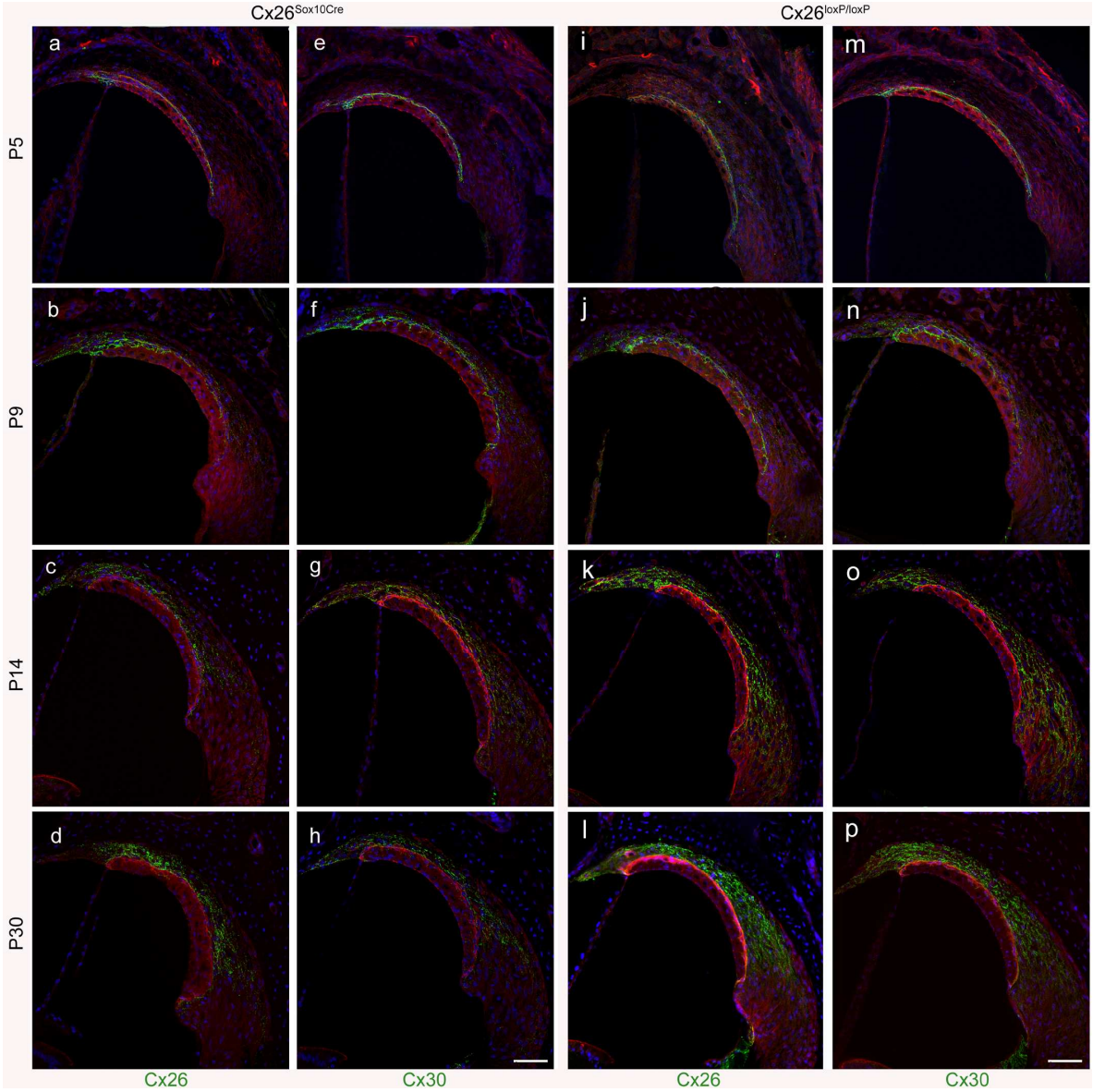

Figure 15. Connexin immunoreactivity in the *stria vascularis* from Cx26^{Sox10Cre} and Cx26$^{loxP/loxP}$ mice. Maximal projection rendering of two consecutive midmodiolar confocal optical sections, taken at 1 mm intervals in the basal cochlear turn of Cx26^{Sox10Cre} (a-h) and Cx26$^{loxP/loxP}$ (i-p) on P5, P9, P14 and P30. Cx26 (a-d, i-l) and Cx30 (e-h, m-p) expression was analysed with selective antibodies (green), nuclei were stained with DAPI (blue) and actin filaments with Texas red conjugated phalloidin (red). Scale bar, 50 µm.

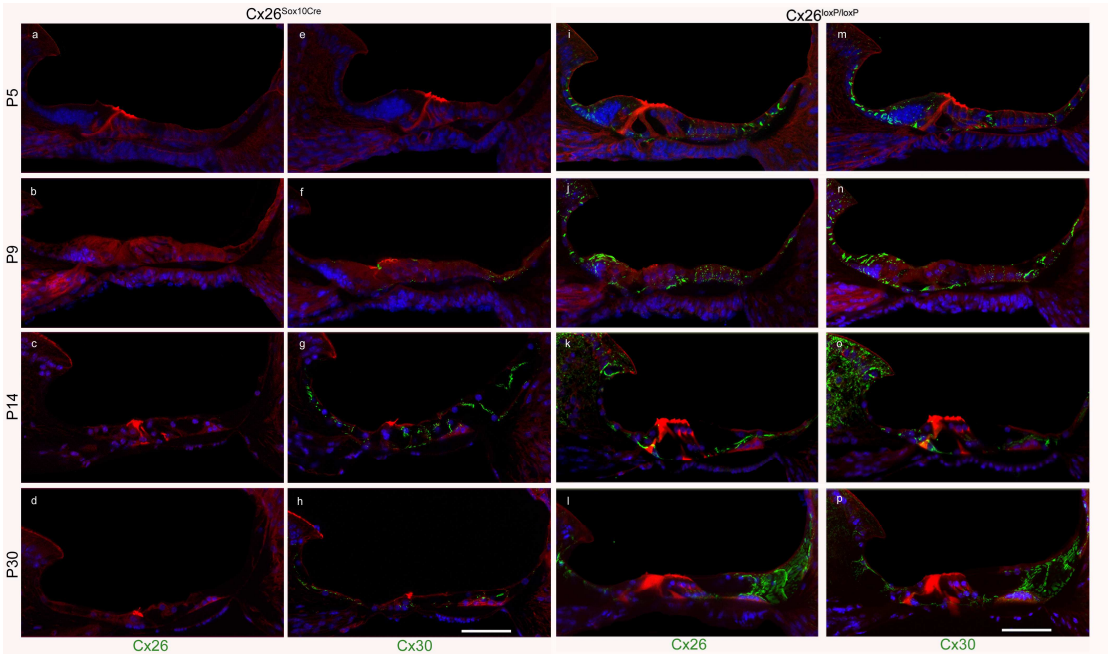

Figure 16. Connexin immunoreactivity in the OoC from Cx26^{Sox10Cre} and Cx26$^{loxP/loxP}$ mice.

Maximal projection rendering of two consecutive midmodiolar confocal optical sections, taken at 1µm intervals in the basal cochlear turn of Cx26^{Sox10Cre} (a-h) and Cx26$^{loxP/loxP}$ (i- p) on P5, P9, P14 and P30. Cx26 (a-d, i-l) and Cx30 (e-h, m-p) expression was analysed with selective antibodies (green), nuclei were stained with DAPI (blue) and actin filaments with Texas red conjugated phalloidin (red). Scale bar, 50 µm.

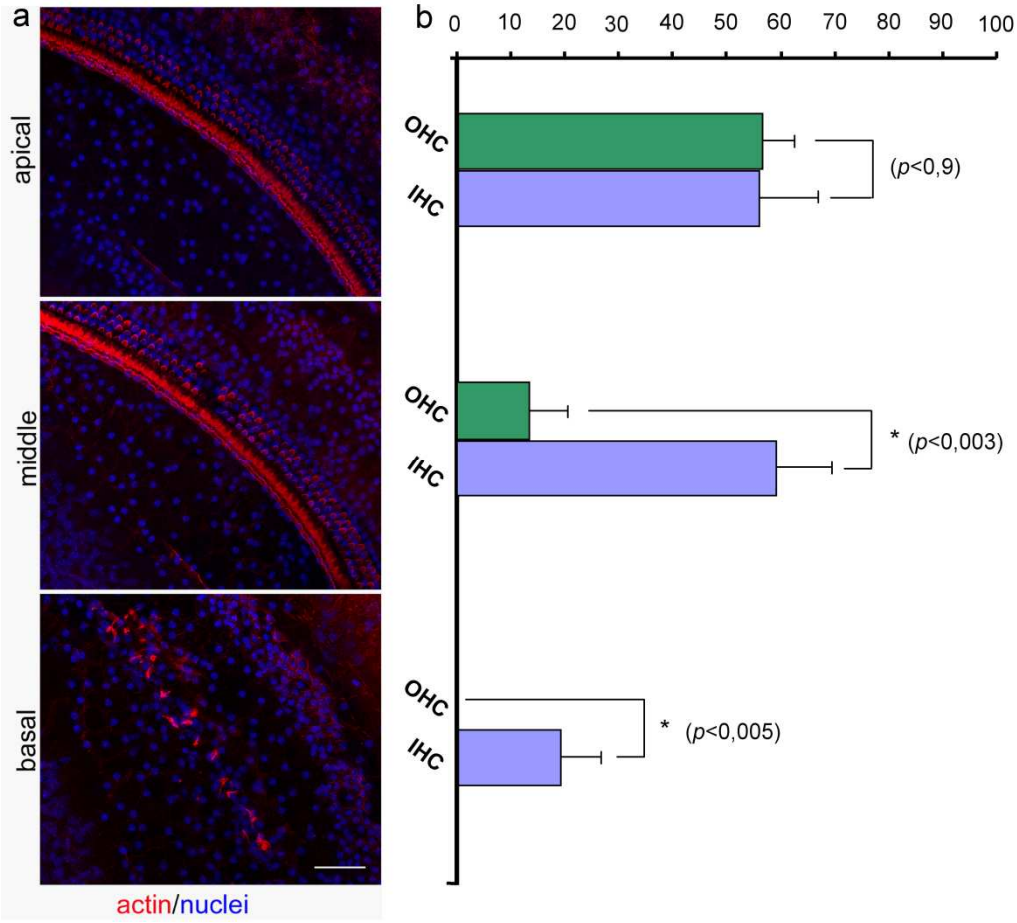

Figure 17. Actin and nuclei staining in P30 cochlea whole mounts and percentage of HC survival. (a) Horizontal sections (orthogonal to the modiolus) of cochlea whole mounts from P30 $Cx26^{Sox10Cre}$ mice. Images from apical, medial and basal regions are obtained by maximal back-projection of 20 confocal optical sections from a 2 µm step z–stack. Actin filaments were stained with Texas red conjugated phalloidin (red) and nuclei with DAPI (blue). Scale bar: 50 µm.**(b)** Percentage of HC survival in the basal, middle and apical turn of $Cx26^{Sox10Cre}$ mice cochleae.

Characterization of gap junction channel permeability in the developing cochlea by fluorescence recovery after photobleaching

Functional gap junction channels are crucial for maturation of different tissues [187]. In particular, Cx26 and Cx30 are essential for survival and development of the organ of Corti [51], [52]. Several lines of experiments indicate that permeability

to larger metabolites, rather than small inorganic ions, may play an important role in the development, physiology and aetiology of connexin-related diseases [188]. In order to determine whether the hearing loss in $Cx26^{Sox10Cre}$ mice may be ascribed to a diminished cell–cell coupling during the crucial post-natal period, as observed in Cx30 ko mice [3], we performed fluorescence recovery after photobleaching assays [189] in cochlear cultures obtained from P5 mice [3], [160], [65], [4]. In particular, we focused on non-sensory cells of the receding greater epithelial ridge, the region of the epithelium that gives rise to the inner hair cells and medial non-sensory cells [190], [191]. We also investigated non-sensory cells in the lesser epithelial ridge, the area thought to give rise to the outer hair cells and lateral non-sensory cells [190], [191] (**Figure 18a**). After overnight incubation *in vitro*, cochlear organotypic cultures were loaded with the acetoxymethyl (AM) ester of the fluorescent tracer calcein (MW 622, net charge 24) that diffuses through gap junction channels of non-sensory cells in cochlear organotypic cultures (see Matherial and Methods). Following the delivery of a 405 nm laser pulse to a restricted tissue area, the intracellular calcein fluorescence was partially restored via diffusion of the indicator dye through gap junction channels from adjacent unbleached cells in wild-type cultures (**Figure 18b, blue traces**). Incomplete recovery of fluorescence intensity is ascribed to the fraction of the calcein pool which is not available for intercellular transfer (immobile fraction), due to trapping into subcellular organelles and/or binding to subcellular structures [192]. These experiments clearly indicate that non-sensory cells in the developing cochlea of wild-type mice are dye-coupled in all cochlear turns. The different time courses of fluorescence traces in the lesser epithelial ridge (**Figure 18b, right**) compared with the greater epithelial ridge (**Figure 18b, left**) is indicative of a substantially larger immobile fraction in the latter. The ablation of Cx26, and the subsequent downregulation of Cx30 [3] caused a substantial reduction of dye coupling levels in $Cx26^{Sox10Cre}$ cultures (**Figure 18b, red traces**). The process of fluorescence recovery after photobleaching was inhibited by pre-incubating cochlear cultures for 20 min in an extracellular medium (EXM, see Materials and Methods) supplemented with 100 mM carbenoxolone, a broad spectrum inhibitor of connexin

channels [155] (**Figure 18b, black traces**). The residual downward peak, which is resistant to carbenoxolone, is due to a small and rapid recovery of fluorescence caused by the diffusion of dye within the cell from deeper, relatively unbleached regions to more superficial, bleached regions.

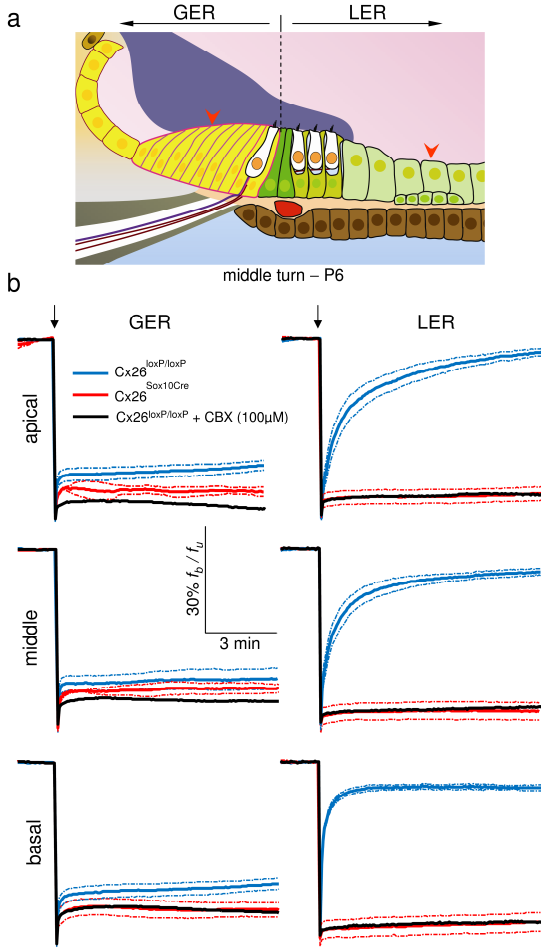

Figure 18. Dye coupling through gap junction channels in the developing cochlea.
(a) Scheme of the sensory epithelium in the developing cochlea (middle turn, P6). Arrowheads indicate the approximate position of laser foci in the receding greater epithelial ridge (GER) and in the lesser epithelial ridge (LER). (b) Shown are plots of fb/fu (bleached over unbleached fluorescence intensity) versus time from the base, middle and apex of the cochlea (see Materials and Methods). Solid lines are averages of n=3 independent experiments; dashed lines indicate 95% confidence intervals. Downward arrows mark the time of laser pulse delivery. CBX is a non-specific inhibitor of gap junction channels [155]. Data acquired by Laura Rodriguez Hernandez.

In vivo delivery

Canalostomy is a surgical technique that is largely used in humans. With a post-auricolar approach, the vestibular system is exposed, permitting to inject drugs with a microsyringe in the posterior semicircular canal (PSC) (see Materials and Methods). In mice, this technique is one of the possible routes to perform gene delivery. Other common approaches are cochleostomy, and the release of drugs through the round window [193]. Canalostomy is the best choice to access the endolymphatic compartment. Thus, while there is a direct communication between the cerebrospinal fluid (CSF) and the perilymph through the cochlear aqueduct [194], endolymph is connected only to the endolymphatic sac, making the endolymphatic compartment a close hydraulic system (**Figure 19**).

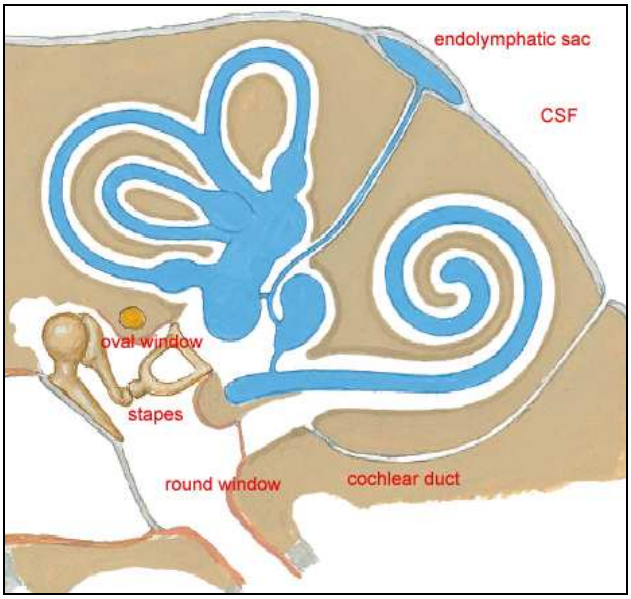

Figure 19. Endolymphatic compartment in the inner ear. The blue area represents the endolymph, defined by the membraneous inner ear, the white area is the perilymph, connected to the CSF through the cochlear duct.

It is well demonstrated that in adult mice canalostomy, in contrast to other approaches, does not affect hearing function [169]. All together, these findings make the vestibular approach a route suitable for gene therapy. Initially, we performed canalostomy on adult mice introducing bromophenol blue and wheat

germ agglutinin-Alexa 568 (WGA-Alexa568) to set injection parameters. We found that delivering a maximum volume of 2 µl at slow speed (3nl/s) preserved the integrity of scala media. Larger volumes and/or higher injection speeds resulted in the rupture of Reissner's membrane and spreading of the dye outside the endolymphatic compartment (perilymphatic space, CSF). The fluid delivered to the posterior semicircular canal reaches the vestibular system and the cochlea. **Figure 20a** shows a cochlea injected with bromophenol blue dye: the blue staining is evident from the base to the apex. Using a fluorescent dye that binds cell membranes (WGA-Alexa568), we verified by confocal fluorescence microscopy that cochleae injected following the procedure described above present with normal microanatomy and intact hair cells and Reissner's membrane (**Figure 20b**). Moreover, 4 weeks after surgery, mice were tested for ABR. No increase in the hearing thresholds was observed following delivery of WGA-Alexa568, in accord with Praetorius et al. [169] (data not shown).

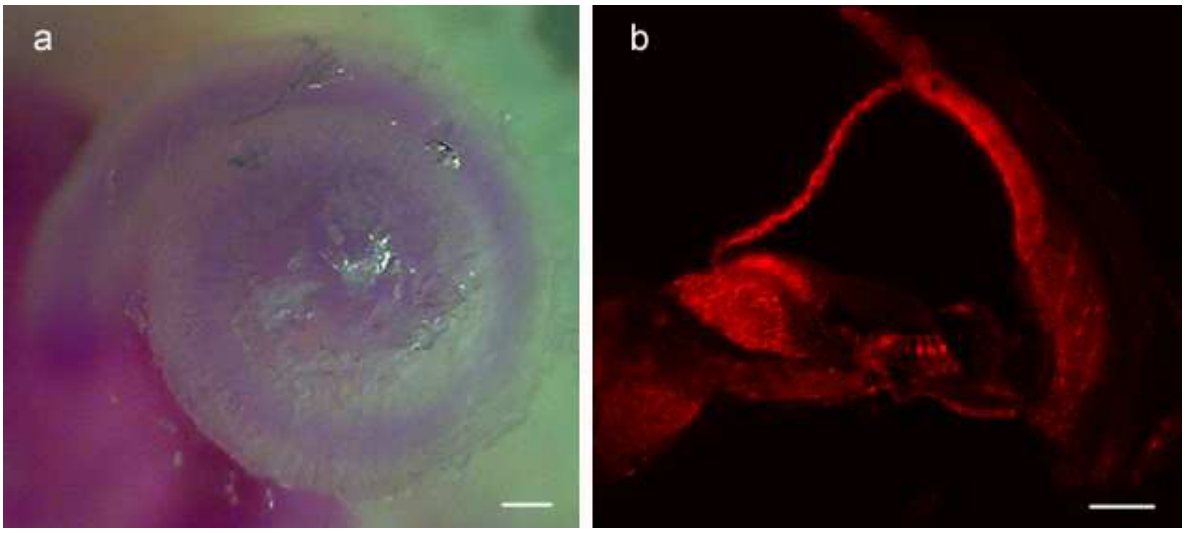

Figure 20. Fluids injected through PSC raise the apex of the cochlea and do not damage the inner ear. (a) After injection by canalostomy in the PSC of 2µl of Bromophenol blue, diluted in artificial endolymph, mice are sacrified and the cochlea was observed under a dissection microscope. The blue staining can be observed in the endolymphatic compartment from the base to the apex of the cochlea. Scale bar: 250 µm. **(b)** After injection by canalostomy in the PSC of 2µl of Alexa 594-conjugated Wheat germ agglutinin (WGA), diluted in artificial endolymph (5µg/ml), the injected cochlea was fixed, cut parallel to the modiolus axis and analysed with fluorescence

microscopy. The WGA staining (red) can be observed in the scala media and the anatomy of the Organ of Corti is intact. Scale bar: 50µm.

We also performed gene delivery using BAAV particles ($2x10^{12}$ particles/ml) carrying the DNA for a reported gene (recombinant beta actin-GFP). This vector has been used *in vivo* to efficiently transduce lungs [195], parotid grands [196], and cochlea [173]. Injected cochleae were extracted and analysed for the presence of beta actin-GFP. As is shown in **Figure 21**, recombinant beta actin-GFP is expressed in the supporting cells of the OoC, including Pillars' and Hensen's cells.

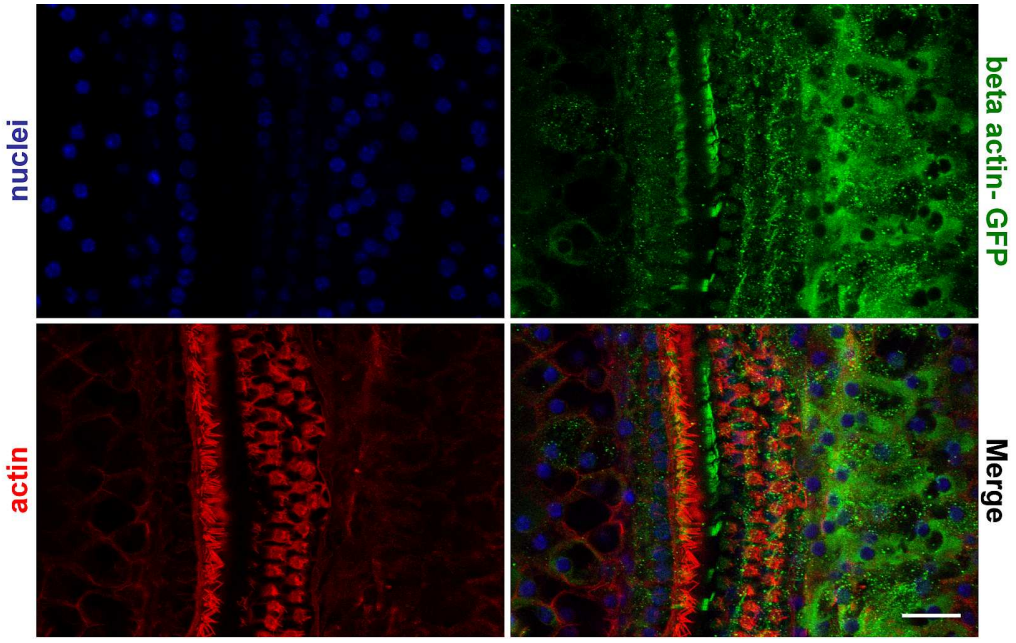

Figure 21. Cochlea whole mount transduced *in vivo* with BAAV beta actin-GFP. Four weeks after delivery of BAAV beta actin-GFP by canalostomy in adult mice, cochleae were extracted and processed for the detection of GFP signal from viral transduction. A signal specific for supporting cells of the OoC can be observed. Scale bar: 25 µm.

Analysis of $Cx26^{Sox10Cre}$ and Cx30 ko mice [52], revealed that the OoC degenerates from P14, leading to an irreversible hearing loss. A therapy whose aim is to rescue Cxs expression and restore hearing function should be applyed early in the development to permit signals from non-sensory cells to mediate normal inner ear's cells differentiation and innervation [197]. For this reason, performing gene delivery on adult mice is unlikely to rescue the deafness

phenotype. Hair cell regeneration studies were performed at embryonic stage [198], but this approach presents high variability as the technique is extremely intricate and prone to a high mortality for embryos and mothers. As a compromise, we decided to carry on with canalostomy, performing it in newborn mice at P4, an age at which several cell signaling processes are still underway and decide cell fate [161].

Performing surgery on such young mice is not an easy task. First of all, protocols to induce anesthesia on pups are not available, and pharmacokinetics of young mice is completely different from that of adult. Sedation is often achieved by hypothermia, a method used for non invasive surgeries when it is necessary only to maintain still the pup and no profound wound is made. Since we needed to perform a dorsal incision (3mm of length) and separate the trapezius fibers, a deeper anesthesia was required. We thus adopted another method commonly used to sedate pups, i.e. isofluorane inhalation [199]. More than 15 minutes were required to obtain a deep sleep, since breathing of newborn mice is very slow. Moreover, canalostomy affects the head of the pup, thus maintenance of anesthesia by tubes applied to the muzzle was not an option. By trial and error we finally managed set anesthesia dosage (see Matherials and Methods), maintaining the percentage of survivors around 80-90%. Approach to the head of newborn mouse requires great care. The cochlea of pups is smaller than that of adult mice, and the bony capsule is not yet developed. Hence a needle smaller than the one used for surgery on adult was required (36G). **Figure 22** shows side-by-side the semicircular canals and syringe needles used for adult **(a)** and P4 **(b)** mice canalostomy.

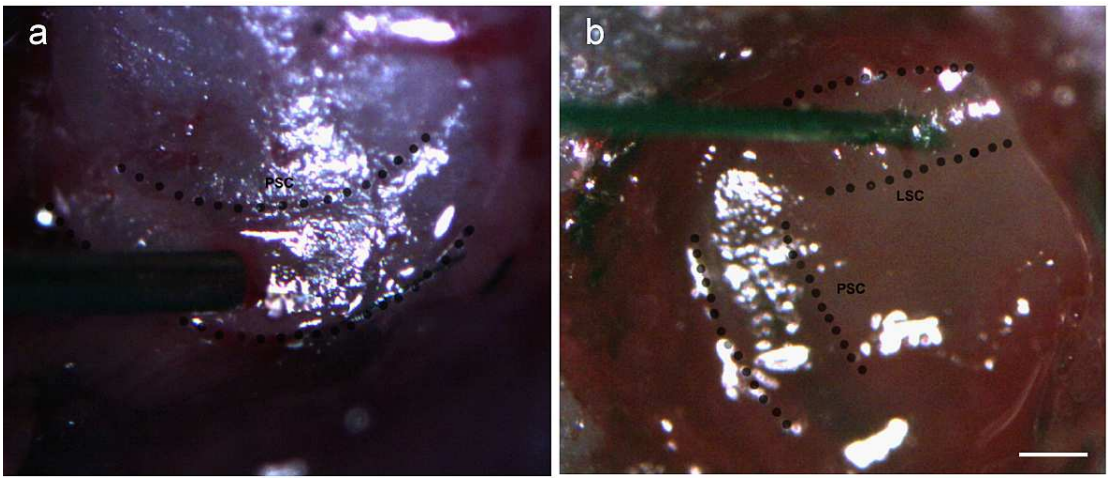

Figure 22. Syringe needle- semicircular canal complex. (a) A 33 G syringe needle is inserted in the PSC of adult mice, **(b)** a 36 G syringe needle in the LSC of P4 mice. Scale bar: 200µm.

Microinjections via canalostomy in pups were performed via the lateral semicircular canal (LSC), which is not easily accessible in adult. As in the adult, injected dyes reached the apex of the cochlea, but fail to enter the posterior and superior canal. For this reason, and for the reduced size of the cochlea, we set the maximum injected volume at 1µl, i.e. half that used for canalostomy in adult mice. Postoperative mortality due to cannibalism or lack of care by the dam was worked out weaning pups with a step mother, or, when necessary, with artificial milk administered by a feeding needle. Hearing in mice that had undergone canalostomy at P4 was tested 4 weeks after surgery by recording ABRs. The pool of mice injected with BAAV-containing solution presented no significant hearing loss, as shown in **Figure 23** (blue trace, control $Cx26^{loxP/loxP}$ mice, not injected; violet trace, $Cx26^{loxP/loxP}$ mice injected with BAAV beta actin-GFP). To test the efficacy of the delivery method, we injected a solution of tannic acid, an ototoxic compound commonly used to stain lateral tip links of hair cell stereocilia [200]. ABR analysis, performed 4 weeks later, revealed a hearing loss of 20-50 dB at all tested frequencies (**Figure 23**, green trace). These results indicate microinjection via canalostomy in P4 pups is a viable method that, if used judiciously, does not compromise hearing function.

Our initial attempts to alter connexin expression by this method focussed on ablating Cx26 in $Cx26^{loxP/loxP}$ mice by injecting a BAAV construct encoding for a

Cre recombinase, and thus aimed to reproduce *in vivo* the results obtained in cochlear cultures (Ortolano, 2008). Gene delivery of Cre recombinase led to a partial increase of hearing thresholds (**Figure 23**, light blue trace).

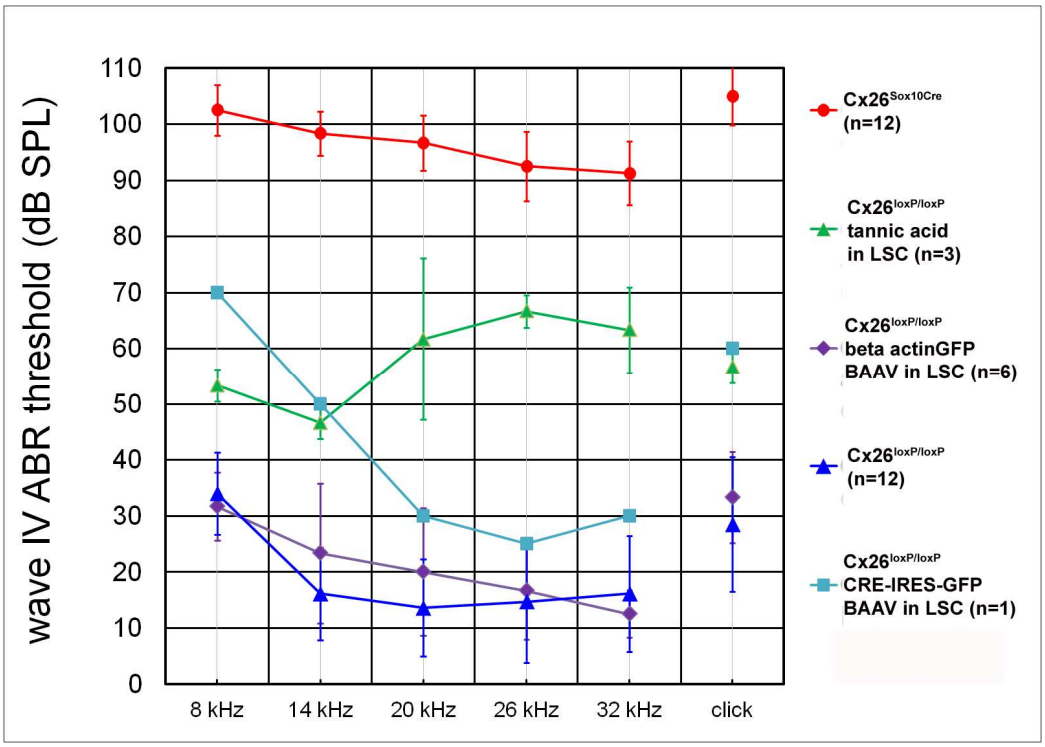

Figure 23. *In vivo* recordings from Cx26$^{loxP/loxP}$ mice 4 weeks after surgery. Audiograms for tone bursts at 8-14-20-26-32 kHz and for click obtained from Cx26$^{loxP/loxP}$ mice that were injected at P4 with 1µl of tannic acid (2%) (green line, n=2), BAAV beta actin GFP (10^{13} p/ml) (violet line, n=2) or BAAV Cre IRES GFP(10^{13} p/ml) (light blue line, n=1), diluted in artificial endolymph. Blue line: Cx26$^{loxP/loxP}$, red line Cx26^{Sox10Cre}. Bars represent standard deviation. Note that click responses are plotted at an arbitrary point on the frequency axis (the position does not reflect the frequency content of click stimuli).

At the time of writing, available constructs to restore Cxs in knockout mice are not yet optimized for in vivo experiments, although they were successfully used for experiments in cochlear organotypic culture [3].

DISCUSSION

In this study we analyzed a new DFNB1 mouse model, $Cx26^{Sox10Cre}$, with targeted deletion of the Cx26 gene (GJB2) in cells deriving from the neural crests and in the otic vesicle. ABR recordings revealed that these mice are profoundly deaf and present with a ~70% reduced EP (**Fig. 13**). Hearing thresholds were similar to those of Cx30 full ko mice. While Cx30 ko mice have a EP around 4mV, the residual EP $Cx26^{Sox10Cre}$ is tenfold higher, around 40mV. This striking difference correlates with difference in Cxs protein expression in different inner ear compartments in the two types of transgenic mice. Thus, immunoflurescence results obtained in thick cochlear slices from Cx30 ko mice show complete lack of Cx30 proteins at all ages. Instead the expression of Cx26, which is reduced in cochlear cultures at P5, particularly in supporting cells of the lesser epithelial ridge [3], is similar to that of wt mice by P30. In $Cx26^{Sox10Cre}$, on the other hand, Cx26 and Cx30 are still expressed in the spiral ligament and in the basal and intermediate cells of the stria vascularis (**Fig. 14**). These data agree with the general assumption that gap junctions network in the stria vascularis are crucial for K^+ homeostasis in the endolymphatic compartment. Although recent studies revealed that the EP depends on an electrically isolated space and two K^+-diffusion potentials in the stria vascularis that exclude connexins contribution [201], technical difficulties in the EP recordings let the real pathway still unknown.

Data presented here, indicate clearly that preservation of normal expression of Cx26 and Cx30 in the OoC is crucial for inner ear development and hair cells survival. Gap-FRAP experiments showed reduced cell–cell communication, both in the GER and in the LER of $Cx26^{Sox10Cre}$ mice (this work) (**Fig. 18**). During maturation of the inner ear, connexin channels and hemichannels permit the exchange of intercellular Ca^{2+} signals (ICS) [160], [3], [65] which are fundamental for HC innervation and differentiation [197], and the normal development of the hearing function [4]. Indeed, after hearing onset, OoC cells in mutant mouse appear immature, the tunnel of Corti do not open and HCs degenerate (**Fig. 16**).

From a gene therapy perspective, the studies presented here on the $Cx26^{Sox10Cre}$ mouse model, highlight the importance of an early intervention. Restoration of normal Cxs levels in DFNB1 mouse models could be a way to rescue hearing function. These pilot studies might, in future, lead to the development of therapeutic interventions in humans, particularly in children. In mice, differentiation pathways are active before hearing onset, thus efficient gene delivery should be executed at this stage. Our preliminary results highlight the possibility of obtaining genetic modification, by the introduction of a Cre recombinase in the inner ear of $Cx26^{loxP/loxP}$ mice. Although differences in Cx26 expression between injected and control cochleae could not be detected by immunoflurescence, ABR recordings revealed a sizeable increase of auditory thresholds (**Fig. 23**). This happened also in the case of $Cx30^{T5M/T5M}$ mice, affected by a similar hearing loss, and a Cxs expression downregulation appreciable only by western blots [4].

Protein expression for *in vivo* delivery will be optimized by addition of a modified Kozak sequence at the translational start site of Cxs constructs. Modifications in BAAV production and delivery will include use of a long stuffer sequence to prevent reverse packaging from the AAV inverted-terminal repeats, and co-injection with a surfactant, to allow consistent and predictable delivery of a given dose of vector. Infact, BAAV Cxs constructs were used to efficiently tranduce cochlear cultures, but *in vivo*, mechanisms that regulate gene expression are quite different. Such kind of modifications were also used to optimize AAV2 vectors to obtain a reversal of blindness in animal models of leber congenital amaurosis [202].

NOTE

In the following, title and Abstracts of the five publications to which G. Crispino contributed in the course of her Ph.D. studies are listed. In each case, the portion of the results contributed by G. Crispino to each publication is highlighted.

Coordinated control of connexin 26 and connexin 30 at the regulatory and functional level in the inner ear

Saida Ortolano, Giovanni Di Pasquale, **Giulia Crispino**, Fabio Anselmi, Fabio Mammano, John A. Chiorini

Proceedings of National Academy of Sciences. 2008, 105(48):18776-81

Abstract

Connexin 26 (Cx26) and connexin 30 (Cx30) are encoded by two genes (*GJB2* and *GJB6*, respectively) that are found within 50 kb in the same complex deafness locus, DFNB1. Immunocytochemistry and quantitative PCR analysis of Cx30 KO mouse cultures revealed that Cx26 is downregulated at the protein level and at the mRNA level in nonsensory cells located between outer hair cells and the stria vascularis. To explore connexin coregulation, we manipulated gene expression using the bovine adeno-associated virus. Overexpression of Cx30 in the Cx30 KO mouse by transduction with bovine adeno-associated virus restored Cx26 expression, permitted the formation of functional gap junction channels, and rescued propagating Ca^{2+} signals. Ablation of Cx26 by transduction of $Cx26^{loxP/loxP}$ cultures with a Cre recombinase vector caused concurrent downregulation of Cx30 and impaired intercellular communication. The coordinated regulation of Cx26 and Cx30 expression appears to occur as a result of signaling through PLC and the NF-κB pathway, because activation of IP_3-mediated Ca^{2+} responses by stimulation of P2Y receptors for 20 min with 20 nM ATP increased the levels of Cx26

transcripts in Cx30 KO cultures. This effect was inhibited by expressing a stable form of the IκB repressor protein that prevents activation/translocation of NF-κB. Thus, our data reveal a Ca^{2+}-dependent control in the expression of inner ear connexins implicated in hereditary deafness as well as insight into the hitherto unexplained observation that some deafness-associated DFNB1 alleles are characterized by hereditable reduction of both *GJB2* and *GJB6* expression.

Results

The contribution of this work was the production of viral particles used in all experiments and the qPCR analysis of Cx26 and Cx30 mRNA levels in the skin and liver of P5 Cx30 ko mice. These data showed comparable levels of Cx26 in the skin of WT and Cx30 KO mice . We also found comparable levels of Cx26 in the liver of WT and Cx30 KO mice, whereas Cx30 mRNA was not detectable in WT mouse liver, as previously reported [150]. (**Fig. 12**)

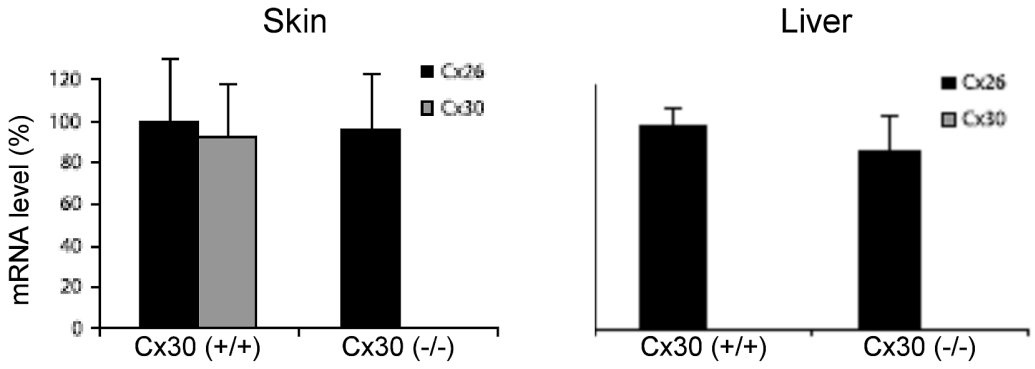

Figure 24. Cx26 and Cx30 mRNA levels in liver and skin from Cx30 KO mice. Histogram representation of Cx26 and Cx30 qPCR products amplified from reverse-transcribed mRNAs extracted from fresh liver or skin tissue of P5 WT [Cx30(-/-)] and KO [Cx30(-/-)] mice (*n*=3 for each indicated condition; error bars represent SD). Note that Cx30 mRNA is not detectable in the liver of WT mice.

ATP release through connexin hemichannels and gap junction transfer of second messengers propagate Ca2+ signals across the inner ear

Anselmi F, Hernandez VH, **Crispino G**, Seydel A, Ortolano S, Roper SD, Kessaris N, Richardson W, Rickheit G, Filippov MA, Monyer H, Mammano F.

Proceedings of National Academy of Sciences. 2008, 105(48):18770-75

Abstract

Extracellular ATP controls various signaling systems including propagation of intercellular Ca(2+) signals (ICS). Connexin hemichannels, P2x7 receptors (P2x7Rs), pannexin channels, anion channels, vesicles, and transporters are putative conduits for ATP release, but their involvement in ICS remains controversial. We investigated ICS in cochlear organotypic cultures, in which ATP acts as an IP(3)-generating agonist and evokes Ca(2+) responses that have been linked to noise-induced hearing loss and development of hair cell-afferent synapses. Focal delivery of ATP or photostimulation with caged IP(3) elicited Ca(2+) responses that spread radially to several orders of unstimulated cells. Furthermore, we recorded robust Ca(2+) signals from an ATP biosensor apposed to supporting cells outside the photostimulated area in WT cultures. ICS propagated normally in cultures lacking either P2x7R or pannexin-1 (Px1), as well as in WT cultures exposed to blockers of anion channels. By contrast, Ca(2+) responses failed to propagate in cultures with defective expression of connexin 26 (Cx26) or Cx30. A companion paper demonstrates that, if expression of either Cx26 or Cx30 is blocked, expression of the other is markedly down-regulated in the outer sulcus. Lanthanum, a connexin hemichannel blocker that does not affect gap junction (GJ) channels when applied extracellularly, limited the propagation of Ca(2+) responses to cells adjacent to the photostimulated area. Our results demonstrate that these connexins play a dual crucial role in inner ear Ca(2+) signaling: as hemichannels, they promote ATP release, sustaining long-range ICS

propagation; as GJ channels, they allow diffusion of Ca(2+)-mobilizing second messengers across coupled cells.

Results

By using antibodies against Cx26 extracellular loop peptides [203], we detected immunofluorescence signals near the apex of fixed, but not permeabilized, cochlear supporting and epithelial cells (Fig. 13), suggesting that unpaired connexons may be present in the apical plasma membrane, which prompted us to further test the hypothesis that Cx hemichannels release ATP in this system.

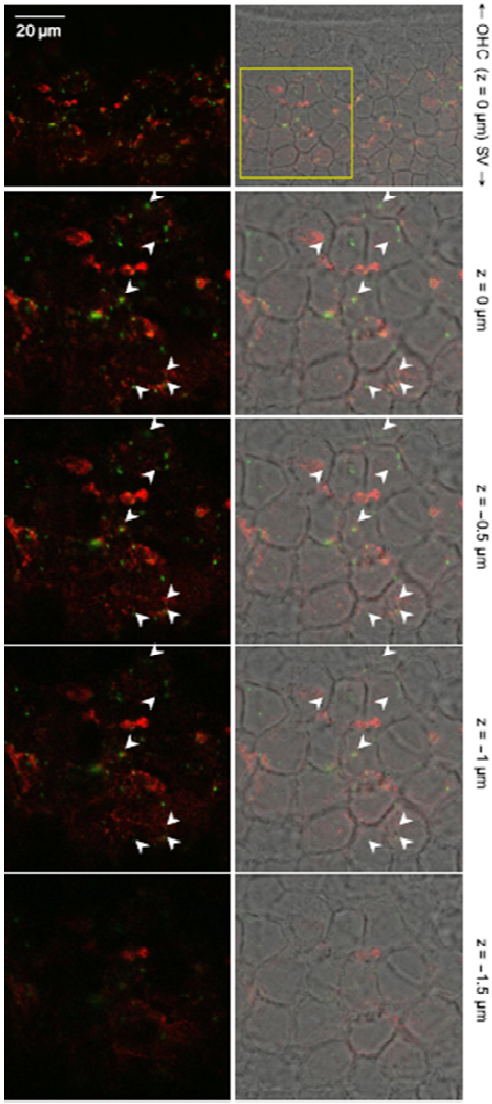

Figure 25. Connexin immunoreactivity near the endolymphatic surface of the organ of Corti. Through focus confocal image sequence (z-stack) of cochlear supporting and epithelial cells in the region comprised between outer hair cells (OHC) and stria vascularis (SV), immuno-labeled with Abs directed against peptides corresponding to the extracellular loops of Cx26 (primary antibodies) and green-fluorescent secondary antibodies. Cell plasma membranes in these fixed, but non-permeabilized, preparations were stained with red-fluorescent wheat germ agglutinin. *Left*, merged green and red channels. *Right*, overlay of *Left* images on the corresponding grayscale transmitted light differential interference contrast images. Arrowheads points to apical plasma membrane Cx26 signals from locations that, *in vivo*, would be exposed to endolymph. Scale bar: 20µm.

ATP-mediated cell-cell signaling in the organ of Corti: the role of connexin channels

Majumder P, **Crispino G**, Rodriguez L, Ciubotaru CD, Anselmi F, Piazza V, Bortolozzi M, Mammano F.

Purinergic Signalling, 2010, 6(2):167-87

Abstract

Connexin 26 (Cx26) and connexin 30 (Cx30) form hemichannels that release ATP from the endolymphatic surface of cochlear supporting and epithelial cells and also form gap junction (GJ) channels that allow the concomitant intercellular diffusion of Ca(2+) mobilizing second messengers. Released ATP in turn activates G-protein coupled P2Y(2) and P2Y(4) receptors, PLC-dependent generation of IP(3), release of Ca(2+) from intracellular stores, instigating the regenerative propagation of intercellular Ca(2+) signals (ICS). The range of ICS propagation is sensitive to the concentration of extracellular divalent cations and activity of ectonucleotidases. Here, the expression patterns of Cx26 and Cx30 were characterized in postnatal cochlear tissues obtained from mice aged between P5 and P6. The expression gradient along the longitudinal axis of the cochlea, decreasing from the basal to the apical cochlear turn (CT), was more pronounced in outer sulcus (OS) cells than in inner sulcus (IS) cells. GJ-mediated dye coupling was maximal in OS cells of the basal CT, inhibited by the nonselective connexin channel blocker carbenoxolone (CBX) and absent in hair cells. Photostimulating OS cells with caged inositol (3,4,5) tri-phosphate (IP(3)) resulted in transfer of ICS in the lateral direction, from OS cells to IS cells across the hair cell region (HCR) of medial and basal CTs. ICS transfer in the opposite (medial) direction, from IS cells photostimulated with caged IP(3) to OS cells, occurred mostly in the basal CT. In addition, OS cells displayed impressive rhythmic activity with oscillations of cytosolic free Ca(2+) concentration ([Ca(2+)](i)) coordinated by the propagation of Ca(2+) wavefronts sweeping repeatedly through the same tissue area along the coiling axis of the cochlea.

Oscillations evoked by uncaging IP(3) or by applying ATP differed greatly, by as much as one order of magnitude, in frequency and waveform rise time. ICS evoked by direct application of ATP propagated along convoluted cellular paths in the OS, which often branched and changed dynamically over time. Potential implications of these findings are discussed in the context of developmental regulation and cochlear pathophysiology.

Results

It has been previously documented that development of the cochlear GJ system precedes the functional maturation of the murine inner ear [37], which takes place between the second and third postnatal week [204]. To better characterize connexin expression in our experimental model, we performed immunolabeling of Cx26 and Cx30 with selective antibodies. Labeling was similar, but not identical, for Cx26 (**Fig. 26a**) and Cx30 (**Fig. 26b**). For both connexins, expression was evident in several sub-compartments of the cochlear duct even at this early post natal stage that precedes by one week the onset of hearing [205]. In particular, our confocal images highlight the expression of connexins at point of contacts between supporting and epithelial cells of the OoC on both sides of the HCR (which comprises the RL) as well as in basal and intermediate cells of the SV. Furthermore, both Cx26 and Cx30 showed marked immunoreaction in the spiral limbus and the spiral ligament. Immunolabeling intensity decreased markedly in OS cells along the *longitudinal* axis, from the *basal* to the *apical* end the cochlea. However, this expression gradient was less evident in IS cells, which showed intense immunolabeling in all cochlear turns (CTs). IHCs and OHCs showed no sign of immunoreactivity to Cx26 or Cx30 antibodies, consistent with the notion that sensory cells are not coupled by GJ to any other cell in the OoC. Using antibodies against Cx26 extracellular loop peptides (CELAbs) [203], we detected immunofluorescence signals corresponding to unpaired connexons (i.e., connexin hemichannels) in the cell plasma membrane. In particular, CELAbs decorated the endolymphatic surface of the epithelium, except the hair cells, from IS cells across the RL to OS cells, with maximal intensity in the basal CT (**Fig. 27**).

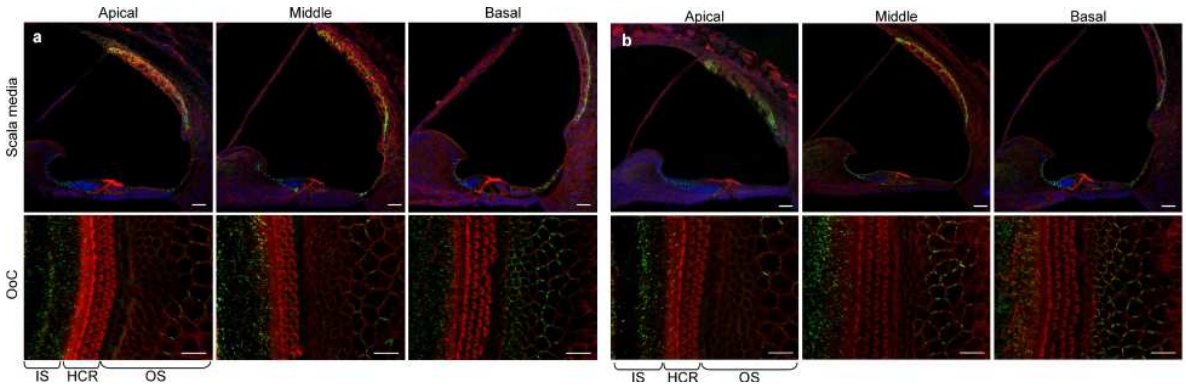

Figure 26. Cx26 and Cx30 immunoreactivity. *Top*: maximal projection rendering of two consecutive midmodiolar confocal optical sections, taken at 1 µm intervals in the indicated CTs, from cochlear preparations of P6 mice. Cx26 and Cx30 expression was probed, respectively, by a Cx26 and Cx30 selective antibody (*green*), nuclei were stained with DAPI (*blue*) and actin filaments with Texas Red conjugated phalloidin (*red*). *Scale bars* 30 µm. *Bottom:* Cx26 and Cx30 immunolabeling of P5 cochlear cultures, processed after 1 day in vitro. Images are maximal projection rendering of confocal optical sections selected from a *z* stack of 20 images taken at 0.5 µm intervals. *OoC* organ of Corti, *IS* inner sulcus, *HCR* hair cell region, *OS* outer sulcus. *Scale bars* 30 µm

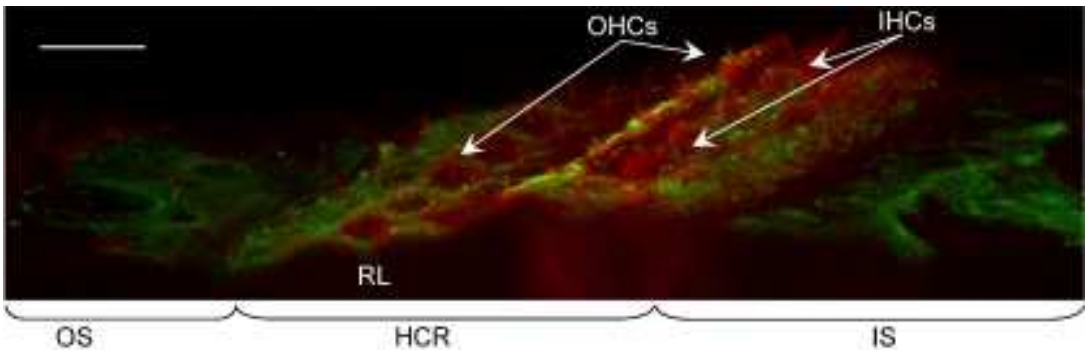

Figure 27. Cx26 hemichannels at the endolymphatic surface of the OoC. Three-dimensional reconstruction of the OoC in the basal CT obtained by the maximal projection rendering of 14 confocal optical sections, taken at 1.5 µm intervals in a slice cut from a P6 mouse cochlea. Cx26 hemichannel expression was probed by CELAbs (*green*) and actin filaments were stained with Texas Red conjugated phalloidin (*red*). *IS* inner sulcus, *HCR* hair cell region, *OS* outer sulcus, *RL* reticular lamina, *OHCs* outer hair cells, *IHCs* inner hair cells. *Scale bar* 10 µm

The novel PMCA2 pump mutation Tommy impairs cytosolic calcium clearance in hair cells and links to deafness in mice

Bortolozzi M, Brini M, Parkinson N, **Crispino G**, Scimemi P, De Siati RD, Di Leva F, Parker A, Ortolano S, Arslan E, Brown SD, Carafoli E, Mammano F.

The Journal of Biological Chemistry, 2010, 285(48):37693-703.

Abstract

The mechanotransduction process in hair cells in the inner ear is associated with the influx of calcium from the endolymph. Calcium is exported back to the endolymph via the splice variant w/a of the PMCA2 of the stereocilia membrane. To further investigate the role of the pump, we have identified and characterized a novel ENU-induced mouse mutation, Tommy, in the PMCA2 gene. The mutation causes a non-conservative E629K change in the second intracellular loop of the pump that harbors the active site. Tommy mice show profound hearing impairment from P18, with significant differences in hearing thresholds between wild type and heterozygotes. Expression of mutant PMCA2 in CHO cells shows calcium extrusion impairment; specifically, the long term, non-stimulated calcium extrusion activity of the pump is inhibited. Calcium extrusion was investigated directly in neonatal organotypic cultures of the utricle sensory epithelium in Tommy mice. Confocal imaging combined with flash photolysis of caged calcium showed impairment of calcium export in both Tommy heterozygotes and homozygotes. Immunofluorescence studies of the organ of Corti in homozygous Tommy mice showed a progressive base to apex degeneration of hair cells after P40. Our results on the Tommy mutation along with previously observed interactions between cadherin-23 and PMCA2 mutations in mouse and humans underline the importance of maintaining the appropriate calcium concentrations in the endolymph to control the rigidity of cadherin and ensure the function of interstereocilia links, including tip links, of the stereocilia bundle.

Results

We performed confocal imaging immunoassays in the neonatal utricle preparation using antibodies selective for the PMCA2 (**Fig. 28**). P7 utricle cultures from wild

type, heterozygous, and homozygous *Tommy* mice presented with selective localization of the PMCA2 in the plasma membrane of the stereocilia with comparable levels of fluorescence. Although not quantitative, these results suggest that the differences in recovery after Ca^{2+} photoliberation highlighted above reflected a dysfunction of the pump more than problems with its expression or targeting. Immunofluorescence was also used to monitor the progressive degeneration of the organ of Corti, which correlates with the lack of auditory function in the homozygote (**Fig. 29a**). By immunolabeling transversal and orthogonal sections of the cochlea, we observed a progressive base to apex loss of PMCA2 in the hair cells of homozygous *Tommy* mice after P40 (**Fig. 29b**). At P60, PMCA2 immunofluorescence signal was virtually absent in the basal part of the cochlea, and signs of hair cell degeneration were evident by the lack of several nuclei stained with DAPI.

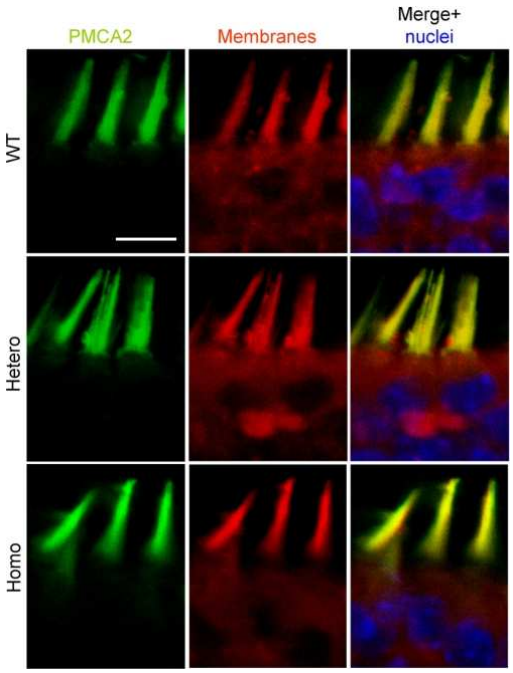

Figure 28. PMCA2 immunolabeling in neonatal utricle. Confocal imaging immunoassays of PMCA2 (stained by Alexa 488 conjugated, *green*) in P7 utricle cultures from wild type, heterozygous, and homozygous *Tommy* mice. Membranes (*red*) are stained by FM4-64FX, whereas nuclei (*blue*) are stained by DAPI. *Scale bar*, 10 µm.

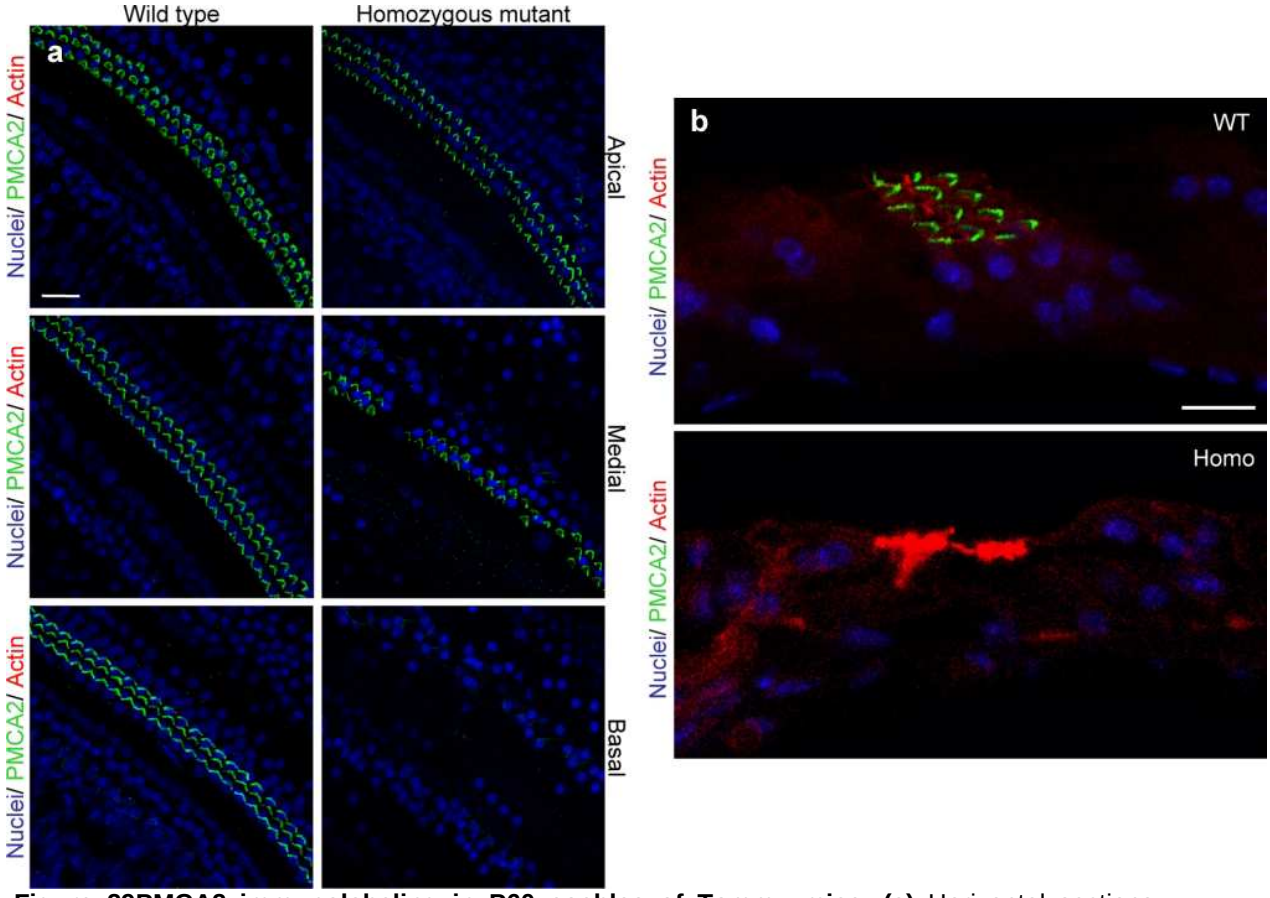

Figure 29PMCA2 immunolabeling in P60 cochlea of Tommy mice. (a) Horizontal sections (orthogonal to the modiolus) of cochlea whole mounts from P60 wild type (*left column*) and homozygous (*right column*) *Tommy* mice are shown. Images from apical, medial, and basal regions are obtained by maximal back-projection of 20 confocal optical sections from a 2-µm step z-stack of wild type and homozygous *Tommy* mice. PMCA2 expression was probed by a PMCA2 selective antibody (Alexa 488 conjugated, *green*), and nuclei were stained with DAPI (*blue*). *Scale bar*, 15 µm. **(b)** PMCA2 immunolabeling in basal cochlear transversal sections (parallel to the modiolus) of P60 Tommy mice. Images were obtained by maximal back-projection of 2–6 confocal optical sections from a 1-µm step z-stack of wild type (*top panel*) and homozygous (*bottom panel*) *Tommy* mice. Actin filaments were stained with phalloidin (Texas Red-conjugated, *red*) and nuclei with DAPI (*blue*). *Scale bar*, 15 µm.

The human deafness-associated connexin 30 T5M mutation causes mild hearing loss and reduces biochemical coupling among cochlear non-sensory cells in knock-in mice.

Schütz M, Scimemi P, Majumder P, De Siati RD, **Crispino G**, Rodriguez L, Bortolozzi M, Santarelli R, Seydel A, Sonntag S, Ingham N, Steel KP, Willecke K, Mammano F.

Human Molecular Genetics, 2010, 19(24):4759-73

Abstract

Mutations in the GJB2 and GJB6 genes, respectively, coding for connexin26 (Cx26) and connexin30 (Cx30) proteins, are the most common cause for prelingual non-syndromic deafness in humans. In the inner ear, Cx26 and Cx30 are expressed in different non-sensory cell types, where they largely co-localize and may form heteromeric gap junction channels. Here, we describe the generation and characterization of a mouse model for human bilateral middle/high-frequency hearing loss based on the substitution of an evolutionarily conserved threonine by a methionine residue at position 5 near the N-terminus of Cx30 (Cx30T5M). The mutation was inserted in the mouse genome by homologous recombination in mouse embryonic stem cells. Expression of the mutated Cx30T5M protein in these transgenic mice is under the control of the endogenous Cx30 promoter and was analysed via activation of the lacZ reporter gene. When probed by auditory brainstem recordings, $Cx30^{T5M/T5M}$ mice exhibited a mild, but significant increase in their hearing thresholds of about 15 dB at all frequencies. Immunolabelling with antibodies to Cx26 or Cx30 suggested normal location of these proteins in the adult inner ear, but western blot analysis showed significantly down-regulated the expression levels of Cx26 and Cx30. In the developing cochlea, electrical coupling, probed by dual patch-clamp recordings, was normal. However, transfer of the fluorescent tracer calcein between cochlear non-sensory cells was reduced, as

was intercellular Ca(2+) signalling due to spontaneous ATP release from connexin hemichannels. Our findings link hearing loss to decreased biochemical coupling due to the point-mutated Cx30 in mice.

Results

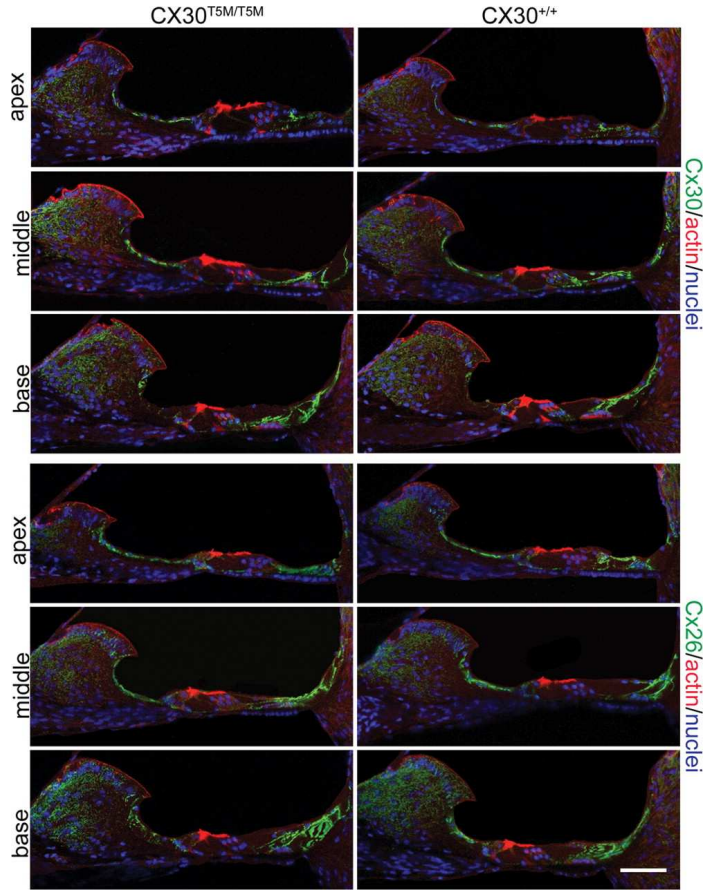

Figure 30 Connexin immunoreactity in the adult organ of Corti. Maximal projection rendering of two consecutive midmodiolar confocal optical sections, taken at 1 µm intervals in the indicated cochlear turns of $Cx30^{T5M/T5M}$ (left) and $Cx30^{+/+}$ mice (right) on P30. Cx30 and Cx26 expression was analysed with selective antibodies (green), nuclei were stained with DAPI (blue) and actin filaments with Texas red conjugated phalloidin (red). Scale bar, 50 µm.

To characterize connexin expression in the $Cx30^{T5M/T5M}$ transgenic mice, we performed immunolabelling with antibodies specific for Cx30 or Cx26 protein (**Fig. 30** On P30, labelling patterns were similar, but not identical, for Cx26 and Cx30. No discernible differences between $Cx30^{+/+}$, $Cx30^{+/T5M}$ and $Cx30^{T5M/T5M}$ mice were

noticed. Thus, in all three genotypes, Cx26 and Cx30 showed immunoreactivity in several sub-compartments of the cochlea at contact sites between supporting and epithelial cells of the organ of Corti on both sides of the hair cell region. Inner hair cells and outer hair cells showed no sign of immunoreactivity to Cx26 or Cx30 antibodies, in accord with the notion that sensory cells are not coupled by gap junction to any other cell type in the organ of Corti.

Connexin immunoreactivity was evident in the spiral limbus, spiral ligament (**Fig. 3**), as well as basal and intermediate cells of the stria vascularis.

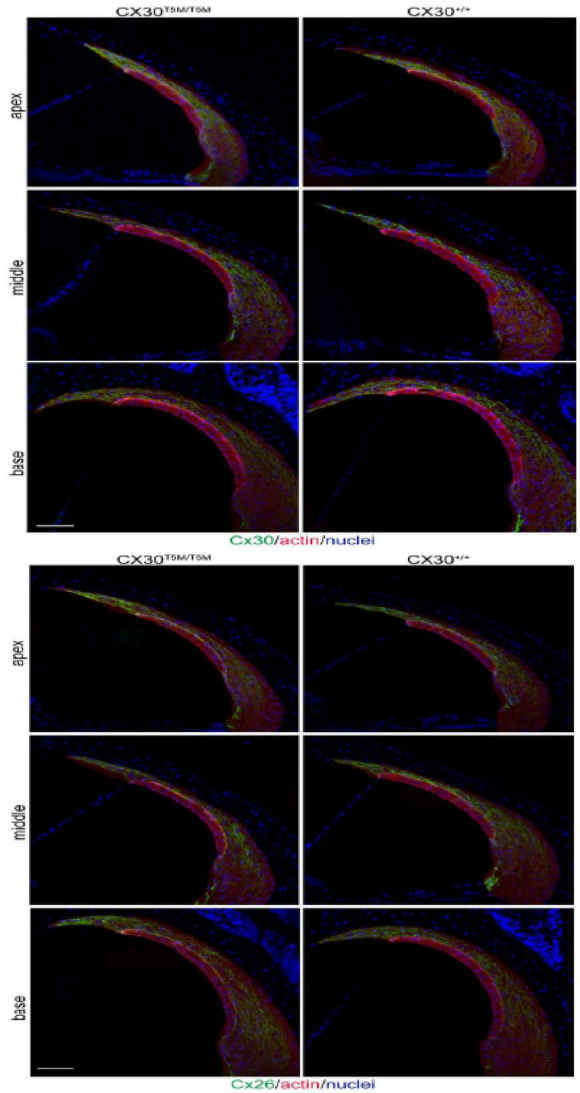

Figure 23. Cx30 (top) and Cx26 (bottom) expression in the adult stria vascularis. Maximal projection rendering of 2 consecutive midmodiolar confocal optical sections, taken at 1 µm intervals

in the indicated cochlear turns of $Cx30^{T5M/T5M}$ and $Cx30^{+/+}$ mice on P30. Cx26 and Cx30 expression was analyzed with specific antibodies (green), nuclei were stained with DAPI (blue) and actin filaments with Texas Red conjugated phalloidin (red). Scale bar, 50 µm.

References

1. Forge, A., et al., *The inner ear contains heteromeric channels composed of cx26 and cx30 and deafness-related mutations in cx26 have a dominant negative effect on cx30.* Cell Commun Adhes, 2003. **10**(4-6): p. 341-6.
2. Rabionet, R., P. Gasparini, and X. Estivill, *Molecular genetics of hearing impairment due to mutations in gap junction genes encoding beta connexins.* Hum Mutat, 2000. **16**(3): p. 190-202.
3. Ortolano, S., et al., *Coordinated control of connexin 26 and connexin 30 at the regulatory and functional level in the inner ear.* Proc Natl Acad Sci U S A, 2008. **105**(48): p. 18776-81.
4. Schutz, M., *The human deafness-associated connexin 30 T5M mutation causes mild hearing loss and reduces biochemical coupling among cochlear non-sensory cells in knock-in mice.* Human Mol Genet, 2010. **19**.
5. Pickles, J.O., *An introduction to the physiology of Hearing*. 2nd ed ed. 1988: Academic press. 26-77.
6. Merchan, M.A., J.A. Merchan, and M.D. Ludena, *Morphology of Hensen's cells.* J Anat, 1980. **131**(3): p. 519-23.
7. Spicer, S.S. and B.A. Schulte, *Differences along the place-frequency map in the structure of supporting cells in the gerbil cochlea.* Hear Res, 1994. **79**(1-2): p. 161-77.
8. Yeaman, C., K.K. Grindstaff, and W.J. Nelson, *New perspectives on mechanisms involved in generating epithelial cell polarity.* Physiol Rev, 1999. **79**(1): p. 73-98.
9. Wangemann, P., Schacht, J., *Homeostatic mechanism in the cochlea*, in *The Cochlea*, P. Dallos, Popper, A., Fay, R., Editor. 1996, Springer-Verlag: New York. p. 130-185.
10. von Bekesy, G., *DC resting potential inside the cochlea partition.* J Acoust Soc Am, 1952. **24**: p. 72-76.
11. Marcus, D., *Acoustic Transduction*. second edition ed. Cell Physiology, ed. N. Sperelakis. 1995: Academic press. 692-694.
12. Slepecky, N.B. and Y. Ogata, *[Immunohistochemical labeling of inner ear tissues embedded in polyethylene glycol 4000--comparative study with araldite and unicryl embedded sections].* Nippon Jibiinkoka Gakkai Kaiho, 1996. **99**(3): p. 361-9.
13. von Bekesy, G., *Experiments in hearing*. 1960, New York: McGraw-Hill.
14. Greenwood, D.D., *A cochlear frequency-position function for several species--29 years later.* J Acoust Soc Am, 1990. **87**(6): p. 2592-605.
15. Crawford, A.C. and R. Fettiplace, *The mechanical properties of ciliary bundles of turtle cochlear hair cells.* J Physiol, 1985. **364**: p. 359-79.
16. Howard, J. and J.F. Ashmore, *Stiffness of sensory hair bundles in the sacculus of the frog.* Hear Res, 1986. **23**(1): p. 93-104.
17. Corey, D.P. and A.J. Hudspeth, *Ionic basis of the receptor potential in a vertebrate hair cell.* Nature, 1979. **281**(5733): p. 675-7.
18. Corey, D.P. and A.J. Hudspeth, *Response latency of vertebrate hair cells.* Biophys J, 1979. **26**(3): p. 499-506.
19. Corey, D.P. and A.J. Hudspeth, *Kinetics of the receptor current in bullfrog saccular hair cells.* J Neurosci, 1983. **3**(5): p. 962-76.
20. Crawford, A.C., M.G. Evans, and R. Fettiplace, *The actions of calcium on the mechano-electrical transducer current of turtle hair cells.* J Physiol, 1991. **434**: p. 369-98.

21. Ricci, A.J., A.C. Crawford, and R. Fettiplace, *Tonotopic variation in the conductance of the hair cell mechanotransducer channel.* Neuron, 2003. **40**(5): p. 983-90.
22. Shotwell, S.L., R. Jacobs, and A.J. Hudspeth, *Directional sensitivity of individual vertebrate hair cells to controlled deflection of their hair bundles.* Ann N Y Acad Sci, 1981. **374**: p. 1-10.
23. Lumpkin, E.A., R.E. Marquis, and A.J. Hudspeth, *The selectivity of the hair cell's mechanoelectrical-transduction channel promotes Ca2+ flux at low Ca2+ concentrations.* Proc Natl Acad Sci U S A, 1997. **94**(20): p. 10997-1002.
24. Ricci, A.J. and R. Fettiplace, *Calcium permeation of the turtle hair cell mechanotransducer channel and its relation to the composition of endolymph.* J Physiol, 1998. **506 (Pt 1)**: p. 159-73.
25. Ohmori, H., *Mechano-electrical transduction currents in isolated vestibular hair cells of the chick.* J Physiol, 1985. **359**: p. 189-217.
26. Ottersen, O.P., et al., *Molecular organization of a type of peripheral glutamate synapse: the afferent synapses of hair cells in the inner ear.* Prog Neurobiol, 1998. **54**(2): p. 127-48.
27. Sadanaga, M. and T. Morimitsu, *Development of endocochlear potential and its negative component in mouse cochlea.* Hear Res, 1995. **89**(1-2): p. 155-61.
28. Xia, A., et al., *Expression of connexin 26 and Na,K-ATPase in the developing mouse cochlear lateral wall: functional implications.* Brain Res, 1999. **846**(1): p. 106-11.
29. Johnstone, B.M. and P.M. Sellick, *The peripheral auditory apparatus.* Q Rev Biophys, 1972. **5**(1): p. 1-57.
30. Johnstone, B.M., J.R. Johnstone, and I.D. Pugsley, *Membrane resistance in endolymphatic walls of the first turn of the guinea-pig cochlea.* J Acoust Soc Am, 1966. **40**(6): p. 1398-404.
31. Hudspeth, A.J., *Extracellular current flow and the site of transduction by vertebrate hair cells.* J Neurosci, 1982. **2**(1): p. 1-10.
32. Kubisch, C., et al., *KCNQ4, a novel potassium channel expressed in sensory outer hair cells, is mutated in dominant deafness.* Cell, 1999. **96**(3): p. 437-46.
33. Langer, P., S. Grunder, and A. Rusch, *Expression of Ca2+-activated BK channel mRNA and its splice variants in the rat cochlea.* J Comp Neurol, 2003. **455**(2): p. 198-209.
34. Boettger, T., et al., *Deafness and renal tubular acidosis in mice lacking the K-Cl co-transporter Kcc4.* Nature, 2002. **416**(6883): p. 874-8.
35. Boettger, T., et al., *Loss of K-Cl co-transporter KCC3 causes deafness, neurodegeneration and reduced seizure threshold.* Embo J, 2003. **22**(20): p. 5422-34.
36. Kikuchi, T., et al., *Potassium ion recycling pathway via gap junction systems in the mammalian cochlea and its interruption in hereditary nonsyndromic deafness.* Med Electron Microsc, 2000. **33**(2): p. 51-6.
37. Cohen-Salmon, M., F.J. del Castillo, and C. Petit, *Connexins Responsiblbe for Hereditary Deafness - The Tale Unfolds*, in *Gap Junctions in Development and Disease*, E. Winterhager, Editor. 2005, Springer-Verlag: Berlin. p. 111-134.
38. Jagger, D.J. and A. Forge, *Compartmentalized and signal-selective gap junctional coupling in the hearing cochlea.* J Neurosci, 2006. **26**(4): p. 1260-8.
39. Kikuchi, T., et al., *Gap junctions in the rat cochlea: immunohistochemical and ultrastructural analysis.* Anat Embryol (Berl), 1995. **191**(2): p. 101-18.
40. Marcus, D.C., et al., *KCNJ10 (Kir4.1) potassium channel knockout abolishes endocochlear potential.* Am J Physiol Cell Physiol, 2002. **282**(2): p. C403-7.
41. Takeuchi, S., M. Ando, and A. Kakigi, *Mechanism generating endocochlear potential: role played by intermediate cells in stria vascularis.* Biophys J, 2000. **79**(5): p. 2572-82.

42. Wangemann, P., et al., *Loss of KCNJ10 protein expression abolishes endocochlear potential and causes deafness in Pendred syndrome mouse model.* BMC Med, 2004. **2**: p. 30.
43. Sakagami, M., et al., *Cellular localization of rat Isk protein in the stria vascularis by immunohistochemical observation.* Hear Res, 1991. **56**(1-2): p. 168-72.
44. Offner, F.F., P. Dallos, and M.A. Cheatham, *Positive endocochlear potential: mechanism of production by marginal cells of stria vascularis.* Hear Res, 1987. **29**(2-3): p. 117-24.
45. Marcus, D.C., et al., *Protein kinase C mediates P2U purinergic receptor inhibition of K+ channel in apical membrane of strial marginal cells.* Hear Res, 1998. **115**(1-2): p. 82-92.
46. Zidanic, M. and W.E. Brownell, *Fine structure of the intracochlear potential field. I. The silent current.* Biophys J, 1990. **57**(6): p. 1253-68.
47. Konishi, T., P.E. Hamrick, and P.J. Walsh, *Ion transport in guinea pig cochlea. I. Potassium and sodium transport.* Acta Otolaryngol, 1978. **86**(1-2): p. 22-34.
48. Asher, D.L. and I. Sando, *Perilymphatic communication routes in the auditory and vestibular system.* Otolaryngol Head Neck Surg, 1981. **89**(5): p. 822-30.
49. Jentsch, T.J., *Neuronal KCNQ potassium channels: physiology and role in disease.* Nat Rev Neurosci, 2000. **1**(1): p. 21-30.
50. Wangemann, P., *K+ cycling and the endocochlear potential.* Hear Res, 2002. **165**(1-2): p. 1-9.
51. Cohen-Salmon, M., et al., *Targeted ablation of connexin26 in the inner ear epithelial gap junction network causes hearing impairment and cell death.* Curr Biol, 2002. **12**(13): p. 1106-11.
52. Teubner, B., et al., *Connexin30 (Gjb6)-deficiency causes severe hearing impairment and lack of endocochlear potential.* Hum Mol Genet, 2003. **12**(1): p. 13-21.
53. Marcus, D.C. and T. Chiba, *K+ and Na+ absorption by outer sulcus epithelial cells.* Hear Res, 1999. **134**(1-2): p. 48-56.
54. Komune, S., et al., *Mechanism of lack of development of negative endocochlear potential in guinea pigs with hair cell loss.* Hear Res, 1993. **70**(2): p. 197-204.
55. Takeuchi, S. and M. Ando, *Voltage-dependent outward K(+) current in intermediate cell of stria vascularis of gerbil cochlea.* Am J Physiol, 1999. **277**(1 Pt 1): p. C91-9.
56. Housley, G.D., *Extracellular nucleotide signaling in the inner ear.* Mol Neurobiol, 1998. **16**(1): p. 21-48.
57. Wangemann, P., et al., *Muscarinic receptors control K+ secretion in inner ear strial marginal cells.* J Membr Biol, 2001. **182**(3): p. 171-81.
58. Wangemann, P., *Adrenergic and muscarinic control of cochlear endolymph production.* Adv Otorhinolaryngol, 2002. **59**: p. 42-50.
59. McGuirt, J.P. and B.A. Schulte, *Distribution of immunoreactive alpha- and beta-subunit isoforms of Na,K-ATPase in the gerbil inner ear.* J Histochem Cytochem, 1994. **42**(7): p. 843-53.
60. Wangemann, P., et al., *K+ secretion in strial marginal cells is stimulated via beta 1-adrenergic receptors but not via beta 2-adrenergic or vasopressin receptors.* J Membr Biol, 2000. **175**(3): p. 191-202.
61. Ishii, K., W.G. Zhai, and M. Akita, *Effect of a beta-stimulant on the inner ear stria vascularis.* Ann Otol Rhinol Laryngol, 2000. **109**(7): p. 628-33.
62. Kanoh, N., *Effect of norepinephrine on ouabain-sensitive, K+-dependent p-nitrophenylphosphatase activity in strial marginal cells of the cochlea in normal and reserpinized guinea pigs.* Acta Otolaryngol, 1998. **118**(6): p. 817-20.

63. Kanoh, N., *Effects of epinephrine on ouabain-sensitive, K(+) -dependent P-nitrophenylphosphatase activity in strial marginal cells of guinea pigs.* Ann Otol Rhinol Laryngol, 1999. **108**(4): p. 345-8.
64. Davis, H., *Energy into nerve impulses:the inner ear.* Adv Sci, 1953. **9**: p. 420-425.
65. Majumder, P., Crispino, G., Rodriguez, L., Ciubotaru, C.D., Anselmi, F., and V. Piazza, Bortolozzi, M. and Mammano, F., *ATP-mediated*
cell-cell signaling in the organ of Corti: the role of connexin channels. Purinergic Signal., 2010. **6**: p. 167–187.
66. Saez, J.C., et al., *Plasma membrane channels formed by connexins: their regulation and functions.* Physiol Rev, 2003. **83**(4): p. 1359-400.
67. Simon, A.M. and D.A. Goodenough, *Diverse functions of vertebrate gap junctions.* Trends Cell Biol, 1998. **8**(12): p. 477-83.
68. Revel, J.P. and M.J. Karnovsky, *Hexagonal array of subunits in intercellular junctions of the mouse heart and liver.* J Cell Biol, 1967. **33**(3): p. C7-C12.
69. Bruzzone, R., T.W. White, and D.L. Paul, *Connections with connexins: the molecular basis of direct intercellular signaling.* Eur J Biochem, 1996. **238**(1): p. 1-27.
70. Bittman, K., *Cell coupling and uncoupling in the ventricular zone of developing neocortex.* J Neuroscience, 1997. **17**.
71. Owens, D., *Patterns of intracellular calcium fluctuation in precursor cells of the neocortical ventricular zone.* J Neuroscience, 1998. **18**.
72. Elias, L., *Gap junction adhesion is necessary for radial migration in the neocortex.* Nature, 2007. **448**.
73. Donahue, L., *Decreased gap-junctional communication associated with segregation of the neuronal phenotype in the RT4 cell-line family.* Cell Tissue Res, 1998.
74. Harris, A.L., *Emerging issues of connexin channels: biophysics fills the gap.* Q Rev Biophys, 2001. **34**(3): p. 325-472.
75. Yeager, M.a.N., B.J., *Structure and biochemestry of gap junction*, in *Gap junction*, E.L. Hertzberg, Editor. 2000. p. 31-98.
76. Wagner, C.A., *Function of connexins in the renal circulation.* 2008.
77. Musil, L.S. and D.A. Goodenough, *Multisubunit assembly of an integral plasma membrane channel protein, gap junction connexin43, occurs after exit from the ER.* Cell, 1993. **74**(6): p. 1065-77.
78. Martin, P.E., et al., *Multiple pathways in the trafficking and assembly of connexin 26, 32 and 43 into gap junction intercellular communication channels.* J Cell Sci, 2001. **114**(Pt 21): p. 3845-55.
79. Gaietta, G., et al., *Multicolor and electron microscopic imaging of connexin trafficking.* Science, 2002. **296**(5567): p. 503-7.
80. Jordan, K., et al., *The origin of annular junctions: a mechanism of gap junction internalization.* J Cell Sci, 2001. **114**(Pt 4): p. 763-73.
81. Laing, J.G., et al., *Proteolysis of connexin43-containing gap junctions in normal and heat-stressed cardiac myocytes.* Cardiovasc Res, 1998. **38**(3): p. 711-8.
82. Fallon, R.F. and D.A. Goodenough, *Five-hour half-life of mouse liver gap-junction protein.* J Cell Biol, 1981. **90**(2): p. 521-6.
83. Beardslee, M.A., et al., *Rapid turnover of connexin43 in the adult rat heart.* Circ Res, 1998. **83**(6): p. 629-35.
84. Berthoud, V.M., S. Bassnett, and E.C. Beyer, *Cultured chicken embryo lens cells resemble differentiating fiber cells in vivo and contain two kinetic pools of connexin56.* Exp Eye Res, 1999. **68**(4): p. 475-84.

85. Beyer, E.C., D.L. Paul, and D.A. Goodenough, *Connexin family of gap junction proteins.* J Membr Biol, 1990. **116**(3): p. 187-94.
86. Goodenough, D.A., J.A. Goliger, and D.L. Paul, *Connexins, connexons, and intercellular communication.* Annu Rev Biochem, 1996. **65**: p. 475-502.
87. Kumar, N.M. and N.B. Gilula, *The gap junction communication channel.* Cell, 1996. **84**(3): p. 381-8.
88. Suchyna, T.M., et al., *Different ionic selectivities for connexins 26 and 32 produce rectifying gap junction channels.* Biophys J, 1999. **77**(6): p. 2968-87.
89. Falk, M.M., et al., *Cell-free synthesis and assembly of connexins into functional gap junction membrane channels.* Embo J, 1997. **16**(10): p. 2703-16.
90. Falk, M.M., *Connexin-specific distribution within gap junctions revealed in living cells.* J Cell Sci, 2000. **113 (Pt 22)**: p. 4109-20.
91. Haubrich, S., et al., *Incompatibility of connexin 40 and 43 Hemichannels in gap junctions between mammalian cells is determined by intracellular domains.* Mol Biol Cell, 1996. **7**(12): p. 1995-2006.
92. White, T.W. and R. Bruzzone, *Multiple connexin proteins in single intercellular channels: connexin compatibility and functional consequences.* J Bioenerg Biomembr, 1996. **28**(4): p. 339-50.
93. Niessen, H., et al., *Selective permeability of different connexin channels to the second messenger inositol 1,4,5-trisphosphate.* J Cell Sci, 2000. **113 (Pt 8)**: p. 1365-72.
94. Goldberg, G.S., P.D. Lampe, and B.J. Nicholson, *Selective transfer of endogenous metabolites through gap junctions composed of different connexins.* Nat Cell Biol, 1999. **1**(7): p. 457-9.
95. Bevans, C.G., et al., *Isoform composition of connexin channels determines selectivity among second messengers and uncharged molecules.* J Biol Chem, 1998. **273**(5): p. 2808-16.
96. Goldberg, G.S., V. Valiunas, and P.R. Brink, *Selective permeability of gap junction channels.* Biochim Biophys Acta, 2004. **1662**(1-2): p. 96-101.
97. Bennett, M.V., et al., *Gap junctions: new tools, new answers, new questions.* Neuron, 1991. **6**(3): p. 305-20.
98. Elfgang, C., et al., *Specific permeability and selective formation of gap junction channels in connexin-transfected HeLa cells.* J Cell Biol, 1995. **129**(3): p. 805-17.
99. Veenstra, R.D., *Size and selectivity of gap junction channels formed from different connexins.* J Bioenerg Biomembr, 1996. **28**(4): p. 327-37.
100. Veenstra, R.D., et al., *Selectivity of connexin-specific gap junctions does not correlate with channel conductance.* Circ Res, 1995. **77**(6): p. 1156-65.
101. Niessen, H. and K. Willecke, *Strongly decreased gap junctional permeability to inositol 1,4, 5-trisphosphate in connexin32 deficient hepatocytes.* FEBS Lett, 2000. **466**(1): p. 112-4.
102. Gilula, N.B., O.R. Reeves, and A. Steinbach, *Metabolic coupling, ionic coupling and cell contacts.* Nature, 1972. **235**(5336): p. 262-5.
103. Peracchia, C., X.G. Wang and L.L. Peracchia, *Behavior of chemical- and slow voltage-sensitive gating of connexin channels: the "cork" gating hypothesis*, ed. C. Peracchia. Vol. Gap Junctions. Molecular Basis of Cell Communication in Health and Disease. 2000, San Diego, CA: Academic Press. 271–295.
104. Firek, L. and R. Weingart, *Modification of gap junction conductance by divalent cations and protons in neonatal rat heart cells.* J Mol Cell Cardiol, 1995. **27**(8): p. 1633-43.
105. Veenstra, R.D. and R.L. DeHaan, *Cardiac gap junction channel activity in embryonic chick ventricle cells.* Am J Physiol, 1988. **254**(1 Pt 2): p. H170-80.

106. Enkvist, M.O. and K.D. McCarthy, *Astroglial gap junction communication is increased by treatment with either glutamate or high K+ concentration.* J Neurochem, 1994. **62**(2): p. 489-95.
107. Duthe, F., et al., *Endogenous protein phosphatase 1 runs down gap junctional communication of rat ventricular myocytes.* Am J Physiol Cell Physiol, 2001. **281**(5): p. C1648-56.
108. Peracchia, C., G. Bernardini, and L.L. Peracchia, *Is calmodulin involved in the regulation of gap junction permeability?* Pflugers Arch, 1983. **399**(2): p. 152-4.
109. Bevans, C.G. and A.L. Harris, *Regulation of connexin channels by pH. Direct action of the protonated form of taurine and other aminosulfonates.* J Biol Chem, 1999. **274**(6): p. 3711-9.
110. Bukauskas, F.F., et al., *Gating properties of gap junction channels assembled from connexin43 and connexin43 fused with green fluorescent protein.* Biophys J, 2001. **81**(1): p. 137-52.
111. Bukauskas, F.F. and V.K. Verselis, *Gap junction channel gating.* Biochim Biophys Acta, 2004. **1662**(1-2): p. 42-60.
112. Bukauskas, F.F. and C. Peracchia, *Two distinct gating mechanisms in gap junction channels: CO2-sensitive and voltage-sensitive.* Biophys J, 1997. **72**(5): p. 2137-42.
113. Peracchia, C., X.G. Wang, and L.L. Peracchia, *Is the chemical gate of connexins voltage sensitive? Behavior of Cx32 wild-type and mutant channels.* Am J Physiol, 1999. **276**(6 Pt 1): p. C1361-73.
114. Foote, C., *The pattern of disulfide linkages in the extracellular loop regions of connexin 32 suggests a model for the docking interface of gap junctions.* J. Cell Biol., 1998.
115. Bao, X., *Functional expression in Xenopus oocytes of gap-junctional hemichannels formed by a cysteine-less connexin 43.* J Biol Chem, 2004.
116. Maeda, S., *Structure of the gap junction channel and its implications for its biological functions.* Cell Mol. Life Sci., 2010.
117. Maeda, S., et al., *Structure of the connexin 26 gap junction channel at 3.5 A resolution.* Nature, 2009. **458**(7238): p. 597-602.
118. Ahmad, S., et al., *Connexins 26 and 30 are co-assembled to form gap junctions in the cochlea of mice.* Biochem Biophys Res Commun, 2003. **307**(2): p. 362-8.
119. Forge, A., et al., *Gap junctions in the inner ear: comparison of distribution patterns in different vertebrates and assessement of connexin composition in mammals.* J Comp Neurol, 2003. **467**(2): p. 207-31.
120. Kelsell, D.P., et al., *Connexin 26 mutations in hereditary non-syndromic sensorineural deafness.* Nature, 1997. **387**(6628): p. 80-3.
121. Grifa, A., et al., *Mutations in GJB6 cause nonsyndromic autosomal dominant deafness at DFNA3 locus.* Nat Genet, 1999. **23**(1): p. 16-8.
122. Hilgert, N., *Forty-six genes causing nonsyndromic hearing impairment: which ones should be analyzed in DNA diagnostics?* Mutat Res, 2009. **681**.
123. Morton, C.C., *Newborn hearing screening--a silent revolution.* N Engl J Med, 2006.
124. Morton, C.C., *Gene discovery in the auditory system using a tissue specific approach.* Am J Med Genet A, 2004. **130**(1): p. 26-8.
125. Dror, A., *Hearing loss: mechanisms revealed by genetics and cell biology.* Annu Rev Genet, 2009.
126. Stojkovic, T., et al., *Sensorineural deafness in X-linked Charcot-Marie-Tooth disease with connexin 32 mutation (R142Q).* Neurology, 1999. **52**(5): p. 1010-4.

127. Liu, X.Z., et al., *Mutations in connexin31 underlie recessive as well as dominant non-syndromic hearing loss.* Hum Mol Genet, 2000. **9**(1): p. 63-7.
128. Richard, G., et al., *Mutations in the human connexin gene GJB3 cause erythrokeratodermia variabilis.* Nat Genet, 1998. **20**(4): p. 366-9.
129. Liu, X.Z., et al., *Mutations in GJA1 (connexin 43) are associated with non-syndromic autosomal recessive deafness.* Hum Mol Genet, 2001. **10**(25): p. 2945-51.
130. Zelante, L., et al., *Connexin26 mutations associated with the most common form of non-syndromic neurosensory autosomal recessive deafness (DFNB1) in Mediterraneans.* Hum Mol Genet, 1997. **6**(9): p. 1605-9.
131. Snoeckx, R.L., et al., *GJB2 mutations and degree of hearing loss: a multicenter study.* Am J Hum Genet, 2005. **77**(6): p. 945-57.
132. Richard, G., *Connexin gene pathology.* Clin Exp Dermatol, 2003. **28**(4): p. 397-409.
133. Chaib, H., et al., *A gene responsible for a dominant form of neurosensory non-syndromic deafness maps to the NSRD1 recessive deafness gene interval.* Hum Mol Genet, 1994. **3**(12): p. 2219-22.
134. Abe, S., et al., *Connexin 26 gene (GJB2) mutation modulates the severity of hearing loss associated with the 1555A-->G mitochondrial mutation.* Am J Med Genet, 2001. **103**(4): p. 334-8.
135. Kikuchi, T., et al., *Gap junction systems in the rat vestibular labyrinth: immunohistochemical and ultrastructural analysis.* Acta Otolaryngol, 1994. **114**(5): p. 520-8.
136. Mammano, F., et al., *Ca2+ signaling in the inner ear.* Physiology (Bethesda), 2007. **22**: p. 131-44.
137. Beyer, E.C.a.W., K., *Gap junction genes and their regulation*, in *Gap Junction*, B. E., Editor. 2000, Hertzberg. p. 1-29.
138. Denoyelle, F., et al., *Prelingual deafness: high prevalence of a 30delG mutation in the connexin 26 gene.* Hum Mol Genet, 1997. **6**(12): p. 2173-7.
139. White, T.W., et al., *Connexin mutations in deafness.* Nature, 1998. **394**(6694): p. 630-1.
140. Estivill, X., et al., *Connexin-26 mutations in sporadic and inherited sensorineural deafness.* Lancet, 1998. **351**(9100): p. 394-8.
141. Morell, R.J., et al., *Mutations in the connexin 26 gene (GJB2) among Ashkenazi Jews with nonsyndromic recessive deafness.* N Engl J Med, 1998. **339**(21): p. 1500-5.
142. Gerido, D.A. and T.W. White, *Connexin disorders of the ear, skin, and lens.* Biochim Biophys Acta, 2004. **1662**(1-2): p. 159-70.
143. Bruzzone, R., et al., *Functional analysis of a dominant mutation of human connexin26 associated with nonsyndromic deafness.* Cell Commun Adhes, 2001. **8**(4-6): p. 425-31.
144. Bruzzone, R., et al., *Loss-of-function and residual channel activity of connexin26 mutations associated with non-syndromic deafness.* FEBS Lett, 2003. **533**(1-3): p. 79-88.
145. D'Andrea, P., et al., *Hearing loss: frequency and functional studies of the most common connexin26 alleles.* Biochem Biophys Res Commun, 2002. **296**(3): p. 685-91.
146. Wang, H.L., et al., *Functional analysis of connexin-26 mutants associated with hereditary recessive deafness.* J Neurochem, 2003. **84**(4): p. 735-42.
147. Denoyelle, F., et al., *Connexin 26 gene linked to a dominant deafness.* Nature, 1998. **393**(6683): p. 319-20.
148. Loffler, J., et al., *Sensorineural hearing loss and the incidence of Cx26 mutations in Austria.* Eur J Hum Genet, 2001. **9**(3): p. 226-30.
149. Morle, L., et al., *A novel C202F mutation in the connexin26 gene (GJB2) associated with autosomal dominant isolated hearing loss.* J Med Genet, 2000. **37**(5): p. 368-70.

150. Dahl, E., et al., *Molecular cloning and functional expression of mouse connexin-30,a gap junction gene highly expressed in adult brain and skin.* J Biol Chem, 1996. **271**(30): p. 17903-10.
151. Kelley, P.M., et al., *Human connexin 30 (GJB6), a candidate gene for nonsyndromic hearing loss: molecular cloning, tissue-specific expression, and assignment to chromosome 13q12.* Genomics, 1999. **62**(2): p. 172-6.
152. Common, J.E., et al., *Functional studies of human skin disease- and deafness-associated connexin 30 mutations.* Biochem Biophys Res Commun, 2002. **298**(5): p. 651-6.
153. del Castillo, I., et al., *A deletion involving the connexin 30 gene in nonsyndromic hearing impairment.* N Engl J Med, 2002. **346**(4): p. 243-9.
154. del Castillo, I., et al., *Prevalence and evolutionary origins of the del(GJB6-D13S1830) mutation in the DFNB1 locus in hearing-impaired subjects: a multicenter study.* Am J Hum Genet, 2003. **73**(6): p. 1452-8.
155. Rozental, R., S. Miduturu, and D.C. Spray, *How to close a gap junction channel*, in *Connexin Methods and Protocols*, R. Bruzzone and C. Giaume, Editors. 2001, Humana Press: Totowa, NJ. p. 447-476.
156. Levesque, S.A., et al., *Specificity of the ecto-ATPase inhibitor ARL 67156 on human and mouse ectonucleotidases.* Br J Pharmacol, 2007. **152**(1): p. 141-50.
157. Komoszynski, M.A., *Comparative studies on animal and plant apyrases (ATP diphosphohydrolase EC 3.6.1.5) with application of immunological techniques and various ATPase inhibitors.* Comp Biochem Physiol B Biochem Mol Biol, 1996. **113**(3): p. 581-91.
158. Molnar, J. and L. Lorand, *Studies on apyrases.* Arch Biochem Biophys, 1961. **93**: p. 353-63.
159. Contreras, J.E., et al., *Gating and regulation of connexin 43 (Cx43) hemichannels.* Proc Natl Acad Sci U S A, 2003. **100**(20): p. 11388-93.
160. Anselmi, F., et al., *ATP release through connexin hemichannels and gap junction transfer of second messengers propagate Ca2+ signals across the inner ear.* Proc Natl Acad Sci U S A, 2008. **105**(48): p. 18770-5.
161. Kelly, M.C. and P. Chen, *Development of form and function in the mammalian cochlea.* Curr Opin Neurobiol, 2009. **19**(4): p. 395-401.
162. Schutz, M., *The connexin26 S17F mouse mutant represents a model for the human hereditary keratitis-ichthyosis-deafness syndrome.* Hum Mol Genet, 2011. **20**.
163. White, T.W. and D.L. Paul, *Genetic diseases and gene knockouts reveal diverse connexin functions.* Annu Rev Physiol, 1999. **61**: p. 283-310.
164. Gabriel, H.D., et al., *Transplacental uptake of glucose is decreased in embryonic lethal connexin26-deficient mice.* J Cell Biol, 1998. **140**(6): p. 1453-61.
165. Lautermann, J., et al., *Expression of the gap-junction connexins 26 and 30 in the rat cochlea.* Cell Tissue Res, 1998. **294**(3): p. 415-20.
166. Valiunas, V., et al., *Biophysical properties of mouse connexin30 gap junction channels studied in transfected human HeLa cells.* J Physiol, 1999. **519 Pt 3**: p. 631-44.
167. Jero, J., et al., *A surgical approach appropriate for targeted cochlear gene therapy in the mouse.* Hear Res, 2001. **151**(1-2): p. 106-114.
168. Jero, J., et al., *Cochlear gene delivery through an intact round window membrane in mouse.* Hum Gene Ther, 2001. **12**(5): p. 539-48.
169. Praetorius, M., et al., *Hearing preservation after inner ear gene therapy: the effect of vector and surgical approach.* ORL J Otorhinolaryngol Relat Spec, 2003. **65**(4): p. 211-4.
170. Praetorius, M., et al., *A novel vestibular approach for gene transfer into the inner ear.* Audiol Neurootol, 2002. **7**(6): p. 324-34.

171. Gubbels, S., *Functional auditory hair cells produced in the mammalian cochlea by in utero gene transfer.* Nature, 2008.
172. Schmidt, M., et al., *Cloning and characterization of a bovine adeno-associated virus.* J Virol, 2004. **78**(12): p. 6509-16.
173. Shibata, S., *Gene transfer using bovine adeno-associated virus in the guinea pig cochlea.* Gene Ther, 2009.
174. Di Pasquale, G., et al., *A novel bovine virus efficiently transduces inner ear neuroepithelial cells.* Mol Ther, 2005. **11**(6): p. 849-55.
175. Matsuoka, T., et al., *Neural crest origins of the neck and shoulder.* Nature, 2005. **436**(7049): p. 347-55.
176. Watanabe, K., et al., *Expression of the Sox10 gene during mouse inner ear development.* Brain Res Mol Brain Res, 2000. **84**(1-2): p. 141-5.
177. Kaludov, N., B. Handelman, and J.A. Chiorini, *Scalable purification of adeno-associated virus type 2, 4, or 5 using ion-exchange chromatography.* Hum Gene Ther, 2002. **13**(10): p. 1235-43.
178. Pfaffl, M.W., *A new mathematical model for relative quantification in real-time RT-PCR.* Nucleic Acids Res, 2001. **29**(9): p. e45.
179. Steel, K.P.a.B., C., *Another role for melanocytes: their importance for normal stria vascularis development in the mammalian inner ear.* Development, 1989. **107**: p. 453–463.
180. Santarelli, R., Arslan, E., Carraro, L., Conti, G., Capello, M. and Plourde, G., *Effects of isoflurane on the auditory brainstem responses and middle latency responses of rats.* Acta Otolaryngol, 2003. **123**: p. 176–181.
181. Di Virgilio, F., T.H. Steinberg, and S.C. Silverstein, *Organic-anion transport inhibitors to facilitate measurement of cytosolic free Ca2+ with fura-2.* Methods Cell Biol, 1989. **31**: p. 453-62.
182. Bry, C., *Loss of connexin 26 in mammary epithelium during early but not during late pregnancy results in unscheduled apoptosis and impaired development.* Dev. Biol., 2004. **267**.
183. Shibata, S., *Sox10-Venus mice: a new tool for real-time labeling of neural crest lineage cells and oligodendrocytes.* Mol. Brain, 2010.
184. Sauer, B., *Inducible gene targeting in mice using the Cre/lox system.* Methods, 1998.
185. Wang, Y., *Targeted connexin26 ablation arrests postnatal development of the organ of Corti.* Biochem Biophys Res Commun, 2009.
186. Ahmad, S., et al., *Restoration of connexin26 protein level in the cochlea completely rescues hearing in a mouse model of human connexin30-linked deafness.* Proc Natl Acad Sci U S A, 2007. **104**(4): p. 1337-41.
187. Levin, M., *Gap junctional communication in morphogenesis.* Prog Biophys Mol Biol, 2007. **94**(1-2): p. 186-206.
188. Harris, A.L., *Connexin channel permeability to cytoplasmic molecules.* Prog Biophys Mol Biol, 2007. **94**(1-2): p. 120-43.
189. Wade, M.H., J.E. Trosko, and M. Schindler, *A fluorescence photobleaching assay of gap junction-mediated communication between human cells.* Science, 1986. **232**(4749): p. 525-8.
190. Eggston, A.A., *Histopathology of the Ear, Nose, and Throat.* Embriology of the ear, 1947: p. 37-64.
191. Bermingham-McDonogh, O., *Expression of Prox1 during mouse cochlear development.* J. Comp. Neurol., 2006.

192. Rabut, G. and J. Ellenberg, *Photobleaching techniques to study mobility and molecular dynamics of proteins in live cells: FRAP, iFRAP, and FLIP.*, in *Live Cell Imaging*, R.D. Goldman and D.L. Spector, Editors. 2005, Cold Spring Harbor Laboratory: New York. p. 101-126.
193. Paulson, D., *A novel controlled local drug delivery system for inner ear disease.* Laryngoscope, 2008.
194. Walsted, A., *Hearing decrease after loss of cerebrospinal fluid. A new hydrops model?* Acta Otolaryngol, 1991.
195. Di Pasquale, G. and J.A. Chiorini, *AAV transcytosis through barrier epithelia and endothelium.* Mol Ther, 2006. **13**(3): p. 506-16.
196. Zheng, C., *Convenient and reproducible in vivo gene transfer to mouse parotid glands.* Oral. Dis., 2011. **17**.
197. Tritsch, N.X., *Calcium action potentials in hair cells pattern auditory neuron activity before hearing onset.* Nature Neuroscience, 2010. **13**.
198. Brigande, J., *Electroporation-mediated gene transfer to the developing mouse inner ear.* Methods Mol Biol, 2009.
199. Anderson, D., *A vapor exposure model for neonatal mice.* Toxicol Mech Methods, 2002.
200. Tsuprun, V., *Structure of outer hair cell stereocilia side and attachment links in the chinchilla cochlea.* J. Histochem Cytochem, 2002.
201. Hibino, H., *How is the highly positive endocochlear potential formed? The specific architecture of the stria vascularis and the roles of the ion-transport apparatus.* 2010.
202. Bennicelli, J., *Reversal of blindness in animal models of leber congenital amaurosis using optimized AAV2-mediated gene transfer.* MOl. Ther., 2008. **16**.
203. Clair, C., et al., *Extracellular-loop peptide antibodies reveal a predominant hemichannel organization of connexins in polarized intestinal cells.* Exp Cell Res, 2008. **314**(6): p. 1250-65.
204. Eatock, R.A. and K.M. Hurley, *Functional development of hair cells.* Curr Top Dev Biol, 2003. **57**: p. 389-448.
205. Mikaelian, D., B.R. Alford, and R.J. Ruben, *Cochlear Potentials and 8 Nerve Action Potentials in Normal and Genetically Deaf Mice.* Ann Otol Rhinol Laryngol, 1965. **74**: p. 146-57.